The role of the PeBoW-complex in ribosome biogenesis and proliferation of mouse embryonic stem cells

Dissertation

der Fakultät für Biologie

der Ludwig-Maximilians-Universität München

vorgelegt von

Iris Pfisterer

5. November 2007

Diese Arbeit wurde am Institut für Klinische Molekularbiologie und Tumorgenetik des GSF-Forschungszentrums für Umwelt und Gesundheit in München angefertigt.

Erstgutachter:	Prof. Dr. Dirk Eick
Zweitgutachter:	Prof. Dr. Michael Schleicher
Tag der mündlichen Prüfung:	17.12.2007

Ehrenwörtliche Versicherung

Ich versichere hiermit ehrenwörtlich, dass die Dissertation von mir selbstständig und ohne unerlaubte Beihilfe angefertigt worden ist.

Erklärung

Hiermit erkläre ich, dass die Dissertation nicht ganz oder in wesentlichen Teilen einer anderen Prüfungskomission vorgelegt worden ist.
Ich erkläre weiterhin, dass ich mich nicht anderweitig einer Doktorprüfung ohne Erfolg unterzogen habe.

München, im November 2007

Iris Pfisterer

TABLE OF CONTENT

SYNOPSIS

Embryonic stem (ES) cell biology has become a very interesting field for scientific research in recent years. This is not only due to the meanwhile relatively easy propagation of stem cells in culture, but mainly to their very specific features, which offer a wide variety of research perspectives and future therapeutic approaches.

ES cells are undifferentiated, pluripotent cells, meaning that an individual cell has the capability to differentiate into all cell types of a mammalian body. The possibility to differentiate ES cells *in vitro* into specific lineages provides an opportunity to follow up differentiation processes and reveal factors involved in the generation of specific progenitors or committed cell types. With human ES cells, there is a strong effort to use this knowledge for cell replacement therapies to repair damaged organs or as vehicle for drug delivery to specific sites within the body. In addition, such studies can provide further understanding of embryogenesis without the use of transgenic animals.

The pluripotency of stem cells depends on their ability to self-renew. Self-renewal is the ability to proliferate via symmetrical cell divisions without differentiation, therefore ensuring identical pluripotent progeny.

Another specific feature of ES cells is their rapid proliferation rate together with unusual cell cycle kinetics, which is speculated to be as well related to self-renewal and the maintenance of pluripotency (Burdon et al., 2002; Niwa, 2007). In culture, ES cells show an unlimited proliferation potential although they are derived without addition of any immortalizing agent (Suda et al., 1987). Moreover, ES cells do not undergo senescence, do not show contact inhibition, and can grow without the addition of serum, properties also typical of tumor cells. When introduced into somatic tissues, ES cells show indeed tumorigenic potential, which might interfere with their usage for therapeutic purposes (Takahashi et al., 2003a). Studying the unusual proliferation properties of ES cells is therefore an important issue that might also advance our understanding of transformed cells and of the self-renewal process.

Proliferation is a coordinated process between cell growth and cell division. This tight balance is necessary to prevent cells from premature division. In ES cells, which lack some of the usual control points during the cell cycle, not much is known about a possible coordination between these processes. One important regulator of cell growth is ribosome biogenesis, which has recently been linked to cell cycle pro gression. As a

factor, involved in both processes, the PeBoW-complex has been identified. The components of the PeBoW-complex, Pes1, Bop1 and WDR12 have been shown to be necessary for maturation of the large ribosomal subunit and for cell proliferation in mature cell systems. Disruptions in ribosome synthesis, following depletion of the PeBoW-complex, are proposed to be transmitted to the cell cycle machinery via a p53-dependent checkpoint response (Holzel et al., 2005; Pestov et al., 2001). During this work it was investigated whether Pes1, Bop1 and WDR12 have an effect on proliferation of embryonic stem cells and how ribosome biogenesis and proliferation are coordinated in stem cells.

1 INTRODUCTION

1.1 Mouse embryonic stem cells

The hallmark of stem cells, embryonic or adult, is their capacity for self-renewal on one hand and differentiation on the other hand. Embryonic stem cells are pluripotent and represent the origin of all tissues of the mammalian body. Pluripotency is generally defined as the ability to give rise to derivatives of all three germ layers and germ cells; that is, essentially all cell types, found in an adult organism (Boiani and Scholer, 2005; Solter, 2006). In contrast, adult stem cells are further developed and therefore considered as multipotent. They can give rise only to a restricted number of specific cell types within the body, e.g., hematopoietic stem cells can differentiate into the different types of blood cells. Adult stem cells play an important function within the body for replacement of aging or damaged tissues. But not for all tissues exist adult stem cells that can renew them after injury. Therefore, research on embryonic stem cells is expected to provide a promising tool for regenerative medicine.

During early embryonic development, the totipotent zygote develops via blastomeres into the morula, a stage of about 100 cells at day 2-3 post fertilization. The morula gradually reorganizes and expands to give rise to the blastula. At this stage, differentiation events partition the embryo into the outer trophectoderm, which will later form the placenta, and the inner cell mass (ICM), the embryonic component. With further development of the mouse, the ICM gives rise to two distinct lineages: the extraembryonic (or primitive) endoderm, which will form extraembryonic tissues, and the epiblast, which gives rise to the embryo proper (via primitive ectoderm) (Niwa, 2007).

Mouse embryonic stem cells are isolated from the inner cell mass (ICM) of the blastocyst from 3-4 day old preimplantation embryos (Evans and Kaufman, 1981; Martin, 1981). Under addition of the cytokine LIF (leukemia inhibitory factor), mouse ES cells can be propagated in culture unlimited, without loosing their self-renewal properties. LIF can be provided by secretion from feeder cells or, alternatively, it can be added as a recombinant protein into the medium, bypassing the need for feeder cells (Smith et al., 1988; Williams et al., 1988). Withdrawal of LIF from cultivation medium leads to differentiation of ES cells *in vitro*. When ES cells are reintroduced into a blastocyst, they can contribute to all cells of the embryo proper.

In principal, ES cells represent an *in vitro* counterpart of a cell population from the early embryo, the ICM. Nevertheless, the cell population of the ICM exists only for a limited time and then differentiates into the fetus and finally the adult organism. It is presumed that ES cells are a transient population that can be maintained practically indefinitely *in vitro* through selection and adaptation to the culture environment (Buehr and Smith, 2003).

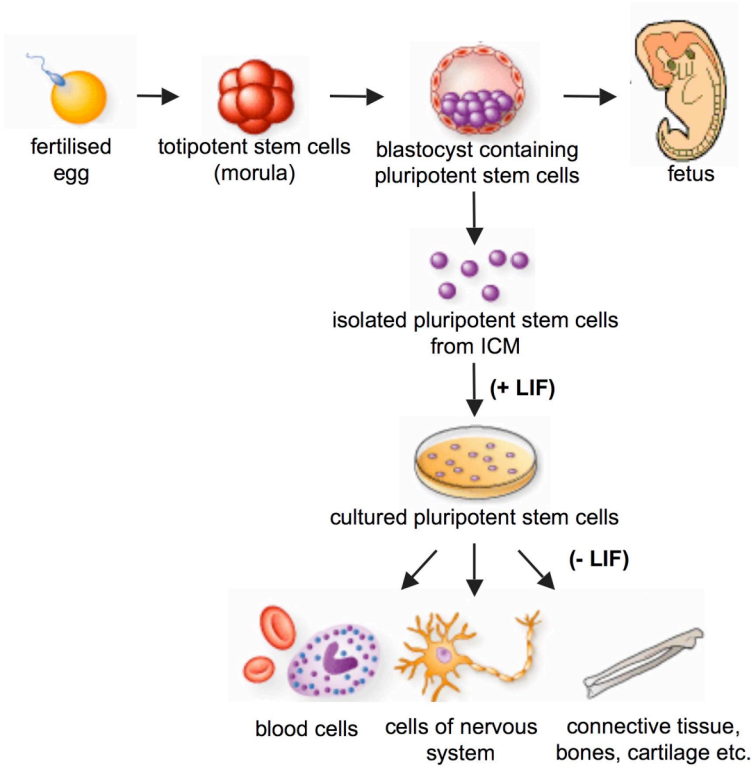

Figure 1: Isolation, cultivation and differentiation of mouse embryonic stem cells. During early embryonic development, the fertilized, totipotent oocyte develops via the morula and blastocyst stages into the fetus. During the early blastomere stages all cells are totipotent, while the blastocyst contains pluripotent cells (the inner cell mass - ICM) and surrounding trophectoderm. Pluripotent embryonic stem cells are isolated from the ICM of a blastocyst. Under addition of leukemia inhibitory factor (LIF), mouse ES cells can be cultured *in vitro* unlimited without loosing their self-renewal properties. In the absence of LIF, they can differentiate into specific cell types like blood cells, nerve cells etc. (Figure was obtained and modified from http://www.biokurs.de/skripten/bs11-76.htm)

1.1.1 Self-renewal of mouse embryonic stem cells

Self-renewal describes the capacity of ES cells to divide without differentiation, so that they remain pluripotent. A variety of pathways are involved in this process. One important factor for the maintenance of pluripotency of mouse ES cell lines *in vitro* is the leukemia inhibitory factor (LIF), which belongs to the interleukin-6 cytokine family. LIF

signals through a heterodimeric receptor complex, consisting of gp130 and LIF receptor (LIFR). By binding of LIF, this complex activates associated JAK kinases (Janus associated tyrosine kinases), which phosphorylate gp130 and LIFR on tyrosine residues. This in turn leads to recruitment and tyrosine phosphorylation of STATs (signal transducer and activator of transcription), predominantly STAT3, by JAKs. Phosphorylation leads to dimerization and translocation of STAT3 dimers into the nucleus, where they control transcription of genes regulating self-renewal. STAT3 activation is essential and sufficient to maintain pluripotency (Matsuda et al., 1999; Niwa et al., 1998). Recently, c-Myc has been identified as one of the major targets of STAT3, involved in self-renewal. Sustained c-Myc activity could maintain ES cell self-renewal in the absence of LIF, while overexpression of a dominant negative mutant promoted differentiation (Cartwright et al., 2005).

Additionally to STAT3, LIF induces other signaling proteins including PI3K (phosphoinositide 3-kinase), Src family tyrosine kinases, and ERKs (extracellular signal-regulated kinases) via the MAPK (mitogen-activated protein kinase) pathway (Anneren et al., 2004; Burdon et al., 1999). Src and PI3K activation have been reported to support self-renewal. Inhibition of PI3K with specific inhibitors led to a differentiated morphology and reduced basal and LIF-stimulated phosphorylation of protein kinase B (PKB or Akt), glycogen synthase 3 (GSK-3) α/β and ribosomal S6 proteins and elevated LIF induced ERK activity (Paling et al., 2004). Furthermore, a myristoylated, active form of Akt maintained the undifferentiated phenotype of mouse ES cells without the addition of LIF. This was independent of the Wnt/β-catenin pathway, supporting the role for PI3K/Akt signaling in self-renewal (Watanabe et al., 2006). In contrast, activation of ERKs leads to differentiation. Apparently, the balance between LIF induced STAT3 plus the other pro self-renewal pathways and ERK signaling is important for the decision of self-renewal versus differentiation (Burdon et al., 2002). SOCS3 (suppressor of cytokine signaling) is also involved in the regulation of self-renewal. Its expression is stimulated by LIF. Overexpression of SOCS3 inhibits the JAK/STAT pathway, thereby regulating LIF signaling in a negative feedback loop. Low expression amounts instead attenuate Shp2-dependent MAPK signaling (Duval et al., 2000; Schmitz et al., 2000).

For efficient self-renewal, LIF signaling needs to collaborate with other factors usually present in the serum added to the culture medium. For example, bone morphogenetic factors (Bmps) have been shown to work in collaboration with LIF. Bmp2 and Bmp4 promote self-renewal in the presence of LIF via upregulation of Ids (inhibitors of

differentiation), which suppress genes involved in neuronal development, and via inhibition the p38 and ERK MAP-Kinase activities (Qi et al., 2004; Ying et al., 2003). Moreover, a range of transcription factors, the most intensively studied being Nanog, Sox2 and Oct4, play an important function (Chambers et al., 2003; Mitsui et al., 2003; Pesce and Scholer, 2001). They seem to build a self-organizing network that prevents differentiation and promotes self-renewal and might also be involved in epigenetic processes, which are important for pluripotency (Niwa, 2007).

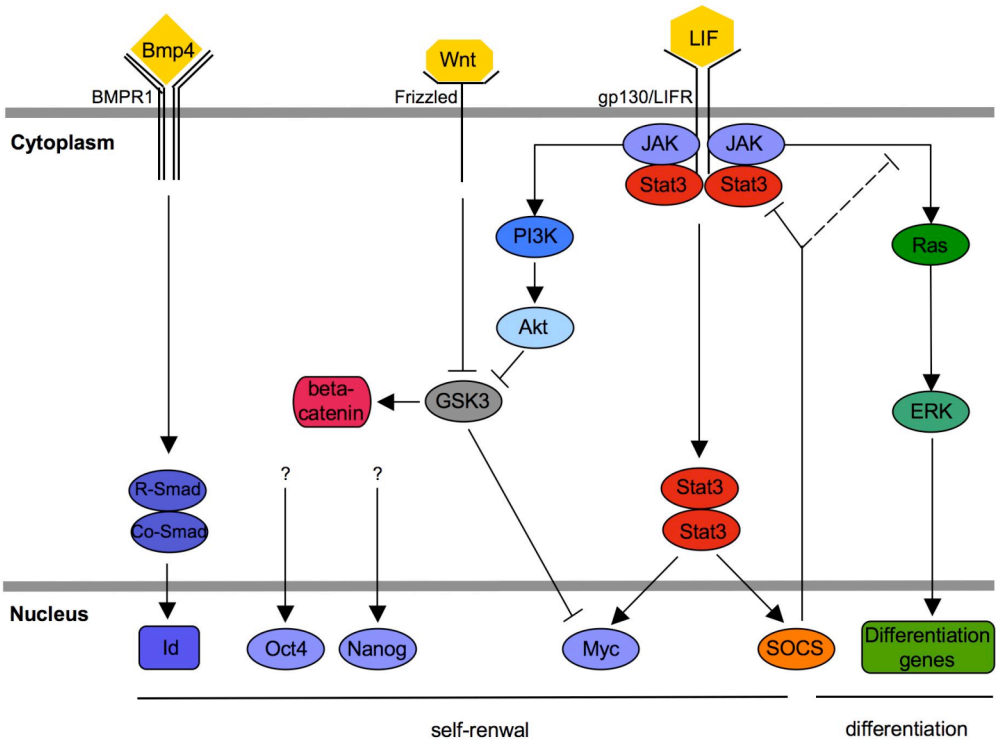

Figure 2: Schematic model of the main pathways involved in self-renewal of mouse embryonic stem cells. A detailed description is given in chapter 1.2.1.

The canonical Wnt pathway seems to have a major function in self-renewal of mouse and of human ES cells, where LIF signaling does not play a role. Wnt factors act through their receptors called Frizzled, leading to stabilization of β-catenin via blocking of glycogen synthase kinase-3β (GSK-3β). Activation of the Wnt signaling by BIO, a pharmacological inhibitor of GSK-3, maintained an undifferentiated phenotype in mouse and human ES cells and sustained the expression of transcription factors like Oct4 and Nanog, involved in the maintenance of pluripotency (Sato et al., 2004). Recently, it has been shown that activation of the Wnt pathway also upregulates the mRNA of STAT3, suggesting a synergistic effect with LIF signaling (Hao et al., 2006). Moreover, as Wnt

signaling has been reported to activate transcription of c-Myc in certain cell-types and c-Myc has been shown to be a target of STAT3, it was supposed that LIF- and Wnt signaling may converge on c-Myc as a common target to promote self-renewal (Cartwright et al., 2005). Recent data suggest though that in human ES cells sustained activation of c-Myc rather leads to apoptosis and differentiation (Sumi et al., 2007).

High telomerase activity is another feature of ES cells, which is related to self-renewal and indefinite replication. Telomerase is a ribonucleoprotein that is involved in maintaining telomere length by adding telomere repeats to the chromosome ends. This plays an important role in chromosome integrity and replicative lifespan (Armstrong et al., 2000; Thomson et al., 1998). Interestingly, the promoter of the catalytic subunit of telomerase (TERT) contains c-Myc binding sites, further approving a role for c-Myc in self-renewal.

In addition, the high proliferation rate and the specific features of the cell cycle of ES cells (see 1.3.2) are also presumed to be involved in the maintenance of pluripotency (Burdon et al., 2002; Niwa, 2007). Interestingly, pathways like PI3K signaling show an overlapping function for both processes.

Finally, the chromatin state and epigenetic modifications play an important role in ES cell pluripotency in determining gene activity. The chromatin of ES cells is different from somatic cells, including nuclear architecture, chromatin structure and dynamics, and histone modifications. The chromatin of ES cells displays for instance characteristics of loosely euchromatin, such as an abundance of acetylated histone modifications (Boyer et al., 2006; Meshorer and Misteli, 2006).

Interestingly, recent data indicate that somatic cells can be reprogrammed *in vitro* into a pluripotent, ES cell-like state (Takahashi and Yamanaka, 2006; Wernig et al., 2007). Reprogramming of fibroblast could be induced by ectopic expression of the transcription factors Oct4, Sox2, c-Myc and Klf4. DNA methylation, gene expression and chromatin state of the induced, reprogrammed cells was similar to those of ES cells (Wernig et al., 2007).

1.1.2 Differentiation of mouse embryonic stem cells

When cultured without addition of LIF, ES cells differentiate spontaneously. On non-adhesive substrates they form spheroid cell aggregates, termed embryoid bodies (EBs) because of their resemblance to post-implantation embryos (Doetschman et al., 1985;

Leahy et al., 1999). The differentiation processes within EBs strongly resemble the processes taking place in a post-implantation embryo, leading to differentiation via derivatives of the three germlayers of ecto-, endo-, and mesoderm into more mature progenitors and committed cell types like cardiomyocytes, endothelial cells, neuronal cells and others. Although multiple cell types form within the EBs, the differentiation appears to be largely unpatterned compared to the precise organization within the early embryo (O'Shea, 2004).

In principle, ES cells are also able to differentiate as a monolayer, but the three-dimensional structure of EBs has the advantage to enhance cell-cell interactions, which may be required for certain developmental programs (Keller, 2005). To favor differentiation of distinct lineages, a variety of different protocols with specific supplements have been established that allow differentiation into almost any cell type. Moreover, ES cells are relatively easily amenable to genetic alterations. Thus, in vitro differentiation of ES cells via EB formation provides a tool to study certain aspects of mouse embryogenesis more rapidly and without the generation of knockout mice.

In the pluripotent state, ES cells show rapid proliferation rates due to unusual cell cycle properties with short gap phases and with most cells being in the S-phase (see chapter 1.3.2). When ES cells start to differentiate, the G1-phase becomes longer and proliferation slows down (White et al., 2005). This goes along with changes in the cell cycle machinery, which is adapting to the “normal” state, known from mature cells.

1.2 Proliferation and cell cycle

Cell proliferation requires a tight coordination between cell growth and cell division to prevent cells from premature division and loss of size (Polymenis and Schmidt, 1999; Thomas, 2000). Coordination of these processes takes place primarily during the cell cycle, which the cells pass during their proliferative stage. The cell cycle can be divided into four different phases. The G1- (gap1) phase is characterized by high biosynthesis and cell growth, during the S- (synthesis) phase DNA replication takes place, in G2- (gap2) phase the cell continues to grow and gets ready for mitosis and during the M- (mitosis) phase the cell divides, leading to transmission of the genetic information from one cell-generation to the next. Transition of cells through the cell cycle is driven by subsequent activation of distinct cyclin-dependent kinases (Cdks). The activity of Cdks is regulated via binding of cyclins and by their phosphorylation state. Each cell cycle

phase is characterized by the expression of distinct cyclins, which in turn activate the respective Cdks (Obaya and Sedivy, 2002). An overview about the cyclin/Cdk complexes, which are active during the different cell cycle phases, is given in table 1. Several checkpoints during the cell cycle (G1-, G2- and M-checkpoint) assure coordination and completion of the processes important to each phase. One important checkpoint, regulating the coordination between cell growth and cell division in mature, mammalian cells, is the G1- or G1/S-phase checkpoint.

Cell cycle phase	Cyclins	Respective Cdks
G1-phase	cyclin D1, D2, D3	Cdk4, 6
G1/S-phase	cyclin E	Cdk2
S-phase	cyclin A	Cdk2
G2-phase	cyclin A	Cdk1
M-phase	cyclin B	Cdk1

Table 1: Overview about the cyclin/Cdk complexes, which are active during distinct cell cycle phases in mammalian cells.

1.2.1 Cell cycle and G1/S-phase checkpoint of mature cells

During early G1-phase the decision is made whether a cell will proliferate and activate the cell cycle or whether it will exit the cycle and go into a quiescent state, the G0-phase. To enter the cell cycle, the availability of mitogenic stimuli from the environment is essential and the cell has to pass the restriction point to be able to enter S-phase.
Mitogenic signaling in early G1-phase usually leads - depending on the cell type - to activation of the MAPK pathway and c-Myc and finally to expression of D-type cyclins (D1, D2, D3) and Cdk4 and Cdk6 (Aktas et al., 1997; Bouchard et al., 1999; Ekholm and Reed, 2000; Lavoie et al., 1996; Perez-Roger et al., 1999). Subsequent association of cyclin D with Cdk4 and Cdk6 leads to phosphorylation and activation of the Cdks, which in turn phosphorylate the retinoblastoma protein (Rb) (Bates et al., 1994; Kato et al., 1993). Rb can be called the gatekeeper of cell cycle. It belongs, together with its relatives p107 and p130, to the so called pocket proteins, whose functions show partial redundancy. Their phosphorylation state plays an essential role for the transition from G1- to S-phase by sequestering the E2F family of transcription factors, which are required for the expression of S-phase entry genes. Hypo-phosphorylated Rb blocks

E2F and therefore S-phase entry in quiescent cells and early G1-phase. During G1-phase Rb is partially phosphorylated by cyclinD/Cdk4 and cyclinD/Cdk6 complexes, which leads to a partial release of E2F, sufficient to activate transcription of its target genes cyclin E and cdc25a. The phosphatase cdc25a removes inhibitory phosphates from Cdk2 and the resulting cyclinE/Cdk2 complex then completes Rb phosphorylation, leading to full release of E2F, expression of its target genes and therefore entry into S-phase (Harbour and Dean, 2000; Helin et al., 1993; Weinberg, 1995). In parallel, the cyclinE/Cdk2 complex is involved in S-phase progression by regulation of factors involved in DNA replication like histone biosynthesis (Zhao et al., 2000). The point where Cdk2 is elevating its own activity in a positive feedback loop via Rb is called the restriction point. At this “stage of no return” the cell has to fully complete the cycle, independent of mitogenic signals (Blagosklonny and Pardee, 2002). In parallel to the Rb/E2F pathway, c-Myc also has a function in passing the restriction point by regulating the expression of cyclinE and cdc25a (Bartek and Lukas, 2001; Santoni-Rugiu et al., 2000).

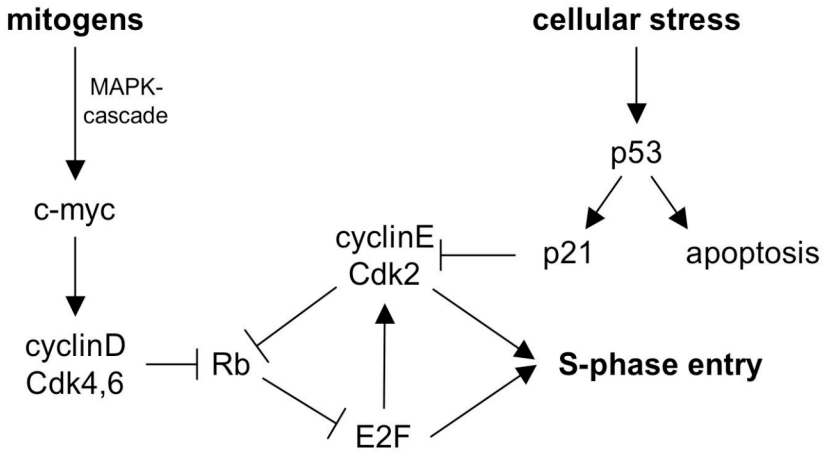

Figure 3: Schematic model of the G1/S-phase checkpoint in mature mammalian cells. Rb is called the gatekeeper of the cell cycle. In the active (hypo-phosphorylated) state Rb blocks the transition of cells from G1-phase into S-phase by binding the E2F family of transcription factors, which are essential for S-phase entry. In case of mitogenic stimulation cyclinD/Cdk4 and cyclinD/Cdk6 complexes are activated, which leads to partial phosphorylation of Rb and thus to partial release of E2F and transcription of their target genes, one of which is cyclin E. This leads to activation of cyclinE/Cdk2 complexes, which further phosphorylate and inactivate Rb, leading to full release of E2F transcription factors, transcription of their target genes and entry into S-phase. On the other hand, cellular stress can inhibit transition of cells into S-phase by blocking cyclinE/Cdk2 activity via the Cdk-inhibitor p21, which is regulated by the tumor suppressor p53. Alternatively, p53 can induce apoptosis.

In contrast to mitogenic signals, which lead to S-phase entry and proliferation, cellular stresses are involved negatively in the regulation of G1/S-phase transition. Cellular stress like DNA damage usually leads to induction of the tumor suppressor p53, which activates expression of the Cdk-inhibitor p21, which in turn targets Cdk2 and Cdk4/6 (Harper et al., 1995; Vogelstein et al., 2000). Inhibition of the kinase activities prevents phosphorylation of Rb and therefore arrests the cells in G1-phase. In addition to a G1-arrest, p53 can also mediate apoptosis. The decision between the two processes is dependent on the overall condition of the cell, e.g., extreme DNA damage, which cannot be repaired during a prolonged G1-phase, would favor the apoptotic pathway.
In addition to p21, other CDK inhibitors can regulate cell cycle progression. Two main families are known. The Cip/Kip family includes $p21^{WAF1/CIP1}$, $p27^{KIP1}$ and $p57^{KIP2}$, which inhibit mainly cyclin E- and cyclin A-dependent Cdk2 activities. The INK4 family includes $p16^{INK4a}$, $p15^{INK4b}$, $p18^{INK4c}$ and $p19^{ARF/INK4d}$, which inhibit the catalytic subunits of Cdk4 and Cdk6. $p19^{ARF/INK4d}$ is involved in the regulation of the tumor suppressor p53 by binding to Mdm2, thereby blocking p53 degradation (Sherr and Roberts, 1999).

1.2.2 Cell cycle of mouse embryonic stem cells

Compared to mature cells, where cell cycle progression and proliferation relies on the balance between mitogenic signals and growth inhibitory signals, cell cycle progression of ES cells seems to rely more on intrinsic factors.
One of the most striking difference between the cell cycle of ES cells and mature cells is that the control mechanisms for the G1/S-phase checkpoint are strongly reduced or absent in mouse ES cells. This goes in line with the majority of cells being in S-phase and a very short G1-phase of roughly 1.5 hours, which can explain the high proliferation potential (Savatier et al., 1994). Doubling time of mouse ES cell lines has been described to be around 10-15 hours. Although the pocket proteins Rb and p107 are expressed in ES cells, they are present almost exclusively in the inactive, hyper-phosphorylated form and cyclinE/Cdk2 and cyclinA/Cdk2 kinase complexes seem to be constitutively active throughout the cycle, suggesting that the cell cycle is constitutively primed for S-phase entry and DNA replication (Savatier et al., 1994; Stead et al., 2002; White et al., 2005). In addition to cyclinE/Cdk2, which was supposed to be the main player in Rb phosphorylation, recently cyclinD3/Cdk6 complexes were shown to be robustly involved in the phosphorylation of Rb (Faast et al., 2004). Instead,

cyclinD/Cdk4 kinase activity is almost undetectable and seems to be dispensable for phosphorylation and inactivation of Rb. Despite the active cyclinD/Cdk6 complex, ES cells do not respond with growth arrest to overexpression of the inhibitor p16, usually targeting cyclinD/Cdk4/6 complexes (Faast et al., 2004; Savatier et al., 1996). Generally, the Cdk inhibitors p16, p21 and p27 are absent in ES cells (Fujii-Yamamoto et al., 2005; Savatier et al., 1996; Stead et al., 2002). Moreover, cell cycle progression of mouse ES cells is independent of persistent serum stimulation and of the Ras/ERK pathway (Jirmanova et al., 2002; Schratt et al., 2001).

Instead, PI3K-dependent signaling plays an important function for the progression of mouse ES cells through G1-phase as well as for inhibition of differentiation (Jirmanova et al., 2002; Paling et al., 2004). Inhibition of PI3K activity by the inhibitor LY294002 led to an accumulation of cells in G1-phase and deletion of Pten, a negative regulator of PI3K, increased proliferation and viability of mouse ES cells (Sun et al., 1999). PI3K activity is also independent of serum stimulation, but relies on LIF stimulation. In addition, a stem cell specific member of the Ras family, termed Eras, which is constitutively active, has been shown to activate PI3K signaling (Takahashi et al., 2003a). Eras-null cells show impaired proliferation as well as reduced tumorigenicity when introduced into somatic tissues. As Eras cannot bind Raf it does not stimulate the MAPK pathway. Furthermore, the protein Tcl1 can increase the activity of Akt by forming a complex with the latter. Tcl1 could be linked to proliferation and self-renewal (Ivanova et al., 2006; Matoba et al., 2006).

Interestingly, the G1/S-phase checkpoint seems to be also impaired after stress. At least DNA damage after irradiation seems not to induce a G1-arrest, although abundant quantities of p53 are synthesized (Aladjem et al., 1998; Hong and Stambrook, 2004). Instead, cells accumulated in S- and G2/M-phase and showed elevated apoptosis. An induced G1-arrest by overexpression of Chk2 kinase, whose function was shown to be impaired in ES cells, could protect ES cells from apoptosis. This indicates that the lack of a G1-checkpoint after DNA damage may favor apoptosis, thereby ensuring genome integrity of the ES cell population (Hong et al., 2007). Moreover, no elevated p21 levels were detected probably due to predominantly cytoplasmic localization of p53. Data with p53 deficient cells indicate a transient, p53-independent arrest in S-phase after UV treatment (Prost et al., 1998) and also p53-independent apoptosis was reported (Aladjem et al., 1998)

1.3 Nucleolus and cell cycle control

The nucleolus, a specialized compartment within the nucleus, is another important factor for regulation of cell proliferation. As the site of ribosome biogenesis, the nucleolus has long been known to be involved in the translation capacity of a cell and therefore in cell growth. More recently, it has been revealed that the nucleolus is also directly involved in cell cycle progression. In fact, it can be considered as a major link between cell growth and cell division (see chapter 1.4.2).

1.3.1 Ribosome biogenesis in mammalian cells

Ribosome biogenesis is a highly complex, well-coordinated, evolutionary conserved process that takes place in the nucleoli (Fromont-Racine et al., 2003). Ribosomes of mammalian cells consist of a large 60S subunit and a smaller 40S subunit, which are comprised of RNA and ribosomal proteins. During ribosome synthesis, the tandem-like repeats of rDNA, present within the nucleolus, are transcribed by RNA Polymerase I (Pol I) into a large precursor ribosomal RNA (47S pre-rRNA). This polycistronic precursor contains the mature 18S, 5.8S and 28S rRNAs interspersed with the non-coding internal transcribed sequences ITS1 and ITS2 and is flanked 5' and 3' by external transcribed spacers (ETS). The 18S rRNA will be the rRNA component of the 40S subunit, while the 5.8S and 28S rRNAs will constitute the RNA component of the 60S subunit, together with the 5S RNA, which is transcribed independently by RNA Polymerase III (Pol III). In addition, up to 80 ribosomal proteins have been identified so far that assemble together with the rRNAs to form the mature ribosomes (Eichler and Craig, 1994; Fatica and Tollervey, 2002; Warner, 1999). After transcription, the large precursor rRNA is rapidly assembled with ribosomal proteins, nonribosomal proteins and small nucleolar RNAs (snoRNAs) into a 90S pre-ribonucleoprotein particle (90S pre-RNP), followed by massive modification of the precursor rRNA by pseudouridylation and methylation. For further maturation, the primary transcript is processed via exo- and endonucleolytic ribonucleases to the mature rRNAs (Eichler and Craig, 1994; Venema and Tollervey, 1999). After cleavage within the ITS1, the 90S precursor splits into the pre-40S and pre-60S particles, which further mature into the 40S and 60S subunits. In yeast, where ribosome biogenesis is better understood than in mammals, over 150 nonribosomal proteins and about the same amount of snoRNAs have been revealed to

be part of these precursor rRNPs and are putatively involved in ribosome biogenesis (Fatica and Tollervey, 2002; Fromont-Racine et al., 2003; Tschochner and Hurt, 2003). In higher eukaryotes, much less is known about the ribosome synthesis machinery. But proteomic analyses of the human nucleolus in the recent years suggest that many of the components have been evolutionary conserved (Andersen et al., 2002; Leung et al., 2006; Scherl et al., 2002; Takahashi et al., 2003b). The general steps involved in the processing of rRNAs in vertebrates are comparable to those in yeast, however, as the ETS and ITS sequences diverge greatly between different eukaryotes, the endo- and exonucleolytic cleavage of the precursor rRNA can vary according to the species, cell type or physiological state (Eichler and Craig, 1994; Hadjiolova et al., 1993). In general, the processing events occur from the 5' to the 3' of the nascent transcript (Strezoska et al., 2000).
Processing of the preribosomal transcripts into the mature rRNAs and assembly of the rRNPs mainly takes place inside the different regions of the nucleolus and later steps in the nucleus. Only addition of the last ribosomal proteins, a final processing step of the 18S rRNA and the final assembly of the two subunits is completed in the cytoplasm, where the mature ribosomes then fulfill their function of mRNA translation (Rouquette et al., 2005).

Ribosome biogenesis places a major energy and biosynthetic demand upon cells, accounting for up to 80% of the energy consumption of a proliferating cell (Thomas, 2000; Warner, 1999). Therefore, it requires precise regulation and coordination with cell cycle progression. In fact, ribosome biogenesis is cell cycle controlled. It is sensitive to nutrient and growth factor signaling and inhibited upon stress signals (Mayer et al., 2005; Mayer and Grummt, 2005; Mayer et al., 2004; Sirri et al., 2002; Voit et al., 1999). On the other hand, proper ribosome biogenesis is essential to keep p53 levels down and thereby ensure proliferation (see chapter 1.4.2). In this light it is not surprising that deregulation of ribosome biogenesis plays a role in cancer (Ruggero and Pandolfi, 2003).

1.3.2 Link of nucleolar disruptions and cell cycle progression

The view of the nucleolus as a mere ribosome producing factory has recently been challenged as it became obvious that it is involved in many more processes than just

ribosome synthesis (Olson et al., 2000). For example, it has been suggested that the nucleolus is involved in the maturation of other ribonucleoprotein particles like the signal recognition particle and telomerase (Mitchell et al., 1999; Politz et al., 2000). In addition, the nucleolus can participate in export or processing of some mRNAs and tRNAs (Bertrand et al., 1998; Schneiter et al., 1995). Most intriguingly, a function of the nucleolus in cell cycle regulation via the tumor suppressor p53 has been described (Olson, 2004; Rubbi and Milner, 2003). p53 is a key regulator of the cell cycle that activates cell cycle arrest and apoptosis during cellular stress. During normal growth, p53 is targeted for degradation by Mdm2, an E3 ubiquitin ligase, and exported to the cytoplasm where it is degraded by the proteasome. Additionally, Mdm2 can bind p53, thereby repressing its transcriptional activity in the nucleus (Haupt et al., 1997; Kubbutat et al., 1997; Oliner et al., 1993). This keeps p53 levels low and cells proliferate.
On the other hand, disturbances in ribosome biogenesis, which is highly sensitive to a lot of cellular stresses, have been shown to lead to an induction of p53, which triggers cell cycle arrest or apoptosis. Several mechanisms have been proposed about how this induction of p53 is mediated. First, impaired ribosome biogenesis can decrease the demand of ribosomal proteins and can therefore lead to accumulation of free ribosomal proteins such as L5, L11 or L23, which can bind and inactivate Mdm2 resulting in stabilization and accumulation of p53 (Dai and Lu, 2004; Dai et al., 2004; Jin et al., 2004; Lohrum et al., 2003; Zhang et al., 2003). Another hypothesis takes into account that cytoplasmic p53 has been detected covalently linked to the 5.8S rRNA of a subset of ribosomes, suggesting that the export of p53 into the cytoplasm may depend on the export of intact ribosomal subunits (Fontoura et al., 1997; Sherr and Weber, 2000).

The model of a crosstalk between ribosome biogenesis and cell cycle via p53 has been expanded by Rubbi and Milner. They propose that p53 induction after different cellular stresses is generally coupled to disruptions within the nucleolus (Rubbi and Milner, 2003). They could demonstrate by micropore UV irradiation that DNA damage only leads to a p53 response, if the nucleolar structure is also affected. In addition, they linked a range of different agents inducing p53 stabilization to disruptions in the nucleolus, including DNA damaging agents, anticancer drugs, inhibitors of RNA synthesis and general stress signals like hypoxia or heat shock. These findings suggest that the nucleolus might function as a universal stress sensor, the disruption of which leads to a rapid p53-mediated checkpoint response, regulating cell cycle progression.

The direct crosstalk between ribosome biogenesis and cell cycle by activation of a critical checkpoint is one possibility for a cell to coordinate division with growth. Another possibility is to measure the translation capacity of a cell. Such mechanisms are known in yeast and drosophila (Polymenis and Schmidt, 1997; Polymenis and Schmidt, 1999; Thomas, 2000). In yeast, cell size is a critical parameter for the cell to pass the restriction point (start). To do so, the cells need a sufficient amount of the G1-Cyclin Cln3. As the Cln3 mRNA contains a second ORF, upstream of the Cln3 ORF, ribosomes bind with less efficiency to the Cln3 ORF. To reach an efficient translation of Cln3 mRNA, the cell has to grow first and produce enough ribosomes to translate also the Cln3 ORF with high efficiency to produce enough protein to finally pass the restriction point. So the translation efficiency of Cln3 is used as a reference for cell cycle regulation (Polymenis and Schmidt, 1997).

In ES cells, not much is known so far about the mechanisms correlating cell growth with cell division. ES cells show novel regulatory pathways for proliferation, lack the normal G1/S-phase checkpoint and have probably an impaired p53 pathway (see chapter 1.3.2). First experimental evidence that the nucleolus and ribosome synthesis are also involved in the regulation of stem cell proliferation is given by studies with the nucleolar protein Nucleostemin, a putative GTPase involved in p53 regulation. Depletion or overexpression of Nucleostemin reduced the proliferation rate of neuronal stem cells and of mutant blastocysts (Beekman et al., 2006; Tsai and McKay, 2002). Moreover, depletion of Bysl (bystin-like) a protein involved in maturation of the small ribosomal subunit showed impaired proliferation of embryonic stem cells (Adachi et al., 2007). Nevertheless, little is known about the underlying mechanisms coordinating the two processes.

1.4 The PeBoW-complex

The PeBoW-complex is one factor involved in the p53-mediated checkpoint response between nucleolus and cell cycle in mature cell systems. It has recently been characterized in mammalian cell lines and consists of the proteins Pes1 (pescadillo) Bop1 (block of proliferation) and WDR12 (WD-repeat protein) (Holzel et al., 2005; Rohrmoser et al., 2007). The PeBoW-complex is located within the nucleoli and it is involved in ribosome biogenesis, namely in the maturation of the large 60S ribosomal

subunit. Knockdowns of its components Pes1, Bop1 or WDR12, by expression of dominant negative mutants or siRNA technology, block processing of the 36/32S precursor rRNA into the mature 28S rRNA and 5.8S rRNA and subsequently the maturation of the large ribosomal subunit. Maturation of the small subunit is not affected (Grimm et al., 2006; Holzel et al., 2005; Strezoska et al., 2000; Strezoska et al., 2002). In addition, an induction of p53 could be examined, followed by a strong cell cycle arrest in G1-phase and an impaired proliferation rate (Grimm et al., 2006; Holzel et al., 2005; Pestov et al., 2001). All three proteins are upregulated by the transcription factor and proto-oncogene c-Myc and incorporation of the single proteins into the PeBoW-complex as well as nucleolar localization seem to be prerequisites for their function ((Grimm et al., 2006; Holzel et al., 2005; Lapik et al., 2004; Rohrmoser et al., 2007).

The structure and function of the PeBoW-complex appears to be conserved throughout evolution. In yeast, a potential homolog of the PeBoW-complex has been identified, which is similarly involved in ribosome biogenesis and cell cycle progression. It consists of the proteins Nop7 (or Yph1), Erb1 and Ytm1, whose homology with the mammalian Pes1, Bop1 and WDR12 averages more than 40% (Du and Stillman, 2002; Miles et al., 2005; Oeffinger et al., 2002). Similar to mammalian cells, depletion of the proteins leads to impaired maturation of the large ribosomal subunit (Miles et al., 2005).

In addition to its role in ribosome biogenesis, the PeBoW-complex has been linked to other processes. In yeast, all three proteins have been identified as part of a bigger complex. Besides 66S ribosomal proteins and preribosomal particle proteins, this complex contained ORC and MCM proteins as well as checkpoint- and cell cycle regulatory proteins, indicating a role in replication and cell cycle control. For Nop7, the yeast homolog of Pes1, a direct involvement in replication could be proven, as its depletion led to an arrest of cells in G1- or G2-phase with no cells in S-phase. This effect was independent of impaired ribosome biogenesis (Du and Stillman, 2002).

Moreover, the PeBoW-complex was linked to a function in mitosis as inactivation of Pes1 and Bop1 in human cell lines leads to abnormal mitoses with altered chromosomal segregation followed by chromosomal instability (CIN) (Killian et al., 2004). As CIN is a hallmark of many tumors, this might indicate a role of the PeBoW-complex in tumorigenesis and indeed increased expression of Bop1 could be detected frequently in colorectal cancers. Furthermore, overexpression of Bop1 increased the percentage of multipolar spindles (Killian et al., 2006). Interestingly, overexpression of Pes1 was reported to be involved in the transformation, but not immortalization, of mouse and human fibroblasts as shown by colony formation in soft agar (Maiorana et

al., 2004). Also, malignant human astrocytomas showed dramatically elevated levels of Pes1, strengthening its role for oncogenic transformation and tumor progression.
Evidence for a function of the proteins during embryogenesis is given by Pes1, which was first identified as *pescadillo* in the zebrafish, where it has an essential function for normal embryonic development (Allende et al., 1996). Lerch-Gaggl et al. report a similar effect in the mouse. Pes1-depleted embryos arrest at the morula stage of development, fail to develop nucleoli and do not accumulate ribosomes (Lerch-Gaggl et al., 2002).

1.4.1 Pes1

A single gene located on chromosome 11 in the mouse genome encodes for murine Pes1, a protein of 584 amino acids and a theoretical size of 67.8 kDa, which is highly evolutionary conserved and shows a homology of 89% to human Pes1 (Haque et al., 2000). The protein contains a highly conserved N-terminal pescadillo-like protein domain (NPLP-domain), a BRCT (BRCA1 C-terminal) domain in the middle of the protein and three nuclear localization sites (NLS). In addition, the C-terminus of Pes1 contains two acidic stretches of amino acids, six bipartite NLS, plus a consensus site for SUMOylation (KΨXE) (Grimm et al., 2006; Haque et al., 2000; Holzel et al., 2007; Kinoshita et al., 2001). C- and N-terminal truncation mutants plus several transposon-derived mutants of Pes1 displayed a dominant negative phenotype, blocking the processing of 36/32S rRNA into mature 28S and 5.8S rRNA and inhibited cell proliferation via a p53-mediated mechanism (Grimm et al., 2006; Lapik et al., 2004). Further, the BRCT domain of Pes1 has been elucidated to be crucial for its nucleolar localization and its function in rRNA processing. BRCT domains facilitate protein-protein interactions and are often found in factors, involved in DNA repair pathways (Holzel et al., 2007).

1.4.2 Bop1

Bop1 (block of proliferation) is an evolutionary conserved gene that encodes a protein of 732 amino acids with a molecular weight of 83 kDa in the mouse. Bop1 contains seven WD40 repeats, which are often involved in the formation of multiprotein complexes as well as two PEST sequences, one at the N-terminus and one in the

middle of the protein. PEST sequences are often associated with short-lived regulatory proteins, indicating a regulatory function for Bop1 (Strezoska et al., 2000; Strezoska et al., 2002). Deletion mutagenesis revealed two dominant negative mutants with an N- or C-terminal deletion, whose phenotype involved a reversible block of proliferation by a G1-arrest and an inhibition of pre-rRNA processing. In mouse cells, the processing of the 36S and 32S rRNA was inhibited, leading to impaired maturation of the 28S and 5.8S rRNA (Pestov et al., 2001; Strezoska et al., 2002).

1.4.3 WDR12

Wdr12 corresponds to a single-copy gene in the mouse genome on chromosome 1, encoding a protein of 423 amino acids with a theoretical molecular weight of 47.3 kDa. The WDR12 (WD repeat) protein contains seven WD40 units and a nuclear localization signal located between the WD domains three and four. At its N-terminus it contains a Notchless-like domain (Nle). It is supposed that the 7 WD40 repeats form a "β-propeller" structure, likewise it has been extensively analyzed in the β-subunits of heterotrimeric G-proteins. Like most WD repeat proteins, WDR12 shows no enzymatic activity, but the propeller structure of the WD40 repeats could play a role for protein-protein interactions. Generally, WD repeat proteins are viewed as regulatory components within higher order complexes, which matches the participation of human WDR12 into the PeBoW-complex (Holzel et al., 2005; Nal et al., 2002).
Deletion of the Nle domain of WDR12 has been shown to induce a dominant negative phenotype. Expression of the mutant in human cells impairs the maturation of 28S rRNA and induces a reversible arrest in G1-phase (Holzel et al., 2005).

1.5 Aim of the project

Cell proliferation is a process where cell growth and cell division have to be tightly coordinated. The nucleolus, as the site of ribosome synthesis, plays an important function in cell growth. Nucleolar disruptions directly signal to the cell cycle machinery and inhibit cell cycle progression. One factor involved in proper nucleolar function is the PeBoW-complex and its single components Pes1, Bop1 and WDR12. The PeBoW-complex has been shown to play a crucial role in ribosome biogenesis as well as cell cycle progression in several cancer cell lines. Knockdowns of its components impair ribosome biogenesis and induce a p53-dependent checkpoint activation, finally leading to a reversible block of proliferation.

Proliferation of embryonic stem (ES) cells is, in comparison to mature cells, very rapid with a quite distinct cell cycle distribution. Their G1-phase is very short and lacks the regulatory mechanisms usually active during G1-phase in other cell types (G1/S-phase checkpoint). ES cells can reenter the S-phase almost directly after mitosis, which is at least one important factor for their rapid proliferation. First evidence for the fact that a proper nucleolar function might be related to proliferation of ES cells comes from studies on Nucleostemin, another nucleolar protein, the knockdown of which leads to impaired proliferation rates of stem cells (Tsai and McKay, 2002).

The goal of this work was to investigate the expression and potential complex formation of the proteins Pes1, Bop1 and WDR12 in mouse ES cells and to assess whether their function in ribosome biogenesis is related to proliferation of ES cells. Based on the different cell cycle kinetics of ES cells, which are missing some of the usual control-points, one main question was to test if inhibition of ribosome biogenesis would be able to activate a p53-dependent checkpoint response in ES cells, as it has been shown in mature cell lines. A knockdown of Pes1, Bop1 and WDR12 via small interfering RNAs served as the major technical feature to investigate the function of those three proteins in ES cells. Furthermore, a possible checkpoint response was investigated by addressing the protein levels of the tumor suppressor p53 and the phosphorylation state of its indirect target Rb (retinoblastoma gene product). As cell system, the germline competent mouse ES cell line CGR8 was used, which can be cultured without the use of feeder cells in the presence of recombinant LIF.

2 MATERIAL

2.1 Cell lines

CGR8	mouse ES cell line obtained from J. Heschelers Lab, Cologne Originally generated from Austin G. Smith, European Collection of Cell Cultures (ECACC) Cat. No. 95011018
NIH3T3	mouse fibroblast cell line

2.2 Media and supplements for cell culture

DMEM (4500mg/ml glucose; contains L-glutamine and pyruvate)	Invitrogen
DMEM (phosphate-free)	Invitrogen
GMEM	Sigma
IMDM	Invitrogen
Optimem1	Invitrogen

Cryoconservation medium for CGR8 cells:
10% DMSO (Roth), 90%FBS (PAA Laboratories)

100 x L-glutamine (200mM)	Invitrogen
100 x MEM (non essential amino acids)	Invitrogen
100x Penicilline/Streptomycine	Invitrogen
FBS	PAA Laboratories
FBS dialysed (phosphate free)	Invitrogen
Gelatine from porcine skin, type A	Sigma
LIF-ESGRO	Chemicon
ß-mercaptoethanol	Sigma
Trypsin/EDTA	Invitrogen

Lipofectamine 2000	Invitrogen
Oligofectamine	Invitrogen
Polyethylenimine	Sigma

2.3 siRNA-oligonucleotides

	sense (5'-3')	antisene (5'-3')
murine Pes1-1 (3' UTR)	CAACGCAGUUCUUAAUCCAtt	UGGAUUAAGAACUGCGUUGtt
murine Pes1-2 (3' UTR)	GCAGUAUGCUUGUCCAAUUtt	AAUUGGACAAGCAUACUGCtt
murine Pes1-3 (ORF 1645)	CUAAGCGCUUGGCCAUCAUtt	AUGAUGGCCAAGCGCUUAGtt
murine Bop1-1 (ORF 768)	GAAGGUGUCUCGAAUGGUAtt	UACCAUUCGAGACACCUUCtt
murine Bop1-2 (ORF 1350)	GAAGACUGUACAUGUUGGAtt	UCCAACAUGUACAGUCUUCtt
murine WDR12-1 (3' UTR)	UGUCCUUCGUGCUUAUAAAtt	UUUAUAAGCACGAAGGACAtt
murine WDR12-2 (3' UTR)	GCAUACAACUAACCUGUAAtt	UUACAGGUUAGUUGUAUGCtt
murine WDR12-3 (5' UTR)	GAUUACGAAUCUAGAUAGAtt	UCUAUCUAGAUUCGUAAUCtt
murine WDR12-4 (3' UTR)	AUCAUAGCACACACUUAUAtt	UAUAAGUGUGUGCUAUGAUtt
control (Luciferase)	UUCUCCGAACGUGUCACGUtt	ACGUGACACGUUCGGAGAAtt

2.4 Antibodies

2.4.1 Primary antibodies

	description	source	WB	IF
α-Pes1	Ab-1; guinea pig polyclonal	Charles River Lab.	1:15000	1:500
	Ab-3; guinea pig polyclonal	Charles River Lab.	1:15000	1:500
α-Bop1	Ab-1; guinea pig polyclonal	Charles River Lab.	1:15000	1:500
	Ab-2; guinea pig polyclonal	Charles River Lab.	1:15000	1:500
	rat monoclonal, clone 1B5	E. Kremmer, GSF	1:10	1:10
	rat monoclonal, clone 5F4	E. Kremmer, GSF	1:10	1:10
	rat monoclonal, clone 8G10	E. Kremmer, GSF	1:10	1:10
	rat monoclonal, clone 1A11	E. Kremmer, GSF	1:10	1:10
α-WDR12	Ab-3; guinea pig polyclonal	Charles River Lab.	1:15000	1:500
	Ab-4; guinea pig polyclonal	Charles River Lab.	1:15000	1:500
	rat monoclonal, clone 6A2	E. Kremmer, GSF	1:10	1:10

α-WDR12	rat monoclonal, clone 6B8	E. Kremmer, GSF	1:10	1:10
	rat monoclonal, clone 8D2	E. Kremmer, GSF	1:10	1:10
α-ß-actin	mouse monoclonal, clone AC-15	Sigma	1:20000	-
α-p21	rabbit polyclonal (C-19)	Santa Cruz	1:1000	-
α-p53	rabbit polyclonal (FL-393)	Santa Cruz	1:500	-
α-p53	mouse monoclonal (PAb 122)	Dianova	-	1:100
α-PARP	rabbit polyclonal (SA-253)	Biomol	1:1000	-
α-Rb	mouse monoclonal, clone G3-245	BD Pharmingen	1:500	-
α-α-tubulin	mouse monoclonal, clone DM1A	Sigma	1:30000	-

2.4.2 Secondary antibodies

α-guinea-pig (HRP), donkey	Dianova	Western blot 1:2500, 1:5000
α-mouse (HRP), goat	Promega	Western blot 1:2500, 1:5000
α-rabbit (HRP), goat	Promega	Western blot 1:2500, 1:5000
α-rat (HRP), goat	Dianova	Western blot 1:2500, 1:5000
α-guinea-pig (Cy3), goat	Dianova	Immunofluorescence 1:300
α-mouse (Cy3), goat	Dianova	Immunofluorescence 1:300
α-rat (Cy3), goat	Dianova	Immunofluorescence 1:300

2.5 Primer

	forward (5'-3')	reverse (5'-3')
Aldolase	GGTCACAGCACTTCGTCGCACAG	TCCTTGACAAGCGAGGCTGTTGGC
Flk1	AGACATTGACATGCACAGTCTACGC	GCTTGGATGACCAGCGTACTTACAG
KLF4	TCCTTTCCTGCCAGACCAGATGC	TGCCCTGTGTGTTTGCGGTAGTG
Nanog	GTTGAAGACTAGCAATGGTCTGATT	GTTGCGTAAGTCTCATATTTCACCT
Oct4	TATTGAGTATTCCCAACGAGAAGAG	GAACAAAATGATGAGTGACAGACAG
Sox2	AAGGGGAGAGATTTTCAAAGAGATA	TCATAAAAGTTTTCTAGTCGGCATC
T-bra	GCTAGATACTAACAACTCCATTTTC	GGTGCTATATATTGCCTTTATTATG

2.6 Markers (protein and DNA)

1kb DNA ladder	Invitrogen
Full range rainbow molecular weight marker	Amersham Biosciences
Pre-stained SDS molecular weight marker	Sigma

2.7 Kits

Alkaline Phosphatase Detection Kit	Chemicon
EndoFree Plasmid Maxi Kit	Qiagen
FITC BrdU Flow Kit	BD Biosciences
LightCycler^{R} FastStart DNA Master SYBR Green I	Roche
QIAprep Spin Miniprep Kit	Qiagen
QIAquick PCR Purification Kit	Qiagen
RNeasy RNA Isolation Kit (Mini/Midi)	Qiagen

2.8 Disposables

Bacteriological plates	Greiner
Cell culture freezing vials	Nunc
Cell culture plastic pipettes (5-, 10-, 25ml)	Costar; Falcon
Cell culture plastic pipettes (50ml)	Falcon
Cell culture plates (6-, 10cm)	Nunc
Cell culture plates (6-, 24-, 48-, 96-well)	Falcon
Cell scraper	Sarstedt
Centrifuge tubes (polypropylene ; 15-, 50ml)	Falcon
Combitips (1ml)	Eppendorf
Cover slips	Menzel-glasses
Eppendorf tubes (1,5-, 2ml)	Eppendorf
FACS (1,4ml U-tube)	Micronic
Filter (PES, 0,2μm)	Nalgene
Filter (for syringe; 0,2μm)	Sartorius
Hyperfilm^{TM} MP (autoradiography film)	GE Healthcare

Hyperfilm^{TM} ECL (chemiluminescence film)	GE Healthcare
LightCycler capillaries	Roche
Nitrocellulose membrane (Hybond ECL)	Amersham Biosciences
Pipette tips	TipOne, Molecular Bio Products
Qiashredder columns	Qiagen
Saran wrap	Toppits
Spectrophotometer plastic cuvettes (UVette)	Eppendorf
μ-slideVI-ibidi	Ibidi
Whatman - blotting paper	Schleicher and Schuell
8-chamber slides	Nunc

2.9 Chemicals, Reagents and Enzymes

Acrylamide/Bisacrylamide (Rotiphorese Gel 30)	Roth
Agarose	Invitrogen
Ammonium peroxide sulfate (APS)	Roth
Annexin V-FITC	BD Biosciences
Bradford	Bio-Rad
Bromphenol blue	Sigma
BSA	Roth
DAPI	Sigma
DEPC	Sigma
DMSO	Roth
dNTPs	Promega
ECL-Western blotting detection reagents	GE-Healthcare
EDTA	Merck
Ethanol	Merck
Ethidiumbromide	Sigma
Formamide	Sigma
Formaldehyde solution 37%	Merck
Gelatine	Sigma
GIEMSA	Merck
Glycerol	Roth
Glycine	Merck

Isopropanol	Merck
LIF-ESGRO	Chemicon
Lipofectamine 2000	Invitrogen
ß-mercaptoethanol	Sigma
Methanol	Merck
Milkpowder	Roth
MLV Reverse transcriptase	Invitrogen
MOPS	Roche
Mounting medium	Dako
Oligonucleotides	Metabion
Oligo(dT)15 Primer	Promega
Oligofectamine	Invitrogen
Paraformaldehyde	Sigma
Polyethylenimine	Sigma
PonceauS	Sigma
^{32} P-orthophosphate	GE Healthcare
Protease inhibitor (complete EDTA free)	Roche
Propidium iodide	Sigma
Restriction enzymes	New England
RNase A	Roche
RNasin ribonuclease inhibitor	Promega
SDS	Roth
TEMED	Roth
Tris	Merck
TritonX-100	Sigma
Trypsin/EDTA	Invitrogen
Trypan blue	Gibco, Invitrogen
Tween-20	Roth

Standard chemicals, which are not mentioned in the list, were obtained from Merck, Sigma or Roth.

3 METHODS

3.1 Cell Culture

3.1.1 Culture conditions of CGR8 cells

CGR8 cells were cultured in GMEM under addition of LIF in an incubator with 37°C, 5% CO_2 and a water saturated atmosphere. Plates were coated with 0.2% gelatine prior to plating of cells. Splitting of cells was performed by trypsinization to detach cells from the plate. First, cells were washed once with 6-10ml PBS (10cm-plate), then 2ml of 1 x Trypsin-EDTA were added and cells were incubated at 37°C for 5 minutes. The enzymatic reaction was stopped by addition of 8ml culture medium. Between 0.5-2ml of the suspension were seeded to a new gelatine-coated 10cm plate containing 10ml of fresh medium.
Alternatively, the cell suspension was centrifuged at 1000rpm for 5 minutes. After removal of the supernatant the pellet was resuspended in fresh medium or used for other assays.

GMEM: 445ml GMEM; 50ml FBS; 5ml 200mM L-glutamine; 250µl 0.1M ß-mercaptoethanol; 50µl LIF (10^6 U/ml)

PBS: 2g KCl; 2g KH_2PO_4; 80g NaCl; 14.3g $Na_2HPO_4x2H_2O$; H_2O ad 10l

3.1.2 Culture conditions of NIH3T3 cells

NIH3T3 cells were cultured in DMEM in an incubator with 37°C, 5% CO_2 and a water saturated atmosphere. Coating of plates with gelatine was not necessary. Splitting of cells was performed by trypsinization as described for CGR8 cells.

DMEM: 442,5ml DMEM (with glucose, L-glutamine, pyruvate); 50ml FBS; 5ml 200mM L-glutamine; 2.5ml 100 x penicilline/streptomycine

3.1.3 Differentiation of CGR8 cells

For differentiation of CGR8 cells according to the “hanging drop” protocol, about 70-80% confluent cells were trypsinized, counted and harvested by centrifugation. The pellet was resuspended in differentiation medium to prepare a suspension with 1 x 10^6 cells/ml. This suspension was diluted to 1:40 to obtain 2.4 x 10^4 cells/ml. About 60-70 drops of 20µl (500 cells) were placed into the lid of a 10cm bacteriological plate. The lid was then placed on a plate filled with 7ml PBS and the drops were incubated at 37°C, 5% CO_2 as “hanging drops” for 2 days. Due to the hanging state, the cells accumulate at the bottom of the drop and form spheroid cell aggregates - embryoid bodies (EBs). After 2 days, the EBs were transferred to 10cm bacteriological dishes containing 10ml of differentiation medium (about 200 EBs/10cm plate). Medium was changed every 48 hours.

Differentiation medium: 390ml IMDM; 100ml FBS; 5ml 200mM L-glutamine; 5ml 100x MEM; 500µl 0.1M ß-mercaptoethanol

3.1.4 Freezing of CGR8 cells in liquid nitrogen

For long term storage CGR8 cells were frozen in liquid nitrogen. 10cm-plates with cells at about 80% confluency were trypsinized, harvested by centrifugation at 1000rpm and the pellets were dissolved in 1ml ice-cold cryoconservation medium, transferred into cryovials and frozen at -80°C. After 2-5 days the cells were transferred into liquid nitrogen.

Cryoconservation medium: 10% DMSO; 90%FBS

3.1.5 Transient transfection of CGR8 cells

For transient expression of genes like eGFP, expression plasmids were transfected into the cells using Lipofectamine 2000. Cells at about 80% confluency were pre-incubated with Optimem for 30 minutes. During this time the transfection mix was prepared. 16µg plasmid and 32µl Lipofectamine 2000 were diluted in 1ml Optimem, respectively. After incubation of 5 minutes at room temperature both vials were mixed and incubated for

another 25 minutes at room temperature to form complexes. After removal of Optimem the transfection mix was added to the cells and incubated for 4-6 hours. Then it was replaced by culture medium. Cells were assayed the following day or later.

3.1.6 Transfection of CGR8 cells with siRNA

Transfection of cells with siRNA was usually performed twice. The day before the first transfection about 1.5 x 10^5 CGR8 cells were seeded in 6-wells. The following day the siRNA transfection mix was prepared: 10µl Lipofectamine 2000 were diluted in 150µl Optimem and incubated for 5 minutes at room temperature. Then, 150µl Optimem, containing 10µl of annealed siRNA (20µM), were added, mixed carefully and incubated for 15 minutes at room temperature. During this time cells were pre-incubated with 1.5ml Optimem. After removal, 600µl Optimem were added per 6-well followed by addition of the 300µl of transfection mix. After incubation of the cells for 5-6 hours, the transfection mix was replaced by normal medium. The following day, the same procedure was repeated with the variation that incubation with the transfection mix took place overnight. 2.5ml of normal medium were added though after 5-6 hours of incubation.

3.1.7 Transfection of NIH3T3 cells with siRNA

For transfection with siRNA, NIH3T3 cells were seeded at a density of about 6 x 10^4 cells per 6-well. The following day the transfection mix was prepared using polyethylenimine as transfection reagent. 10µl of annealed siRNA (20µM) were added to 250µl of Optimem containing 12µl of polyethylenimine and incubated for 15 minutes at room temperature. Then, the transfection mix was added directly to a 6-well containing 2.5ml medium. After incubation for 5-6 hours the transfection mix was replaced by standard cell culture medium. The following day the procedure was repeated.
Alternatively, Oligofectamine was used as transfection reagent. In that case preparation of the transfection mix was performed as described for Lipofectamine 2000 in chapter 3.1.6.

3.1.8 Annealing of siRNA

RNA oligonucleotides were obtained from Curevac GmbH and dissolved at a concentration of 100μM in RNase free water and stored at -20°C. For annealing of siRNAs, 200μl of sense and antisense oligonucleotides (100μM) were mixed with 200μl of annealing buffer respectively and were then pooled. After addition of another 200μl of annealing buffer the final concentration of the siRNA duplex was 20μM. The samples were now aliquoted a 100μl and incubated for 1 minute at 90°C in a thermomixer (Eppendorf). Subsequently, the thermomixer was turned out and samples were slowly cooled down for 30-45 minutes until they reached a temperature of about 50°C. Then the thermomixer was switched on again to 12°C and samples were further cooled down to 12°C. Annealed siRNA was stored at -20°C or -80°C.

Annealing buffer: 30mM HEPES-KOH, pH 7.4; 100mM KCl; 2mM $MgCl_2$; 50mM NH_4Ac

3.1.9 Counting of cells

After trypsinization of adherent cells, their concentration can be determined in a Neubauer-counting chamber. Therefore, 10μl of cell solution were added to the chamber and 4 x 16 squares were counted per sample. The respective mean value times 10^4 corresponds to the amount of cells per 1ml medium. If dead cells should be excluded, cells were stained prior to counting with trypan blue solution (1:1). Living cells with an intact membrane exclude the pigment, while it is up-taken by dead cells. Thus, dead cells with a porous membrane can be distinguished by their blue color.

3.2 Protein Analyses

3.2.1 Generation of antibodies

3.2.1.1 Generation of polyclonal antibodies

Polyclonal antibodies against murine Pes1, Bop1 and WDR12 were generated by immunizing guinea pigs with a mixture of the following two peptides per protein.

Pes1: LEKKKYERGSATNYITRNKARKKL (aa 4-27) and KRKAHDDAVRSEKKAKRT RPV (aa 564-584)
Bop1: GKPHMSPASLPGKRRLEPDQELQIQ (aa 6-30) and SQEHTQVLLHQVSRRR SQSPFRRS HG (aa 541-566)
WDR12: MAQLQARFYSENKKYAV (aa 1-17) and DWTDTGLLLSGGADNKLYSYSYS PTTS (aa 393-418)
Peptides were synthesized by H. Rackwitz, Peptide Specialty Laboratories GmbH, Heidelberg. Guinea pigs of the lineage DH were immunized via 4 injections at 2-week intervals using CFA (1st injection) and IFA (2nd injection onwards) as adjuvant. Dosage was 0,24mg peptide per animal. Final bleeding was performed 8 weeks after the first immunization (Charles River Laboratories GmbH, Sulzfeld). Two sera were raised per protein, designated Pes1-Ab1 and -Ab3, Bop1-Ab1 and -Ab2 and WDR12-Ab3 and -Ab4.

3.2.1.2 Generation of monoclonal antibodies

Monoclonal antibodies against murine Bop1 and WDR12 were generated using the following peptides, coupled to ovalbumine or KLH. Peptides were synthesized by H. Rackwitz, Peptide Specialty Laboratories GmbH, Heidelberg.
Bop1: GKPHMSPASLPGKRRLEPDQELQIQ (aa 6-30) and SQEHTQVLLHQVSRRR SQSPFRRS HG (aa 541-566)
WDR12: MAQLQARFYSENKKYAV (aa 1-17) and DWTDTGLLLSGGADNKLYSYSYS PTTS (aa 393-418)
About 50μg of the peptides coupled to KLH (or ovalbumine) were injected both intraperitoneally and subcutaneously into Lou/C rats using CPG2006 and incomplete Freund's (TIB MOLBIOL) as adjuvant. After a 6-week interval, a final boost was given intraperitoneally and subcutaneously. 3 days later, the rat immune spleen cells were fused with the myeloma cell line P3X63-Ag8.653, according to standard procedures. Hybridoma supernatants were tested in a solid phase immunoassay. The plates were coated overnight with the peptides coupled to ovalbumine (or KLH). After blocking with non-fat milk, the hybridoma supernatants were incubated. Bound rat antibodies were detected with a cocktail of biotinylated mouse mAbs against the rat IgG heavy chains, thus avoiding IgM mAbs. The biotinylated mAbs were visualized with peroxidase-labeled avidin (Vector) and o-phenylendiamine as chromogen in the peroxidase

reaction. The hybridomas designated Bop1-1B5, -5F4, -8G10, -1A11 (Bop1 aa 6-30) and WDR12-6A2 (WDR12 aa 1-17), WDR12-6B8 and -8D2 (WDR12 aa 393-418) were stably subcloned and used for further analysis. The immunoglobulin isotypes were determined using mAbs against the rat IgG heavy chains and light chains. Bop1-5F4 antibody has the IgG subclass IgG2c, WDR12-8D2 the subclass IgG2b. All other antibodies have the subclass IgG2a.

3.2.2 Western Blot Analysis

3.2.2.1 Preparation of protein extracts under denaturing conditions for SDS-PAGE

For the analysis of total cellular proteins by Western blotting, cells were trypsinized, harvested by centrifugation and lysed in 1x Laemmli buffer or, alternatively, they were washed with PBS and lysed directly on the plate in 1x Laemmli buffer and harvested using a cell scraper. One confluent 6-well was lysed in about 150-200µl of buffer. Samples were sonicated with 10 pulses, boiled for 5 minutes at 95°C and stored at -20°C. 10-20µl of the lysates were loaded on a gel.

1x Laemmli buffer: 50mM Tris/HCl pH 7.0; 20% glycerol; 2% SDS; 5% ß-mercaptoethanol; 0.02% bromphenol blue

3.2.2.2 SDS-polyacrylamide gel electrophoresis (SDS-PAGE) and blotting of proteins

For separation of proteins by SDS-polyacrylamide gel electrophoresis, 8%, 10% or 12% polyacrylamide gels with 2mm thickness were used, depending on the size of the analyzed proteins. After loading of the lysates the gels were run at 30mA per gel in 1x SDS running buffer. Pre-stained markers were run simultaneously on the gel to estimate the molecular weight. Proteins separated by SDS-PAGE were transferred to a nitrocellulose membrane via wet blotting in 1x transfer buffer at 450mA and 4°C for 1 hour. Beforehand, all components were soaked in transfer buffer and the blotting sandwich was built the following: sponge, Whatman paper, membrane, gel, Whatman paper, sponge. To control an optimal transfer of the proteins after blotting and to verify equal loading, the membranes were stained for 1 minute in Ponceau S solution and destained with H_2O or TBST.

Stacking gel (10ml): 5,5ml H_2O; 1.7ml 30% acrylamide mix (Rotiphorese Gel 30); 2.5ml 1M Tris/HCl pH 6.8; 0.1ml 10% SDS; 0.1ml 10% APS; 10µl TEMED

Resolving gel 10% (20ml): 5.4ml H_2O; 6.7ml 30% acrylamide mix (Rotiphorese Gel 30); 7.5ml 1M Tris/HCl pH 8.8; 0.2ml 10% SDS; 0.2ml 10% APS; 8µl TEMED

10 x SDS running buffer: 30.2g Tris-base; 144g glycine; 50ml 20%- SDS; H_2O ad 1l

10 x Transfer buffer: 30.2g Tris-base; 144g glycine; 10% methanol; H_2O ad 1l

3.2.2.3 Hybridization with antibodies

After blotting of the proteins (3.2.2.2), the membranes were blocked for at least 30 minutes in TBST containing 5% non-fat milk powder. Incubation with the primary antibody, which was diluted in TBST/5%milk, was performed at 4°C overnight. Subsequently, the membranes were rinsed twice with water and washed three times for 5 minutes in TBST, followed by incubation with the secondary antibody, diluted in TBST/5%milk 1:2500 to 1:5000. After 2 hours of incubation at room temperature, the membranes were washed three times for 5 minutes in TBST and were rinsed five times shortly with water. To detect protein bands, the blots were incubated for 1 minute with ECL-detection solution, followed by exposure to chemiluminescence films.

10 x TBS: 100mM Tris; 1.4M NaCl
1 x TBST: 1 x TBS; 0.1% Tween-20

3.2.2.4 Stripping of membranes

To detect additional proteins on a membrane, which was already used for hybridization, the bound antibodies were removed by shaking the membrane in stripping buffer at 55°C for 15 minutes. Subsequently, the membrane was washed twice for 10 minutes in TBST at room temperature, blocked 30 minutes in blocking buffer, followed by hybridization with the new antibodies.

Stripping buffer: 100mM ß-mercaptoethanol; 2% SDS; 62.5mM Tris/HCl pH 6.7

3.2.3 Native Gels

3.2.3.1 Preparation of protein extracts under native conditions

Cells from three 10cm-plates were trypsinized, harvested by centrifugation, washed twice in PBS and resuspended in 200µl lysis buffer. Subsequently, cells were vortexed for 5 seconds, incubated on ice for 20-30 minutes with sporadic vortexing, vortexed again for 5 seconds and centrifuged at 16400rpm, 4°C for 10 minutes. The supernatants were used directly for analyses on native gels.

Lysis buffer:	50mM Tris/HCl, pH 8.8; 1% NP-40; 150mM NaCl; 1 x protease inhibitor; 1 x phosphatase inhibitors
Protease inhibitor (50x):	1 tablet complete EDTA-free protease inhibitor cocktail (Roche) in 1ml H_2O (1:50)
Phosphatase inhibitors:	100mM sodium orthovanadate 1:100
	1M Na-tartrate 1:500
	100mM Na_2MoO_4 1:100

3.2.3.2 Native gel electrophoresis

Native gel run and blotting was performed at 4°C with all materials pre-cooled. The lysates (3.2.3.1) were mixed 1:1 with 2x sample buffer and loaded to one-phase acrylamide gels (15µl for detection of Pes1, Bop1, WDR12 and 6.5µl for detection of Tubulin). Gels were run at 85V until the samples had entered the gels and then at 100V. After separation, proteins were transferred to a nitrocellulose membrane via wet blotting at 450mA for 1.5 hours in blotting buffer. Hybridization with antibodies was performed as described in chapter 3.2.2.3.

2 x sample buffer:	125mM Tris/HCl pH 6.8; 30% glycine; 0.02% bromphenol blue
1 x Running/blotting buffer:	14.4g glycine; 3.02g Tris-base; H_2O ad 1l
Acrylamide gel (10ml):	3.88ml H_2O; 2.16ml acrylamide mix (Rotiphorese Gel 30); 3.75ml 1M Tris/HCl pH 8.8; 0.1ml 10% APS; 8µl TEMED

3.2.4 Immunofluorescence

Immunofluorescence with CGR8 cells was performed in ibidi μ-slides VI, which were pre-coated with 0.2% gelatine. NIH3T3 cells were analyzed in 8-chamber slides from Nunc. After the respective treatment of the cells they were washed in PBS and fixed for 10 minutes in ice-cold methanol (alternatively for 2 minutes in 1:1 methanol/aceton). Subsequently, they were air-dried and rehydrated with PBS for 5 minutes. After blocking for at least 30 minutes in PBS/10% FBS they were incubated with the primary antibodies overnight at 4°C. Antibodies were diluted in PBS/1.5%FBS. The following day, the cells were washed three times for 3 minutes in PBS/0.04%triton and incubated for 1 hour at room temperature with Cy3-labeled secondary antibodies (1:300 in PBS/1.5%FBS). After three washes with PBS/0.04%triton cells were stained with DAPI (1:10000 of 5mg/ml) to counterstain the nuclei. After another wash, the chambers from the 8-chmaber slides were removed and cells were covered with coverslips and mounting medium; cells in the μ-slides could be analyzed directly under a fluorescence microscope. Digital images were aquired using the Openlab acquisition software (Improvision) and a microscope model Axiovert 200M (Zeiss) with 10x, 20x and 100x objectives connected to a 5-charge-coupled device camera model ORCA-479 (Hamamatsu).

3.3 RNA Analyses

3.3.1 Isolation of total RNA

Total RNA was isolated from cells using the Qiagen RNeasy® Kit according to the manufacturers instructions. Cells were lysed in 300-500μl RLT lysis buffer, depending on their density. DNA digestion with the RNase-Free DNase Set (Qiagen) was included to avoid contamination with genomic DNA. Finally, RNA was eluted with 30-50μl of RNase-free water and stored at -80°C. Concentrations of RNA were determined using an Eppendorf spectrophotometer.

3.3.2 Reverse transcription (RT) of RNA into cDNA

For quantitative PCR analysis the RNA had to be transcribed into cDNA. Therefore 3μg (or 1μg) of RNA were diluted in autoclaved ddH_2O to a final volume of 15μl. After addition of 3.75μl of oligo$(dT)_{15}$ primer (17μM) the samples were incubated at 65°C for 5 minutes to denature secondary structures of RNA and allow the primers to bind to the polyA-tails of mRNA molecules. Afterwards 11.25μl of RT-Mix were added and the reaction was performed for 55 minutes at 37°C, followed by inactivation of the enzyme for 5 minutes at 95°C. Finally, 270μl (or 90μl) of autoclaved ddH_2O were added to dilute the samples.

RT-Mix:
4.5μl NX-buffer (0.4M KCl; 0.1M Tris/HCl pH 8.4; 20mM $MgCl_2$; 2% Tween-20)
3.0μl ß-mercaptoethanol (0.1M)
1.5μl dNTPs (20mM/dNTP)
0.75μl RNasin (40U/μl)
1.5μl Mo-MLV reverse transcriptase (200U/μl)

3.3.3 Quantitative real-time PCR analysis

To monitor relative gene expression levels, quantitative real-time PCR (polymerase chain reaction) was performed with the Light-Cycler method from Roche. Amplification of a defined sequence of the target cDNA is monitored in this system by addition of SYBR Green, a fluorescent dye, which enhances its fluorescence 100 times upon intercalation into double-stranded DNA. Thus, the fluorescence is proportional to the amount of amplified DNA. It is measured after each PCR cycle (real-time). The CP-(crossing point) value, which is determined by the Light-Cycler program, represents the cycle of the PCR when the fluorescence of the samples becomes detectable compared to the background levels. This is depending on the amount of target cDNA. Together with a standard curve, which determines the efficiency of the respective PCR reaction, the CP-value can be used to quantify the relative amount of cDNA. For the generation of a standard curve, samples of a previous PCR reaction with the same oligonucleotides were serially diluted to 10^{-5}, 10^{-7} and 10^{-9} and ran in the Light-Cycler. For quantification of future reactions, the dilution 10^{-5} was included in those as reference (calibrator). The calculation of the standard curves as well as quantification of

the samples was performed by the Light-Cycler program. To account for irregularities within cDNA transcription, the determined concentrations of all samples were normalized to the concentrations of the housekeeping gene Aldolase. As the cDNA, which served as template for the PCR reaction, was transcribed reversely from mRNA, the results finally reflect the relative amount of mRNA copies in the cells at the time of lysis normalized to the levels of Aldolase.
Specificity of the used primers was analyzed by melting curves, determining the melting peak of their products. Their sequences are depicted in chapter 2.6.

PCR Mix:
5.2µl H_2O
0.8µl $MgCl_2$
1µl oligonucleotide-pair (5pmol/µl each)
1µl Roche mix
2µl cDNA (diluted 1:10 in H_2O)

Program for amplification:

Activation/denaturation:	95°C; 10min
Amplification:	95°C; 1sec
(50 cycles)	65°C; 10sec
	72°C; 12sec
Melting curve:	70°C; 10sec and in 0.1°C steps to 97°C
Cooling down:	40°C; 10sec

3.3.4 *In vivo* labeling of RNA with ^{32}P-orthophosphate

For metabolic labeling of rRNA, CGR8 or NIH3T3 cells were pre-incubated in phosphate-free DMEM with 10% dialysed FBS for 30 minutes. Then the starvation medium was replaced by 1ml/6-well phosphate-free DMEM/10%dialysed FBS containing 15µCi ^{32}P-orthophosphate. After 1 hour the radioactive medium was removed and cells were incubated in standard medium with 10% FBS for 3-4 hours, followed by isolation of total RNA with the Qiagen RNeasy Kit according to the manufacturers instructions. 1.2µg of total RNA in 15µl loading buffer were denatured at 55°C for 15 minutes and separated on 1% agarose-formaldehyde gels (100V, approximately 5 hours). After electrophoresis, gels were photographed under UV light to visualize ethidiumbromide-stained RNA. Then the gels were dried at 80°C under

vacuum suction on a Whatman-paper. Dried gels were exposed to X-ray films and rRNA was visualized by autoradiography.

1% formaldehyde gel:	4g agarose; H_20 ad 300ml; boil and allow to cool to 65°C before adding 40ml 10x MOPS and 67ml formaldehyde (37%).
10 x MOPS:	200mM MOPS; 50mM Na-acetat; 1mM EDTA; pH 7.0 with NaOH
Running buffer:	1x MOPS
2 x RNA loading buffer (10ml):	5ml formamide; 1.5ml formaldehyde (37%); 1ml 10x MOPS; 1ml bromphenol blue; 10µl ethidiumbromide; 1.5ml H_20

3.4 Cell Proliferation and Apoptosis

3.4.1 Proliferation assay - cell count

CGR8 cells were plated at a density of $1.5x10^5$ cells per 6-well and transfected twice with the respective siRNAs at the following two days. 6 days after the first siRNA transfection, cell numbers were determined in a Neubauer chamber. At day 3 (or 4) after the first transfection, cells were passaged the following way: control siRNA-transfected cells were split 1:10, while cells transfected with siRNAs against Pes1 or Bop1 were split 1:5 to 1:7.5 depending on their density. This was done to ensure comparable amounts of cells per 6-well after plating. The cell numbers, determined at day 6, were multiplied with the respective dilution factors.
NIH3T3 cells were plated at a density of 6×10^4 per 6-well. Transfection, splitting and cell counts were performed in a similar manner as in CGR8 cells. Trypan blue staining was used to exclude dead cells.

3.4.2 Proliferation assay - GIEMSA staining

Cells were plated at a density of $1.5x10^5$ per 6-well and incubated with or without 5FU (10µM or 20µM) for 48 hours. After washing with PBS, the cells were fixed with methanol (-20°C) for 10 minutes, dried in the airflow of the hood for 2-5 minutes and

stained with GIEMSA solution (1:20) for 30 minutes. Subsequently, the cells were washed by dipping the 6-well plate carefully, to not dislodge cells, 4-6 times into a bowl with ddH_2O. After drying, the 6-wells were scanned with an Epson scanner.

3.4.3 Cell cycle analysis with propidium iodide (PI) staining

To analyze the DNA content of the cells by propidium iodide staining, cells from 1-3 6-wells were washed with PBS, trypsinized and harvested by centrifugation at 1000rpm for 5 minutes. For fixation, cells were resuspended in 1ml of cold 80% ethanol and incubated for 1 hour on ice. Cells were then washed once with PBS and resuspended in 1ml PBS, containing 50μg propidium iodide, 5μl RNase A (10units, Roche) and 2μl EDTA (0.5M). After 30 minutes incubation in the dark and at room temperature, for digestion of RNA, cells were subjected to flow cytometry in a FACScan (Becton Dickinson) to analyze cell cycle distribution within the population. 100000 cells were aquired per sample and analyzed with CellQuest software (Becton Dickinson). Cell debris was excluded by gating cells on a dot blot with forward and sideward scatter.

3.4.4 Cell cycle analysis with bromodeoxyuridine (BrdU) labeling

The FITC BrdU Flow Kit from BD Biosciences was used to analyze BrdU labeled cells. BrdU is a thymidine analogue, which is incorporated into newly synthesized DNA and thus labels cells in S-phase. Cells were labeled in 6-well plates with 10μM BrdU in cell culture medium for 30 minutes. Then, cells were washed twice with PBS, trypsinized and 10^6 cells per sample were fixed and permeabilized in 100μl of BD Cytofix/Cytoperm buffer for 30 minutes on ice. After addition of 1ml 1x BD Perm/Wash buffer and centrifugation for 5 minutes at 1200rpm the cell pellet was resuspended in 100μl of BD Cytperm Plus buffer and incubated for 10 minutes on ice. Following a washing step as described above, cells were refixed with 100μl BD Cytofix/Cytoperm buffer for 5min on ice. After another washing step, cells were treated for 1 hour at 37°C with 30μg DNase per sample to expose incorporated BrdU. After washing the cells again with 1ml 1x BD Perm/Wash buffer, they were stained for 20 minutes at room temperature with FITC-conjugated anti-BrdU antibody, diluted 1:50 in 1x BD Perm/Wash buffer. 25μl of antibody dilution were added per sample. After another washing step, the cell pellets

were resuspended in 10µl 7-AAD solution to stain the total DNA content of the cells. Then, 0.5ml PBS was added to each sample and the stained cells were analyzed in a FACS Calibur flow cytometer (Becton Dickinson). 30000 cells per sample were aquired at a rate of no more than 400 events/second. Cell Quest software (Becton Dickinson) was used for analysis. For setup compensation, the following controls were included: 1) unlabeled cells with BrdU antibody; 2) labeled cells with BrdU antibody; 3) unlabeled cells with 7-AAD; 4) labeled cells with BrdU antibody and 7-AAD.

3.4.5 Annexin V staining

Annexin V staining was used to determine the amount of apoptotic cells. Cells were harvested by trypsinization, washed twice with PBS and resuspended in 1x Annexin V-binding buffer at a concentration of ~$1x10^6$ cells/ml. Then 100µl of the cell suspension ($1x10^5$ cells) were stained by addition of 5µl Annexin V-FITC (BD Biosciences) and 2µl propidium iodide (50µg/ml stock) to distinguish between apoptotic and necrotic cells. After incubation for 15 minutes in the dark and at room temperature, 400µl 1x Annexin V-binding buffer were added and cells were analyzed by flow cytometry using a FACScan and CellQuest analysis software (Becton Dickinson). For setup compensation, the following controls were included: 1) unstained cells, 2) cells stained with Annexin V-FITC alone, 3) cells stained with PI alone. To exclude cell debris, cells were gated on a forward and sideward scatter dot blot.

1x Annexin V-binding buffer: 10mM HEPES/NaOH pH7.4; 140mM NaCl; 2.5mM $CaCl_2$

4 RESULTS

4.1 Expression, localization and complex formation of Pes1, Bop1 and WDR12 in mouse embryonic stem cells

4.1.1 Generation of antibodies for the detection of murine Pes1, Bop1 and WDR12

The mammalian proteins Pes1, Bop1 and WDR12 have been shown to be involved in ribosome synthesis and proliferation of several cancer cell lines. In this work, the function of Pes1, Bop1 and WDR12 in mouse embryonic stem cells (ES cells) was investigated. As a model, the germline-competent mouse ES cell line CGR8 was chosen, which can grow without feeder layers on gelatinized plates in the presence of LIF. This property makes culturing conditions easier and eliminates background signals, derived from feeder cells. CGR8 cells were originally derived by Austin G. Smith from a male day 3.5 blastocyst-stage embryo of the mouse strain 129ola. The morphological phenotype of the cells is described as small and tightly packed cells in a singular cellular layer (ECACC, UK; http://www.ecacc.org.uk/).

As former investigations in our lab about Pes1, Bop1 and WDR12 have been performed exclusively in human cell lines, it was necessary to produce several tools like antibodies and siRNAs for a proper investigation of the murine proteins. Therefore, as first step, polyclonal and monoclonal antibodies for all three murine proteins were generated. For the generation of polyclonal antibodies directed against murine Pes1, two guinea pigs were immunized with a mixture of an N-terminal and a C-terminal peptide of Pes1. Thereby, two antibodies, designated αPes1-Ab1 and αPes1-Ab3 were raised. The polyclonal antibodies αBop1-Ab1 and αBop1-Ab2 against murine Bop1 and αWDR12-Ab3 and αWDR12-Ab4 against murine WDR12 were raised by immunizing guinea pigs with a mixture of an N- and a C-terminal peptide of Bop1 or WDR12, respectively. All antibodies were tested by Western blot analysis on total cell lysates of the mouse ES cell line CGR8 and of the mouse cell line NIH3T3, which are fibroblast-like cells. Pes1, Bop1 and WDR12 are expressed at high levels in CGR8 cells as well as in NIH3T3 cells (Fig.4). All polyclonal antibodies showed a specific staining with both cell lysates, detecting strong bands at the expected positions (Fig.4A-C, lanes 1-4, respectively).

Only αWDR12-Ab3 showed additionally a strong unspecific band with a slightly higher molecular weight (Fig. 4B, lanes 1/2).

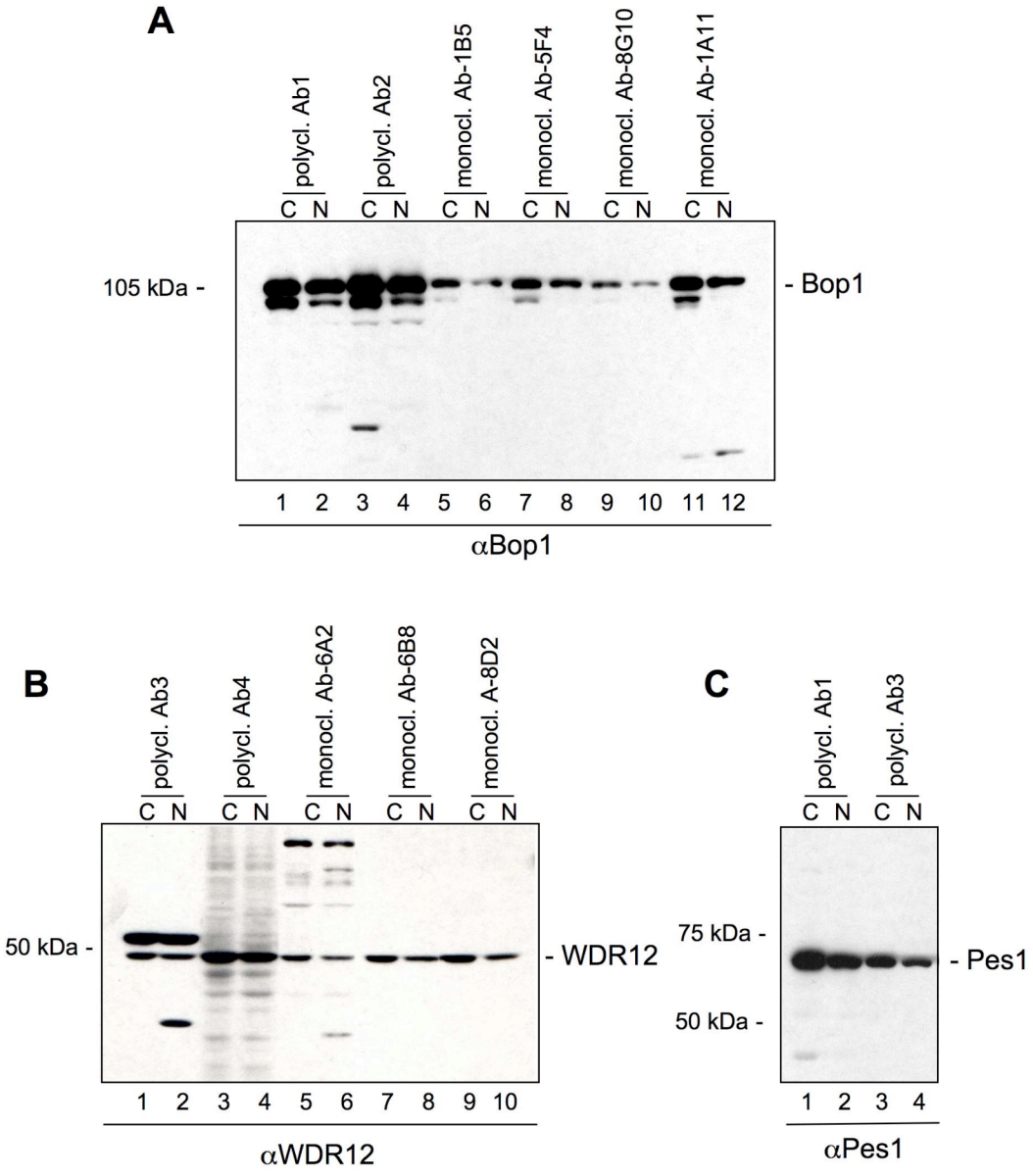

Figure 4: Analysis of Pes1, Bop1 and WDR12 with newly generated antibodies in CGR8 and NIH3T3 cells. The indicated polyclonal and monoclonal antibodies against Bop1 **(A)**, WDR12 **(B)** and Pes1 **(C)** were tested by Western blot analysis on total cell lysates. C: CGR8; N: NIH3T3.

Monoclonal antibodies against murine Pes1, Bop1 and WDR12 were raised in rats. For immunization, the same N- or C-terminal peptides were used as for the generation of the polyclonal antibodies. Four functional monoclonal antibodies against the N-terminus of Bop1 were generated (αBop1-1B5, αBop1-5F4, αBop1-8G10, αBop1-1A11), (Fig.4A,

lanes 5-12), but none against the C-terminal part. For WDR12, one antibody was raised against the N-terminus (αWDR12-6A2), (Fig.4B, lanes 5/6) and two against the C-terminal part (αWDR12-6B8 and αWDR12-8D2), (Fig.4B, lanes 7-10). No functional monoclonal antibody was raised against Pes1. All monoclonal antibodies showed a very high specificity. The fact that the different polyclonal and monoclonal antibodies identified proteins of the same size at the expected positions, further underscores the specificity of the new antibodies. Western blot analyses of Bop1 showed a double band with all tested antibodies (Fig.4A). This might be due to post-translational modifications of Bop1 or to alternative splice variants. Alternatively, the lower band might represent a degradation product.

As the polyclonal antibodies showed very good intensities on the Western blots, they were used for most of the experiments described below. Unless otherwise stated, αPes1-Ab3 was used for detection of Pes1, αBop1-Ab1 for Bop1 and αWDR12-Ab4 for detection of WDR12.

4.1.2 Nucleolar localization of Pes1, Bop1 and WDR12 in CGR8 and NIH3T3 cells

Pes1, Bop1 and WDR12 are expressed at high levels in the embryonic stem cell line CGR8. To get information about the cellular localization of the proteins in ES cells, indirect immunofluorescence analyses were performed. The results showed a predominantly nucleolar localization of all three proteins in CGR8 cells as well as a weak staining of the nucleoplasm (Fig.5A). The staining of WDR12 showed the strongest signal outside the nucleoli with additional staining in the cytoplasm. Whether this is due to unspecific binding of the antibody or whether WDR12 is localized additionally in the cytoplasm remains to be elucidated.

In mouse NIH3T3 cells the localization of Pes1, Bop1 and WDR12 was also mainly nucleolar with a weak nucleoplasmic staining (Fig.5B).

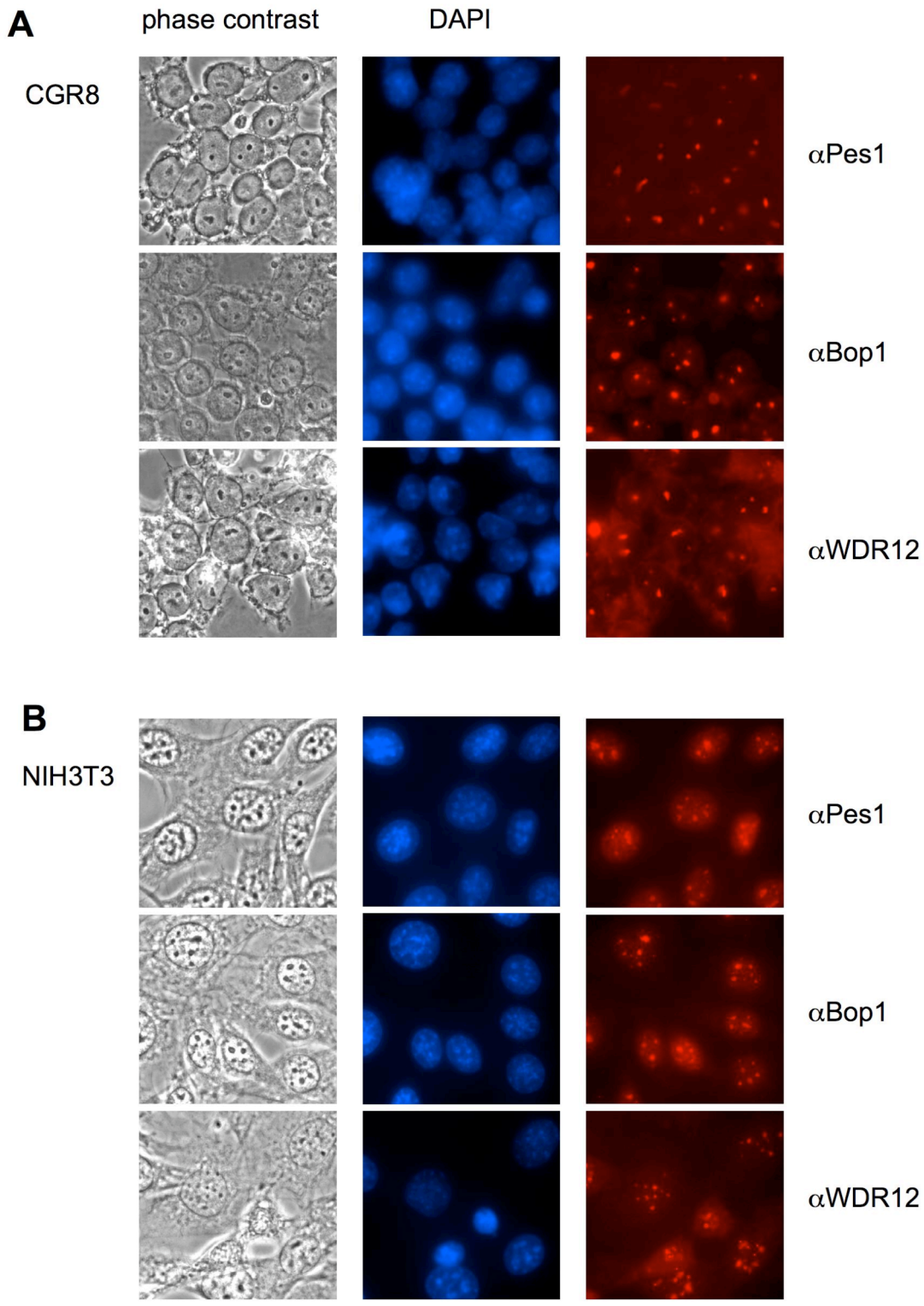

Figure 5: Nucleolar localization of murine Pes1, Bop1 and WDR12. CGR8 **(A)** and NIH3T3 cells **(B)** were fixed with methanol and stained with the polyclonal antibodies αPes1-Ab3, αBop1-Ab1 and αWDR12-Ab4. Antigen-antibody complexes were then detected with Cy3-conjugated anti-guinea pig antibodies and visualized by fluorescence microscopy. Nuclei were counterstained with DAPI.

4.1.3 Stable complex formation of murine Pes1, Bop1 and WDR12

Recent work in our laboratory has shown that Pes1, Bop1 and WDR12 form a stable complex in human U2OS and H1299 cells, termed PeBoW-complex (Holzel et al., 2005, Rohrmoser et al., 2007). To examine whether Pes1, Bop1 and WDR12 also assemble to a complex in mouse cells and especially in embryonic stem cells, native gel electrophoresis was performed with protein extracts of CGR8 and NIH3T3 cells. Cells were lysed using stringent, non-denaturing conditions, followed by the separation of stable core complexes on a polyacrylamide gel. Separation of protein complexes is dependent on their size, shape and charge. Subsequent immunoblot analysis of Pes1, Bop1 and WDR12 showed a single band with all 3 antibodies at the same position in the native gel, representing the PeBoW-complex (Fig.6, lanes 2-4 and 6-8). However, it cannot be excluded that the complex contains additional proteins. Immunoblot analysis of WDR12 showed in addition a faster migrating band, indicating probably free, non-incorporated protein. This band was detected in CGR8 and NIH3T3 cells (Fig.6, lane 4 and 8) and may indicate an additional function of WDR12 besides its integration into the PeBoW-complex.

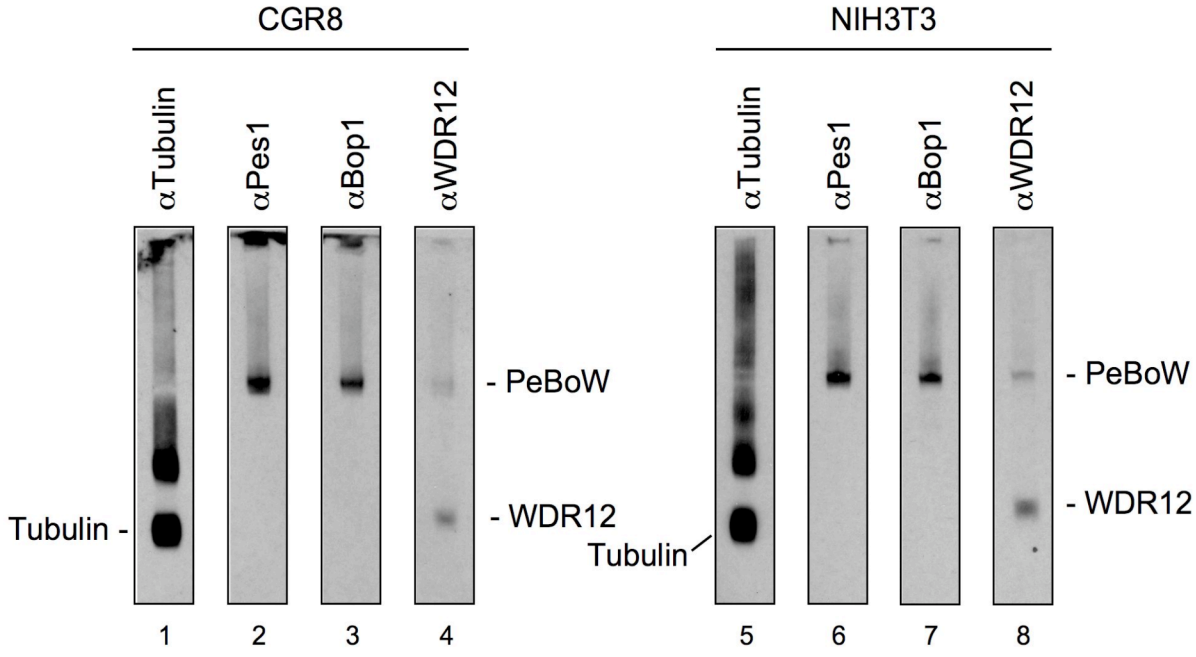

Figure 6: Murine Pes1, Bop1 and WDR12 form a complex. Total cell lysates of CGR8 and NIH3T3 cells were separated by native gel electrophoresis. Pes1 (polyclonal Ab3), Bop1 (polyclonal Ab1), WDR12 (polyclonal Ab4) and α-tubulin were visualized by immunoblotting. Free proteins and complexes, containing the respective factors, are indicated.

4.1.4 Knockdown of murine Pes1, Bop1 and WDR12 by siRNA technology

The method of small interfering RNA (siRNA) knockdowns was chosen to investigate the function of Pes1, Bop1 and WDR12 in embryonic stem cells. Different siRNA sequences for the three genes have been designed and were evaluated in CGR8 cells. The siRNAs were directed either against the open reading frames (ORF) or the untranslated regions (UTR) of the respective mRNAs. As control served a siRNA sequence directed against the Luciferase gene. The protocol for the knockdown and subsequent analysis of the cells was optimized in a way that cells were seeded at low density, followed by transfection of siRNA in duplicate at day 0 and day 1. Analysis of the cells was then performed between day 2 and day 7, depending on the assays (Fig.7A). Evaluation of several siRNA sequences revealed two functional siRNAs against Pes1 and Bop1, respectively (Fig.7B/C). Unfortunately, none out of four tested sequences showed a significant knockdown of WDR12 (Fig.7D). Therefore, functional analyses of the proteins in further experiments were limited to Pes1 and Bop1. As the second functional siRNA against Pes1 (siRNA 3) was evaluated at a later time point, it could not be included in all experiments. As siRNAs often induce off-target effects, it was generally tried to use two different siRNAs per target gene. In case of similar phenotypes, this strongly reduces the possibility that the detected effects might be unspecific. The knockdown efficiencies were varying between different siRNA species, with the siRNAs No.1 against Pes1 and Bop1 giving a better knockdown than the siRNAs No.2 or No.3 (Fig.7B/C, lanes 3/4, respectively). This tendency was reproducible, but nevertheless there were variations between different experiments. Transfection of CGR8 cells with an eGFP expression plasmid showed that about 70% of the cells can be transfected with Lipofectamine 2000 (Fig.7E). Varying intensities of eGFP expression within different cells showed that transfection efficiency differs between single cells. In addition eGFP expression may be also depending on the overall condition of the respective cells.

Knockdowns of the proteins also supplied further proof for the specificity of the antibodies against Pes1 and Bop1. The fact that both bands of Bop1, detected by Western blot analysis, were diminished after siRNA transfection suggests that both bands are specific for Bop1.

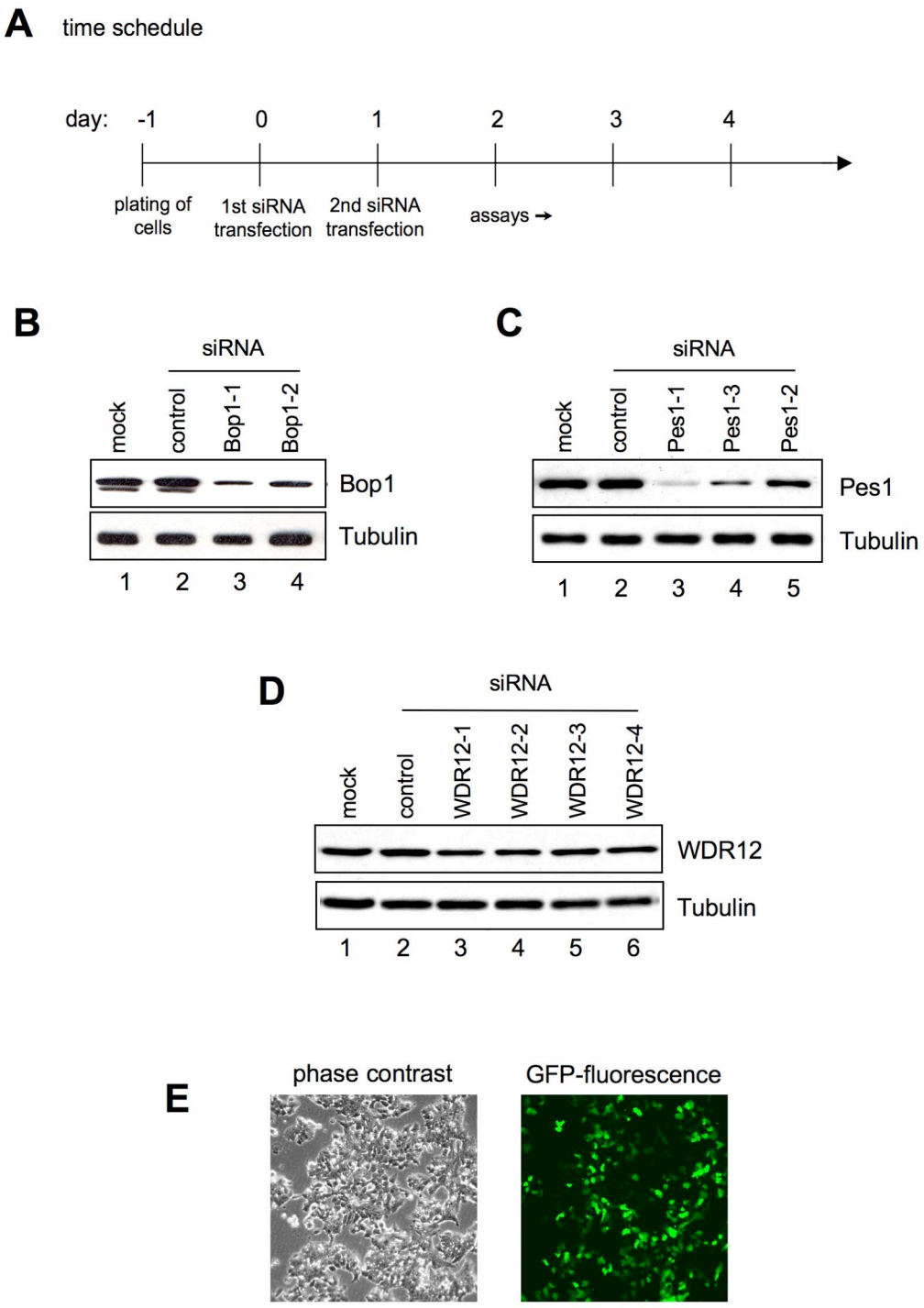

Figure 7: Validation of functional siRNAs for Pes1 and Bop1 but not WDR12. (A) Time schedule of the transfection protocol for siRNA knockdowns. (**B, C, D)** CGR8 cells were transfected twice with the indicated siRNAs using Lipofectamine 2000 as transfection reagent. Two days after the last transfection (day 3), cells were monitored for protein levels of Pes1 (polyclonal Ab3), Bop1 (polyclonal Ab1) and WDR12 (polyclonal Ab4) by Western blot analysis. Mock treated cells were incubated with Lipofectamine 2000. Control siRNA was directed against Luciferase. α-tubulin served as loading control. (**E)** eGFP expression visualized by fluorescence microscopy after transfection of CGR8 cells with an eGFP expression plasmid.

4.1.5 Interdependency of murine Pes1 and Bop1 protein levels

Stability of human Pes1, Bop1 and WDR12 proteins has been shown to be strongly dependent on incorporation into the PeBoW-complex (Rohrmoser et al., 2007). In line with these results, siRNA knockdown experiments showed a strong interdependency of the murine proteins in CGR8 and NIH3T3 cells. Both cell lines were transfected twice with siRNAs against Pes1, Bop1 and WDR12 (according to Fig.7A). Western blot analyses at day 3 showed that depletion of Bop1 also decreases protein levels of Pes1 and vice versa (Fig.8, lanes 2-4 and 8-10). The effect of Pes1 depletion on Bop1 protein levels was stronger though. Interestingly, no clear effect of Pes1 or Bop1 knockdown on the WDR12 protein levels was detectable. This result might be related to the strong intensity of the faster migrating band on the native gels, representing most likely free monomers of WDR12. This further substantiates the hypothesis of an additional function of free WDR12 in mouse cells, independent of its function related to the PeBoW-complex. siRNAs against WDR12, which were shown before not to exert a knockdown of WDR12, served as additional controls and did not show significant effects.

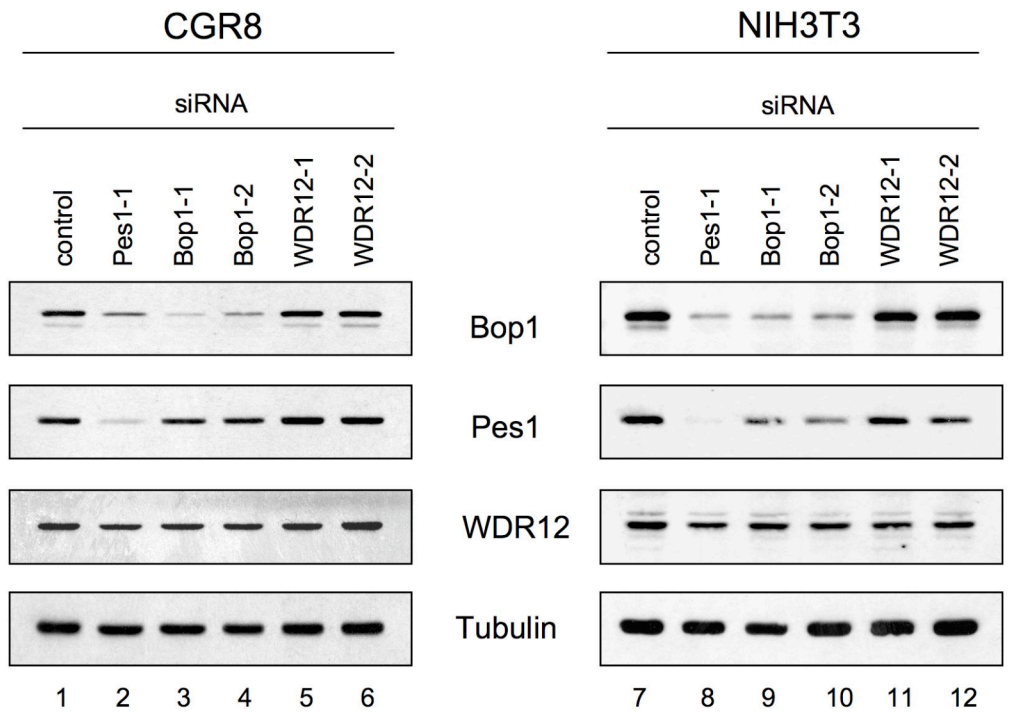

Figure 8: Interdependency of murine Pes1 and Bop1 protein levels. CGR8 **(A)** and NIH3T3 cells **(B)** were transfected twice with the indicated siRNAs. At day 3, protein levels of Pes1, Bop1 and WDR12 were monitored by Western blot analysis. Control siRNA was directed against Luciferase. α-tubulin served as loading control.

4.2 A role for Pes1 and Bop1 in rRNA processing and proliferation of mouse ES cells

4.2.1 Impaired maturation of the 28S rRNA and accumulation of the 36S pre-rRNA upon knockdown of Pes1 and Bop1

Based on the reported function of the PeBoW-complex for ribosome biogenesis, we aimed to investigate whether a knockdown of Pes1 and Bop1 would affect rRNA processing in ES cells. Therefore, maturation of nascent rRNA was analyzed by metabolic labeling of RNA with ^{32}P-orthophosphate. To compare the effects to non-ES cells, the experiment was performed in parallel in mouse NIH3T3 cells. Both cell lines were transfected twice with the respective siRNAs against Pes1, Bop1 and with the control siRNA against Luciferase. Two siRNAs directed against WDR12, which were shown before to have no significant effect on the protein level of WDR12, were included as additional controls in CGR8 cells. Two days after the last transfection, the cells were starved for 30 minutes in phosphate free medium and then RNA was pulse-labeled for 1 hour by addition of ^{32}P-orthophosphate-containing medium. After a chase time of 3-4 hours with normal medium, total RNA was isolated and separated on an agarose-formaldehyde gel. Exposure of the dried gel to an X-ray film led to visualization of labeled, i.e., de novo synthesized and processed ribosomal RNA. Ethidiumbromide staining of total RNA served as loading control. In both cell lines, Pes1- and Bop1-depleted cells showed a reduction of the 28S rRNA levels in comparison to cells treated with control siRNA. In contrast, the amount of the 36S rRNA was increased in the Pes1- or Bop1-depleted cells. The amount of 32S rRNA showed no significant changes, nor did the 45/47S precursor. Also, the amount of 18S rRNA was not changed (Fig.9A). A similar effect was observed at day 2 and day 4, shown at the example of Bop1-depleted CGR8 cells (Fig.9B). The observed effects were comparable between CGR8 and NIH3T3 cells with a slightly stronger decrease of the 28S rRNA in NIH3T3 cells. The intensities of the observed effects were comparable to the knockdown efficiencies, achieved with the respective siRNAs (compare to Fig.8). Namely, the effect observed on 28S rRNA was stronger after depletion of Bop1 with siRNA-1 than with siRNA-2. In cells transfected with siRNAs against WDR12, only a marginal effect was observed.

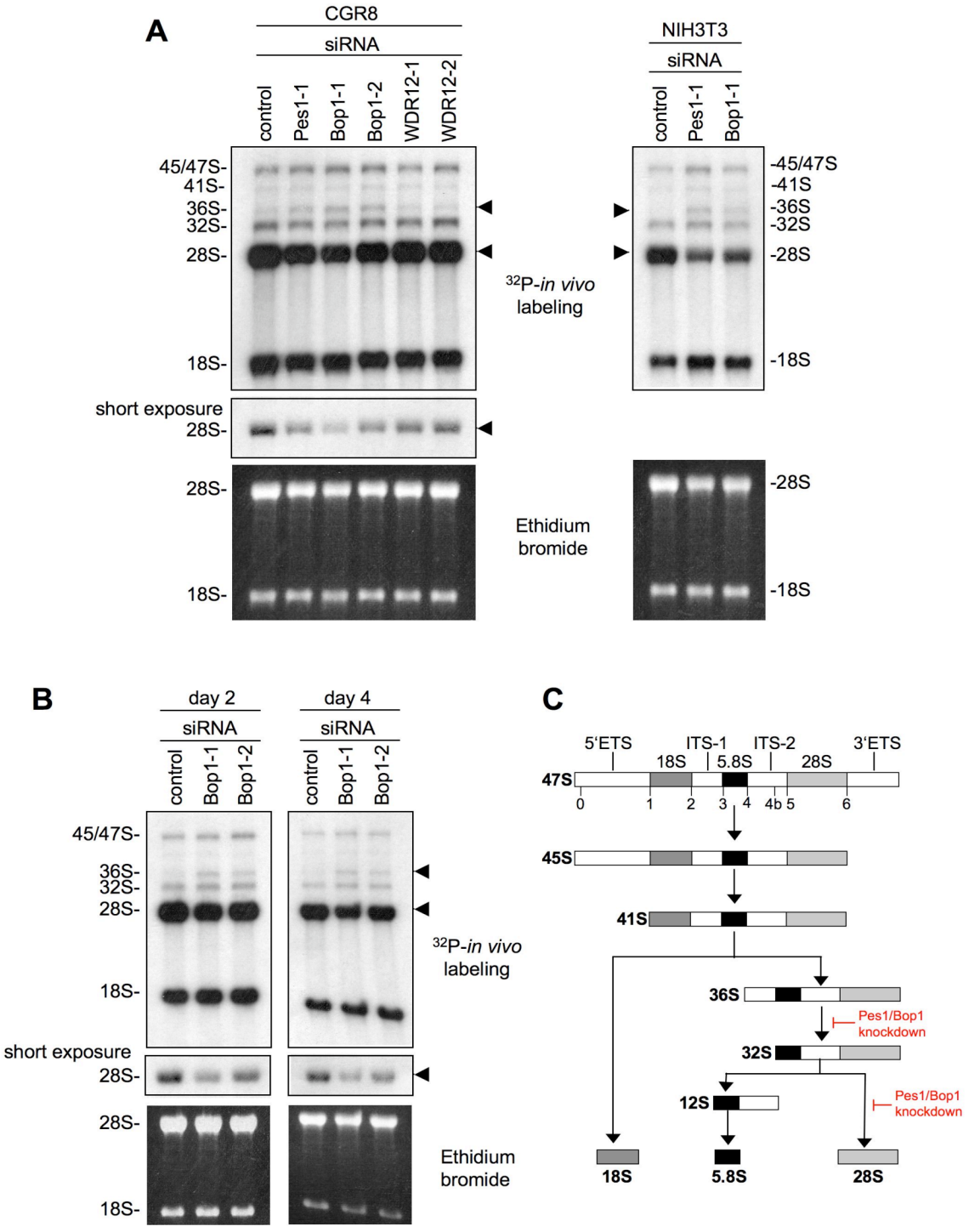

Figure 9: Knockdown of Pes1 or Bop1 inhibits the processing of the 36S and 32S precursors into the 28S rRNA. (**A)** CGR8 and NIH3T3 cells, transfected twice with the indicated siRNAs, were starved for 30 minutes in phosphate-free medium at day 3 (see Fig. 4A). Subsequently, they were pulse-labeled for 1 hour with ^{32}P-orthophosphate. After a chase time of 3-4 hours in regular medium, RNA was isolated, resolved on a 1% formaldehyde gel and visualized by autoradiography. Labeled rRNAs are indicated. Whole RNA staining with ethidiumbromide served as loading control. (**B, C)** CGR8 cells were treated as described in A, except that the pulse-labeling was performed at day 2 and day 4. (**D)** Model of rRNA processing in mammalian cells. Numbers indicate the cleavage sites within the rRNA. Bars indicate the stages, where knockdowns of Pes1 and Bop1 block processing. ETS: external transcribed spacers; ITS: internal transcribed spacers.

The results imply an essential function for Pes1 and Bop1 during rRNA processing of ES cells. As maturation of the 18S rRNA was not affected, Pes1 and Bop1 seem to be involved in the production of the large 60S ribosomal subunit only, whose maturation is dependent on sufficiently processed 28S rRNA. The results further suggest a function for Bop1 and Pes1 during processing of the 36S- into the 32S precursor rRNA and for processing of the 32S precursor rRNA into the mature 28S rRNA. A proposed model for the role of Pes1 and Bop1 in rRNA maturation is shown in figure 9C.

4.2.2 Retarded proliferation of CGR8 and NIH3T3 cells after Pes1 and Bop1 knockdowns

Proliferation of ES cells is very rapid and their cell cycle has distinct features from that of adult cells lacking some of the usual control mechanisms. We were interested to assess the function of the PeBoW-complex for ES cell proliferation under these different conditions. CGR8 and NIH3T3 cells were seeded at low density and transfected twice with the respective siRNAs against Pes1, Bop1 and WDR12 or with a control siRNA directed against Luciferase. To monitor the proliferation rate, cell numbers were determined in triplicate at day 6 (compare to Fig.7A). Knockdown efficiencies were verified by Western blot analysis two days after the second siRNA transfection (Fig.10A-D right panel). Proliferation rates of both, ES cells and NIH3T3 cells, were strongly impaired after knockdowns of Pes1 and Bop1 (Fig.10A-D, left panel). Cell numbers were reduced to 35% compared to the control in CGR8 cells and to 25% in NIH3T3 cells. Again, the knockdown efficiencies correlated directly with the negative effect on proliferation. Knockdowns of WDR12 were again not successful, although a weak reduction of protein could be observed by siRNAs-1 and -2. Additionally, no significant effect was observed on proliferation, except for cells treated with siRNA-2. Those were reduced to 75% compared to cells, treated with control siRNA (Fig.10C). This effect might be related to the weak decrease in WDR12 protein levels. Control siRNA led to a weak reduction of proliferation compared to mock-treated cells, which might be related to siRNA uptake in general.

In summary, Pes1 and Bop1 seem to be essential factors for the high proliferation rate of ES cells. Moreover, the correlation between the degree of impairment on rRNA processing and proliferation, depending on the respective siRNAs, might be indicative of a link between the two processes.

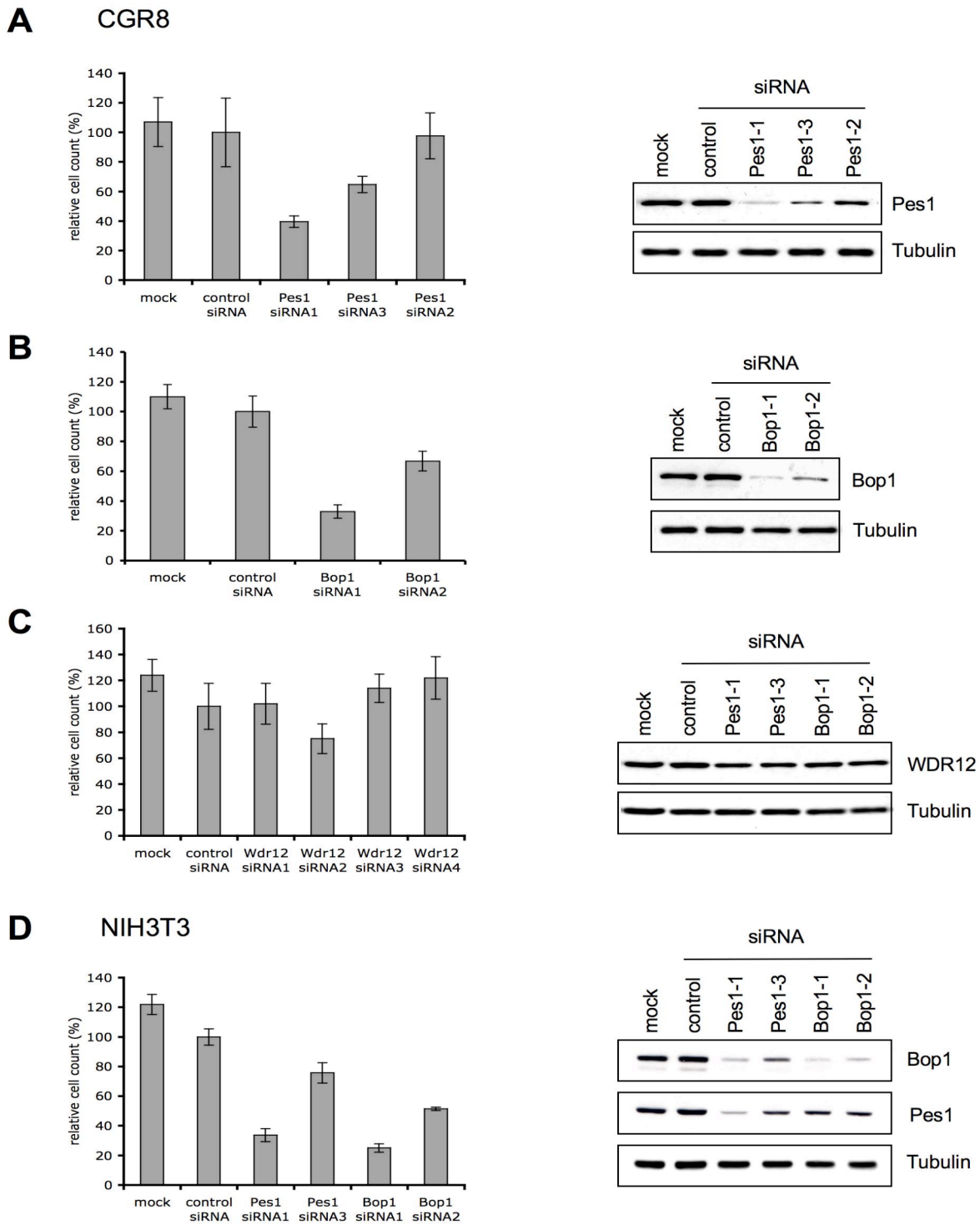

Figure 10: Knockdowns of Pes1 and Bop1 negatively affect proliferation. (A, B, C) CGR8 cells were transfected twice with the indicated siRNAs. At day 6 cell numbers were determined in a Neubauer chamber. Relative cell numbers are shown in a histogram compared to control siRNA-transfected cells, which were set to 100%. Mock cells were treated with Lipofectamine 2000. Error bars indicate the SD. Protein levels of Pes1, Bop1 and WDR12 were analyzed by Western blot analysis. Lysates were made at day 3. (**D)** NIH3T3 cells were treated as described in A and presented as relative cell numbers compared to control siRNA-treated cells, which were set to 100%. Lysates for the corresponding Western blot analyses were made at day 3.

4.3 Expression of Pes1, Bop1 and WDR12 during differentiation and a possible role for self-renewal of ES cells

Much evidence points towards the notion that the high proliferation rate of ES cells is a property linked to their self-renewal capacity. As Pes1 and Bop1 seem to be essential factors for the proliferation of ES cells, the question arose whether Pes1 and Bop1 might have a function in the maintenance of pluripotency. Moreover, we were interested in the expression of Pes1, Bop1 and WDR2 during differentiation of ES cells, as cell cycle kinetics change and proliferation slows down during this process.

4.3.1 Downregulation of Pes1, Bop1 and WDR12 during differentiation

To investigate the expression of Pes1, Bop1 and WDR12 during differentiation, CGR8 cells were allowed to differentiate using the “hanging drop” protocol (Fig.11). For this procedure, undifferentiated CGR8 cells were trypsinized and transferred into medium without LIF. From this cell suspension, drops containing 500 cells were placed into the lid of bacteriological plates and kept upside down in an incubator for two days. During this time the cells start to form spheroid cell aggregates, also called embryoid bodies (EBs). At day 2, the EBs were harvested and further cultivated for 2-12 days in suspension. Alternatively, EBs can be transferred at day 4 or 6 to gelatinized 24-well plates for further cultivation. The differentiation process within EBs strongly reflects the differentiation processes taking place in a proper embryo. Cells differentiate via derivatives of the 3 germlayers of ectoderm, endoderm and mesoderm into lineage specific progenitors and finally into differentiated cells. The advantage of the “hanging drop” method is that the individual EBs develop similar in size and differentiate in a synchronous manner (Wobus et al., 1991).

To assess differentiation of CGR8 cells, EBs were harvested every second day, followed by RNA and protein isolation. One method to monitor the differentiation process is to investigate the expression of certain marker genes by real-time PCR. Therefore, RNA was transcribed into cDNA and analyzed for the expression of specific differentiation- and pluripotency-markers. The markers Oct4, Nanog, Sox2 and KLF4, which are indicative of pluripotency, were downregulated during the differentiation process, while Flk1, an early mesodermal marker, was upregulated, starting to express at day 4 (Fig.12A). T-bra, a gastrulation and early mesodermal marker, was induced at

day 4. Thus, the observed regulation of these markers confirmed differentiation of the cells.

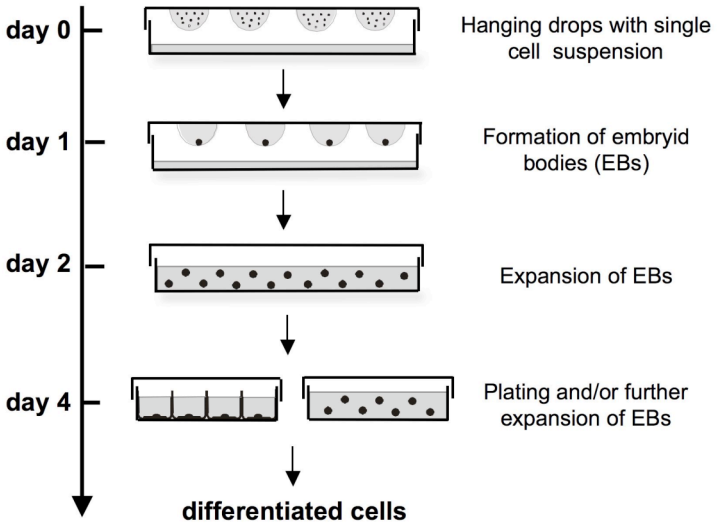

Figure 11: Differentiation of mouse ES cells by the "hanging drop" method. Undifferentiated CGR8 cells with 70-80% confluency were trypsinized, washed with PBS and resuspended in differentiation medium at a final concentration of 2.4 x 10^4 cells/ml. About 70 drops (20μl each) containing 500 cells were placed into the lid of a 10cm plate and incubated upside down for 2 days at 37°C, which leads to formation of embryoid bodies (EBs). At day 2, the EBs were transferred into bacteriological plates containing 10ml of differentiation medium and expanded there for at least two days. Then they were either plated into gelatine-coated 24-well plates or further expanded in the bacteriological plates for several more days. Medium was exchanged every second day. The cells within the EBs differentiated into ectodermal, endodermal and mesodermal cells.

Expression of Pes1, Bop1 and WDR12 was analyzed by Western blot analysis. The levels of all three proteins were downregulated at day 6 of differentiation (Fig.9B). Since ES cells start to adapt to a regulatory cell cycle during differentiation (White et al., 2005), expression and phosphorylation of Rb was determined. Rb switched from its mainly hyper-phosphorylated, inactive form, present in undifferentiated cells, to the hypo-phosphorylated, active form at day 6 of differentiation (Fig.9B), indicating a change towards a regulated Rb-E2F pathway at this stage of differentiation. Interestingly, at day 2 of differentiation a significant induction of the overall amount of Rb could be detected, mainly of the inactive form. A similar effect on Rb was detected after depletion of Pes1 and Bop1 in CGR8 cells (see Fig. 16A). This might suggest that depletion of Pes1 and Bop1 cause certain changes in ES cells, which could reflect a very early differentiation process.

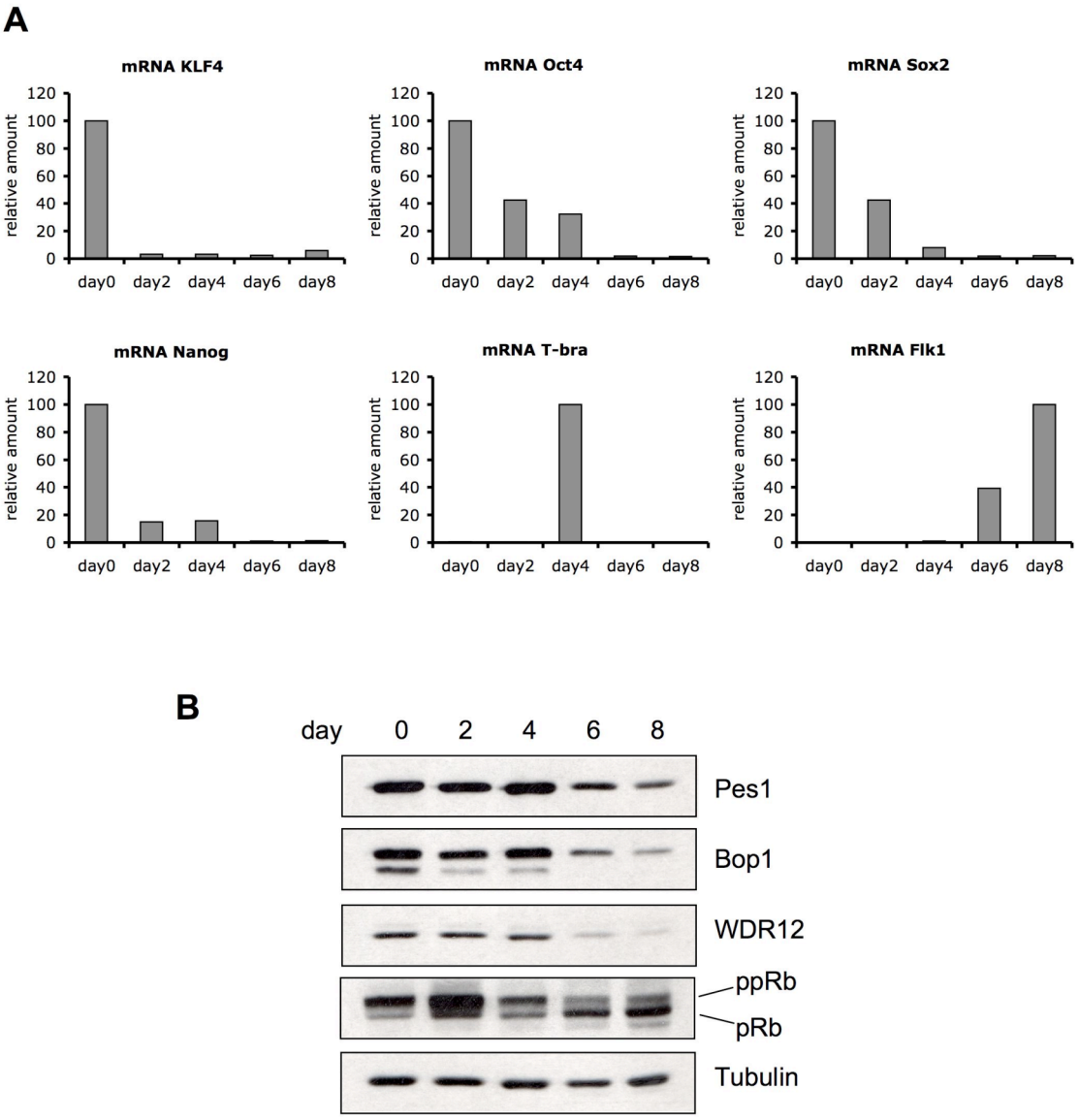

Figure 12: Pes1, Bop1 and WDR12 are downregulated during differentiation and Rb is hypo-phosphorylated. (A) Relative mRNA levels of the indicated genes during differentiation of CGR8 cells, measured by Light-Cycler analysis. Values were normalized to Aldolase. (**B)** Western blots monitoring expression of Pes1, Bop1, WDR12 and Rb during CGR8 cell differentiation. pRb: hypo-phosphorylated Rb; ppRb: hyper-phosphorylated Rb.

4.3.2 Expression of pluripotency markers in CGR8 cells after depletion of Bop1 or Pes1

The proposed link between proliferation and self-renewal of ES cells together with the above described results prompted us to assess whether the PeBoW-complex might be involved in the maintenance of pluripotency and/or whether depletion of Bop1 or Pes1 might induce an early differentiation process in ES cells.

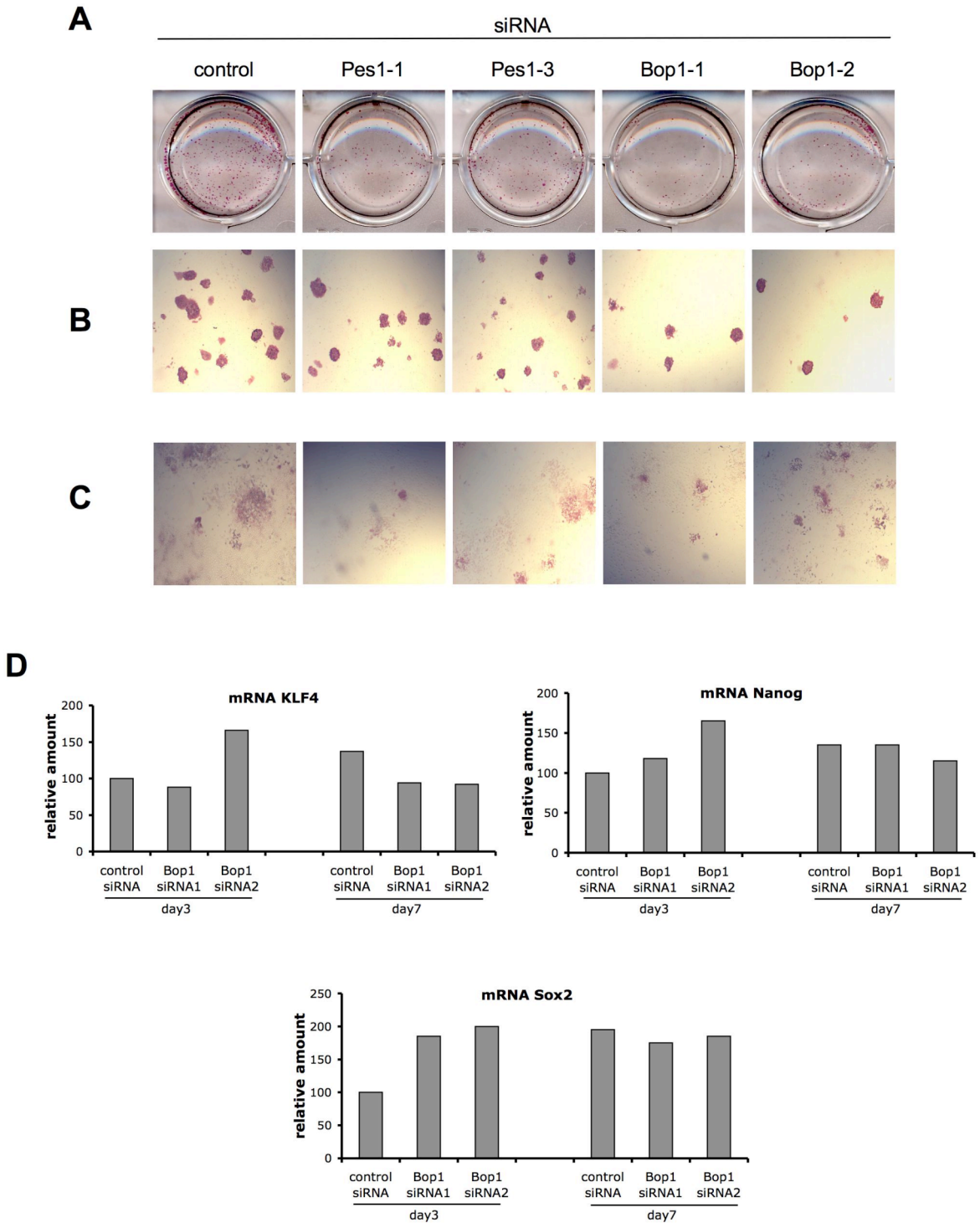

Figure 13: Expression of pluripotency markers after depletion of Pes1 or Bop1. (A) Alkaline phosphatase staining of CGR8 cell colonies. Cells were transfected twice with the indicated siRNA and plated one day after the second transfection to 6-well plates, followed by PFA fixation and AP-staining 5 days later. (**B)** A higher magnification of the images shown in A. (**C)** Cells were treated as in A but cultured without addition of LIF. **(D)** Relative mRNA levels from the indicated genes. CGR8 cells were transfected twice with the indicated siRNAs, RNA was isolated at day 3 and day 7, transcribed to cDNA and analyzed by Light-Cycler analysis. Values were normalized to Aldolase. Mean values of two independent experiments are shown.

One characteristic marker for the undifferentiated state of stem cells is high expression of alkaline phosphatase (AP). To examine AP expression, siRNA transfected cells were seeded at very low densities into 6-well plates and cultured for 5 days with or without addition of LIF to form colonies. Then, cells were analyzed for alkaline phosphatase activity by addition of a substrate, which is transformed by the enzyme into a colored dye. All colonies from control and Pes1- or Bop1-depleted cells that were cultured under addition of LIF stained positive for alkaline phosphatase activity, reflecting the undifferentiated state of the cells. The morphology of the colonies was small with tightly packed cells. Fewer colonies were present in the wells containing Pes1- or Bop1-depleted cells (Fig.13A, B). Cells that were cultured without addition of LIF formed much larger and more widespread colonies. Only about 50% of the cells stained positive for AP, usually the ones in the centre of a colony. Moreover, AP staining was less intense (Fig.13C). Wells with Pes1- and Bop1-depleted cells contained less cells, but no significant change in the morphology of the colonies nor in the intensity of AP staining was observed. This indicates that the early differentiation of Pes1- and Bop1-depleted cells is not disturbed.

In a next step, the mRNA levels of the pluripotency-markers Nanog, Sox2 and KLF4 were investigated. For this test, CGR8 cells were transfected twice with Bop1 and control siRNAs, followed by RNA isolation at day 3 and day 7 and Light-Cycler analysis. None of the three examined markers showed a significant downregulation in Bop1-depleted cells compared to cells transfected with control siRNA (Fig.13D). Although some variations in expression levels were observed, those were less than the differences between the controls at day 3 and 7 and therefore probably not significant. A corresponding downregulation of the same markers at day 2 of differentiation is shown in figure 12A. These first results argue against a change of the cells towards early differentiation upon depletion of Bop1.

4.3.3 Expression and phosphorylation of Rb during differentiation of Bop1-depleted CGR8 cells

Another assumption was that depletion of Pes1 or Bop1 might make CGR8 cells more prone to differentiation if exposed to a differentiation stimulus. This was investigated indirectly by examining the expression and phosphorylation levels of Rb, which were shown to be regulated during differentiation (compare to Fig.9). Bop1 and control siRNA transfected cells were differentiated one day after the second siRNA transfection via the

"hanging drop" protocol. Lysates of each day of differentiation were analyzed by Western blot for the expression and phosphorylation of Rb. The Rb pattern showed no change between Bop1 siRNA-treated and control siRNA-treated cells (Fig.14). In all samples an increase of the overall level of Rb levels was detected at day 1 and day 2 of differentiation and the switch to a predominant expression of the active, hypo-phosphorylated form took place at day 6. Indirectly, this first result points against a favored or faster differentiation of CGR8 cells after Bop1 depletion. However, to clearly argue against favored differentiation, bona-fide differentiation markers should be investigated in addition. Moreover, it has to be considered that the knockdown of Bop1 by siRNA technology is only transient. But as differentiation is a process over several days, a stable and also a more profound knockdown might be important for detectable effects.

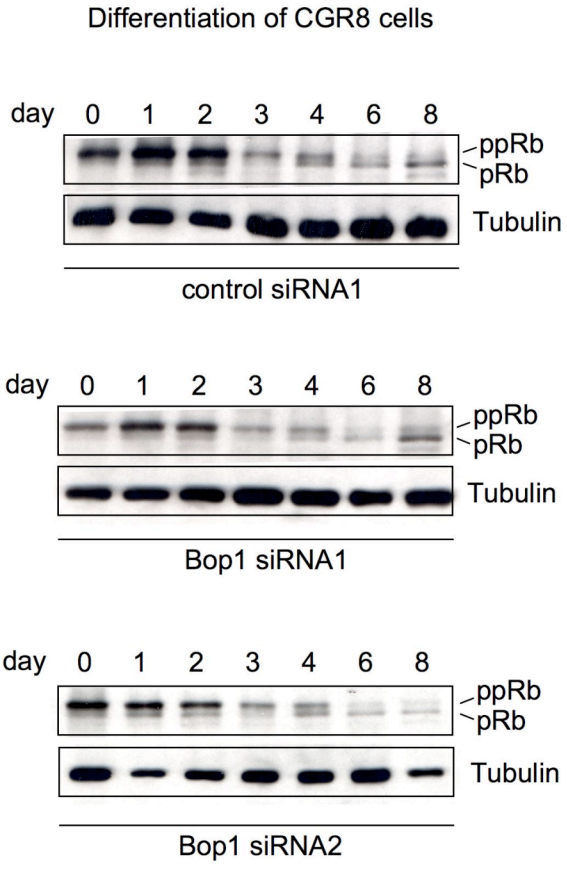

Figure 14: Expression and phosphorylation of Rb is not changed during differentiation of Bop1 depleted CGR8 cells. Cells were transfected twice with the indicated siRNAs and differentiated according to the "hanging drop" protocol, one day after the second siRNA transfection. Total cell lysates from day 1-4, 6 and 8 of differentiation were analyzed by Western blotting. pRb: hypo-phosphorylated Rb; ppRb: hyper-phosphorylated Rb.

4.4 Cross talk between ribosome biogenesis and proliferation of ES cells

4.4.1 Induction of the tumor suppressor p53 in CGR8 cells upon Pes1 and Bop1 depletion

There is strong evidence that nucleolar stress is related to cell proliferation. As we observed defects in ES cell proliferation as well as in rRNA maturation upon depletion of Pes1 and Bop1, we aimed to investigate a link of the two processes in ES cells. One important factor involved in a lot of cellular stresses is the transcription factor and tumor suppressor p53. In mature cells, p53 is induced upon inhibition of ribosome biogenesis and exerts a cell cycle arrest in G1-phase. In ES cells, the function of p53 is not clear. Inactivity of p53 and inability of the cells to undergo a G1-arrest was reported for example after DNA damage (Hong et al., 2004). To examine whether impaired ribosome biogenesis can activate a p53-dependent checkpoint in ES cells, the protein levels of p53 were analyzed by Western blot analysis after Pes1 and Bop1 knockdowns. The amount of p53 was highly induced in Pes1- and Bop1-depleted cells compared to control siRNA-treated cells (Fig.15). Again the intensity of p53 induction was in correlation with the knockdown efficiencies.

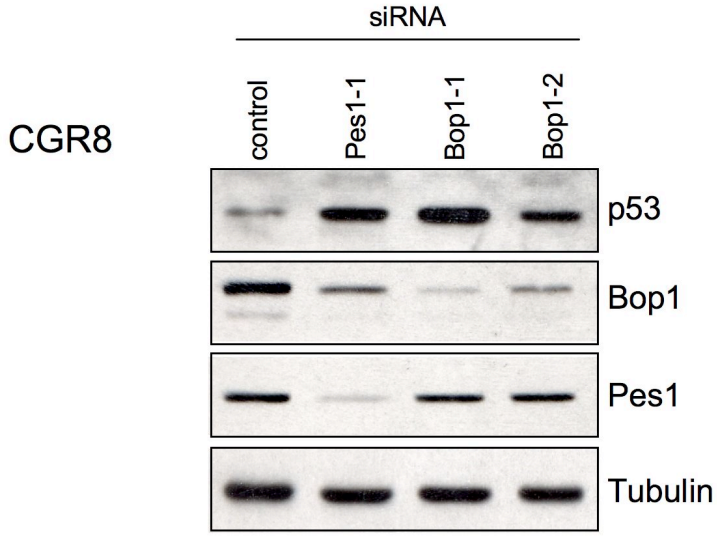

Figure 15: The tumor suppressor p53 is induced in CGR8 cells after depletion of Pes1 and Bop1. CGR8 cells were transfected twice with the indicated siRNAs. p53 protein levels were monitored by Western blot analysis at day 3. Pes1 (polyclonal Ab3) and Bop1 (polyclonal Ab1) are shown to monitor knockdown efficiency. α-tubulin served as loading control.

4.4.2 Investigation of apoptosis after Pes1 and Bop1 knockdown

Apoptosis and cell cycle arrest are two main pathways, which are regulated by p53. To assess whether one of the two mechanisms is activated by the p53 induction after depletion of Pes1 and Bop1, apoptosis and cell cycle distribution of CGR8 cells were analyzed. Apoptosis was investigated via annexin V staining and PARP cleavage.

4.4.2.1 Analysis of apoptosis by annexin V staining

First, the amount of apoptotic cells was examined via annexin V staining. Apoptosis or programmed cell death is an active process, which involves a variety of morphological changes like loss of membrane asymmetry, cell shrinkage and DNA fragmentation. Early features of cells, undergoing apoptosis, are changes in the plasma membrane including exposure of the phospholipid phosphatidylserine (PS) to the outer leaflet of the membrane. In viable cells, PS is located only on the cytoplasmic surface of the membrane. Annexin V is a phospholipid binding protein with high affinity to PS and can be used therefore for the detection of apoptotic cells, which expose PS. Positive stained cells can be counted by FACS analysis. In addition, cells were stained with propidium iodide (PI), which served to distinguish viable from dead cells. Dead cells are permeable for PI due to disruptions in their membrane, while viable cells can exclude PI. Cells that are negative for annexin V and PI staining represent viable cells; double positive cells represent dead cells that may have died by apoptosis or necrosis.
The positive control (cells treated with Actinomycin D) showed a more than 3-fold increase in annexin V positive cells as well as annexin V and PI double positive cells (Fig.16A,B). In contrast, Pes1- and Bop1-depleted cells showed no clear increase of annexin V positive or annexin V and PI double positive cells compared to cells treated with control siRNA. Annexin V staining was measured at day 3 and day 5 post siRNA transfections. A very weak increase of apoptotic cells could be detected for Bop1-depleted cells at day 3 and for Pes1 siRNA3-treated cells (Fig.16A,B). Surprisingly, the controls also showed quite strong variations in the amount of dead cells. One explanation might be the use of different batches of cells for the experiments with Pes1 depletion compared to the experiments after Bop1 depletion, which were performed independently. The increase in dead cells at day 5 might be related to passaging of cells at day 3/4.

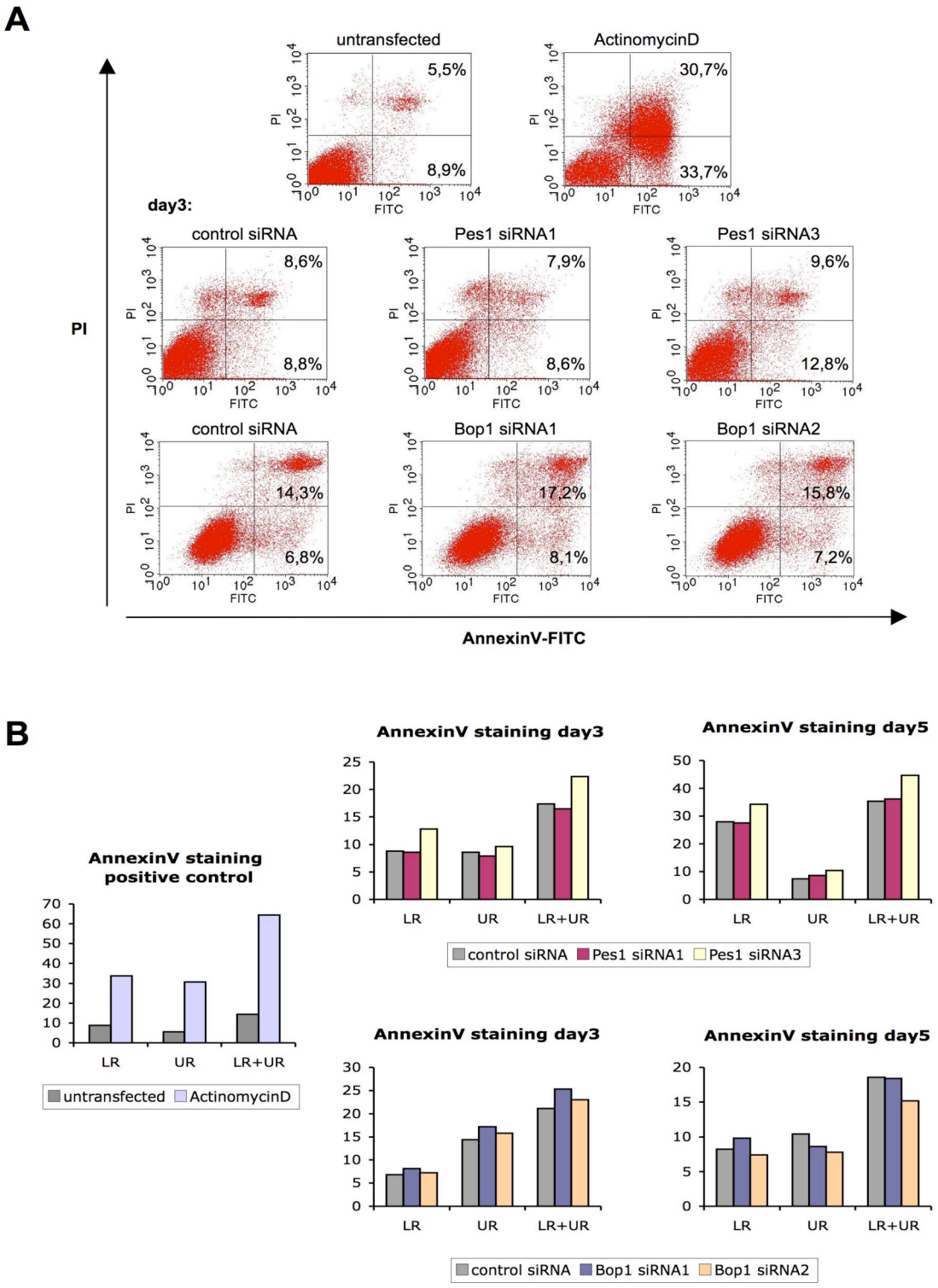

Figure 16: Analysis of cell death after Pes1 and Bop1 depletion. CGR8 cells, transfected twice with the indicated siRNAs, were stained with annexin V and propidium iodide (PI) and analyzed by FACS. Actinomycin D treated cells (overnight with 20nM) served as positive control. (**A)** Dot blots of annexin V/PI stained cells at day 3**. (B)** Results from day 3 and day 5 shown as diagram with LR representing the percentage of annexin V positive cells and UR representing annexin V and PI double positive cells. LR: lower right quadrant, UR: upper right quadrant from the respective dot blots.

4.4.2.2 Analysis of PARP cleavage to examine apoptosis

To verify the absence of a detectable effect on apoptosis, indicated by Annexin V staining, another assay was performed, investigating the cleavage of poly(ADP-ribose)-polymerase (PARP). PARP is involved in DNA damage and repair mechanisms. During apoptosis PARP is cleaved by the protease caspase-3 from the native 116kDa protein into an 85kDA and a 24kDa fragment.

Consistent with the negative results from the annexin V staining, no increase in the cleaved 85kDa form of PARP was observed compared to control siRNA-treated cells after Pes1 or Bop1 knockdowns (Fig.17, lanes 1-6). Actinomycin D treated cells showed an induction of the 85kDA form, which served as positive control (Fig.17, lanes 7-8). A small amount of the 85kDA form could be detected in all transfected cells. Most likely, this is due to a certain amount of apoptosis induced by the transfection stress.

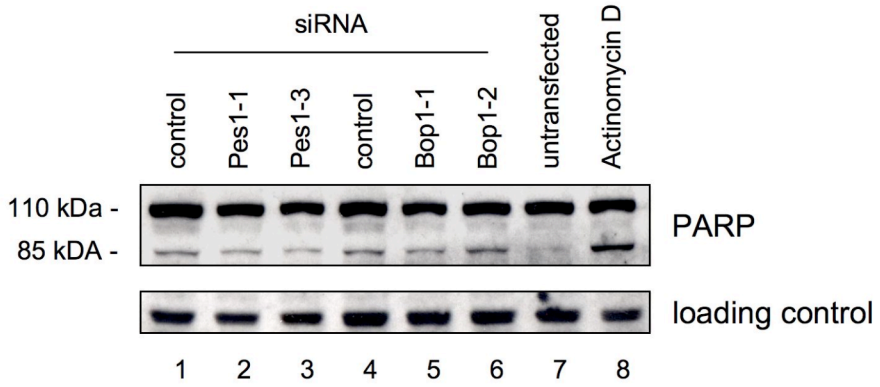

Figure 17: PARP cleavage into the 85kDa fragment is not enhanced upon depletion of Pes1 and Bop1. CGR8 cells were transfected twice with the indicated siRNAs, harvested at day 3 including supernatants, followed by Western blot analysis for detection of PARP. Untreated cells were included as negative control, Actinomycin D treated cells (20nM overnight) as positive control. An unspecific band served as loading control.

4.4.3 Cell-cycle distribution of CGR8 cells after Pes1 and Bop1 depletion

Next, the cell cycle profile of embryonic stem cells was investigated after depletion of Pes1 and Bop1. CGR8 cells were transfected twice with the respective siRNAs and labeled for 30 minutes with 10µM bromodeoxyuridine (BrdU) at day 3 (compare Fig.7A). BrdU is a thymidine analogue, which is incorporated into newly synthesized DNA. Incorporated BrdU was then stained with an anti-BrdU antibody and positive cells were counted by FACS analysis. In parallel, cells were stained with 7-AAD (7-amino

actinomycin D) to measure the DNA content. 7-AAD intercalates into DNA and can be used in place of PI. Its advantage over PI is a minimal spectral overlap with PE and FITC. Pes1- and Bop1-depleted cells showed a slight decrease of cells in S-phase compared to control siRNA-treated cells (Fig.18). In turn, there was a slight increase of cells in G1-phase. BrdU labeling at day 4 showed similar results (data not shown).

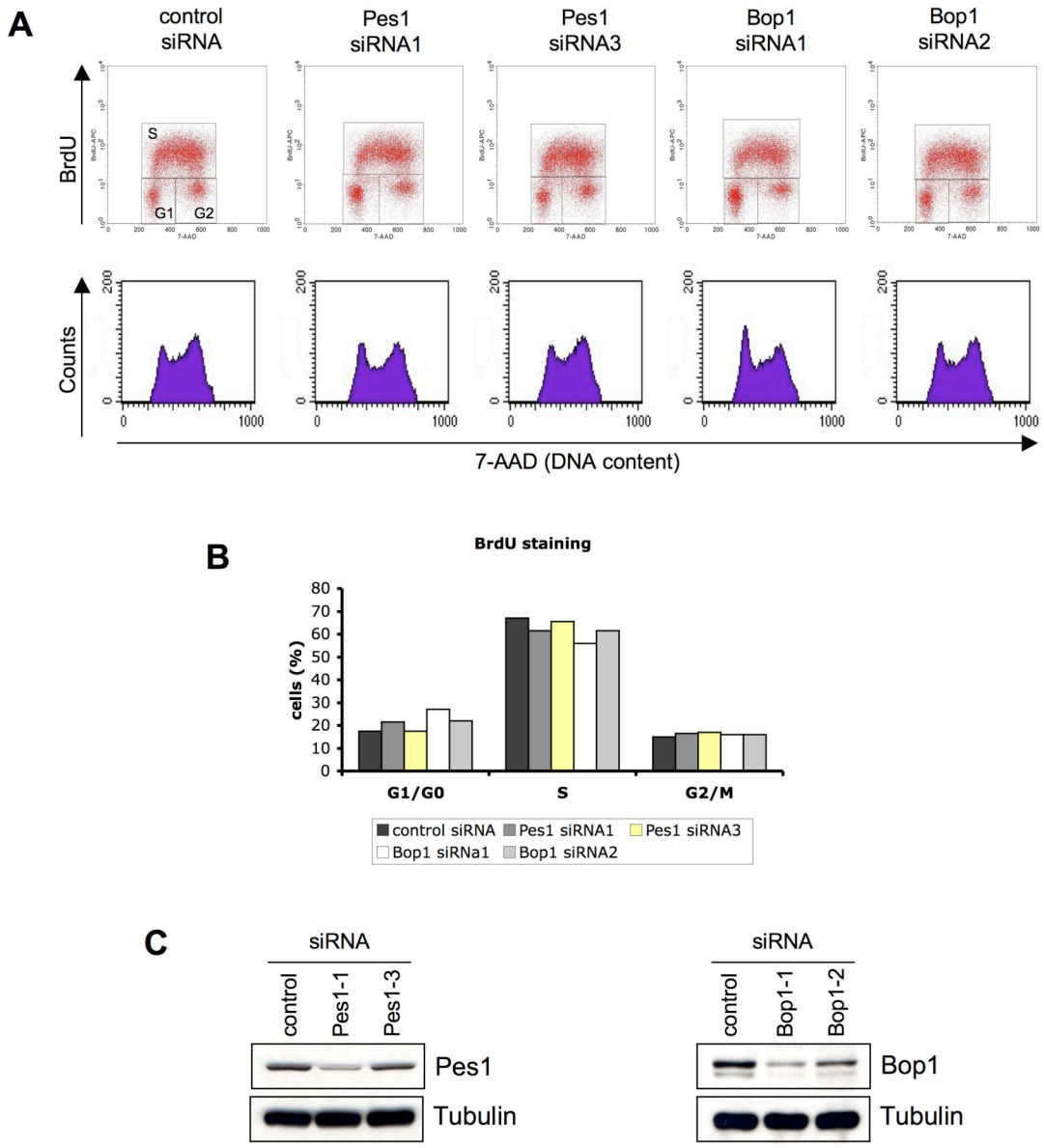

Figure 18: Cell cycle profiles of Pes1 and Bop1 depleted cells, measured by BrdU staining. CGR8 cells were transfected twice with the indicated siRNAs. At day 3, proliferating cells were labeled for 30 minutes with 10µM BrdU, fixed, stained with an anti-BrdU antibody and PI and analyzed by FACS analysis. (**A)** Representative dot blots and histograms of BrdU- and PI-labeled cells with the indicated knockdowns. Cells with a DNA content between 2N and 4N are shown. (**B)** Diagram of the percentage of cells in G1/G0-, S-, and G2/M-phase. Mean values of two independent experiments are shown. Values were calculated using Cell Quest software. (**C)** Respective knockdown efficiencies.

4.4.4 Induction of the retinoblastoma tumor suppressor gene product Rb in CGR8 cells after depletion of Pes1 and Bop1

To further elucidate a putative p53-mediated response mechanism, phosphorylation of the tumor suppressor Rb was investigated, which is one main factor involved in cell cycle arrest. After cellular stress, Rb is usually activated via the p53-p21 pathway. CGR8 and NIH3T3 cells were transfected twice with siRNAs against Pes1, Bop1 and control siRNA. Two days after the second transfection, cells were harvested and Rb was monitored by Western blot analysis. After depletion of Pes1 and Bop1, a strong increase in the overall amount of Rb was observed in both cell lines. In CGR8 cells, the main increase was interestingly in the hyper-phosphorylated, inactive form of Rb (Fig.19A). In addition, a slight increase in the hypo-phosphorylated, active form was visible, which is involved in the regulation of the cell cycle and a G1-checkpoint. The weak increase of cells in G1- and the corresponding decrease of cells in S-phase upon depletion of Pes1 and Bop1 (compare Fig.18) might be correlated with this slight increase of hypo-phosphorylated Rb. The role of the induction of hyper-phosphorylated Rb remains to be elucidated.
In contrast to ES cells, an induction of hypo-phosphorylated, active Rb was observed in NIH3T3 cells after depletion of Pes1 and Bop1, but no increase in hyper-phosphorylated, inactive Rb (Fig.19B). This indicates a functional checkpoint response in those cells, leading to an Rb-mediated arrest of cells in G1-phase.

4.4.5 The cell cycle inhibitor p21 is undetectable in CGR8 cells after depletion of Pes1 or Bop1

To further examine the role of the p53 induction after Pes1 and Bop1 depletion in CGR8 cells, samples of the lysates shown in figure 16A were examined for the Cdk-inhibitor p21. As a direct target gene of p53, p21 can serve to measure the transcriptional activity of p53. On the respective Western blot p21 was hardly detectable even after prolonged exposure times. In Actinomycin D treated NIH3T3 cells, which served as positive control, a strong band could be detected at the expected position of the blot (Fig.19C) even though NIH3T3 cells expressed much lower levels of p53 than CGR8 cells. These data indicate that p53 might not be fully active in CGR8 cells despite its strong induction. To investigate p53 transcriptional activity in more detail, mRNA levels

of p21 should also be examined. Additionally, other mechanisms like promoter silencing or proteasomal degradation of p21 might be explanations why the protein levels of p21 are not induced. Overall, the data support the notion that the p53-p21 pathway, which usually leads to a G1-arrest in mature cells, might not be functional in CGR8 cells after depletion of Pes1 or Bop1.

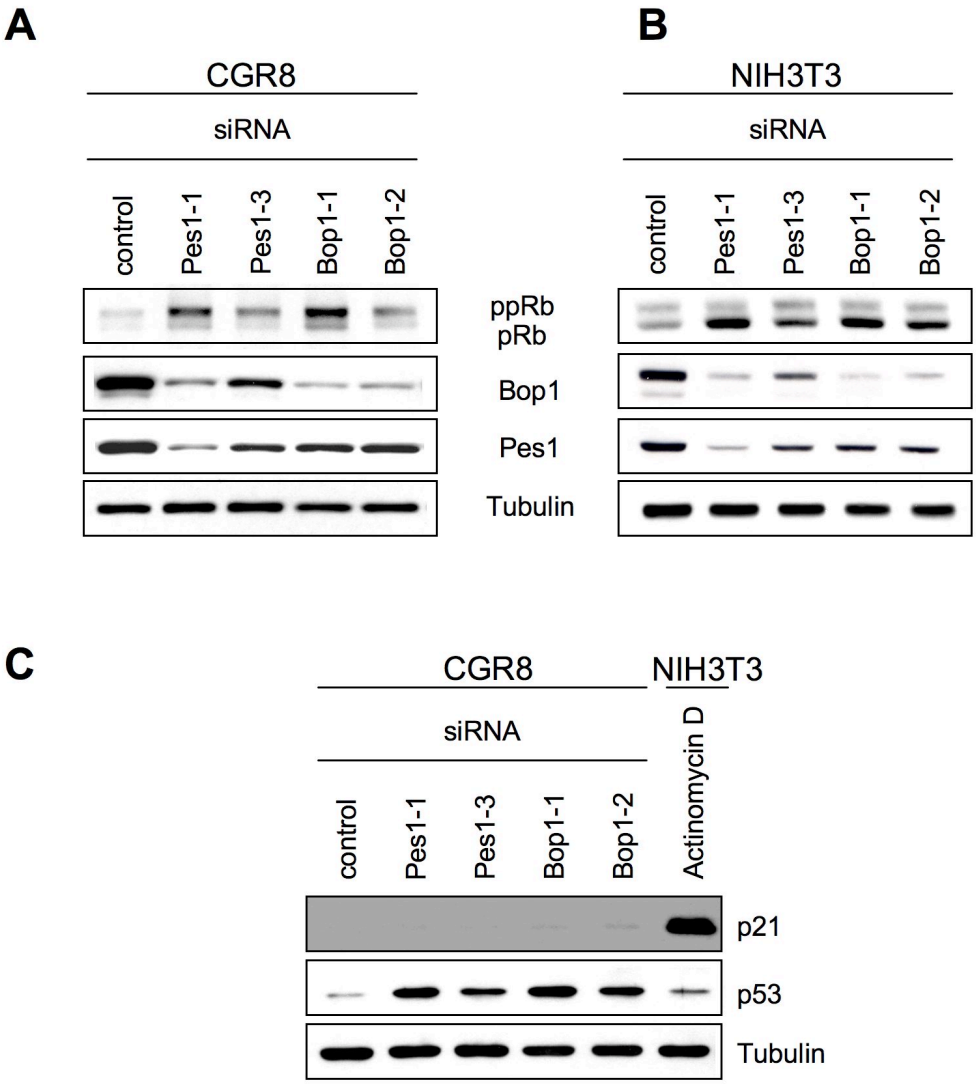

Figure 19: Regulation of Rb, p21 and p53 after Pes1 and Bop1 knockdowns. CGR8 **(A)** and NIH3T3 cells **(B)**, transfected twice with the indicated siRNAs, were harvested at day 3 and expression of Rb was detected by Western blot analysis. Detection of Pes1 and Bop1 confirmed functional knockdowns and α-tubulin verified equal loading. (**C)** The samples from A were monitored for p21 and p53 expression. NIH3T3 cells, treated overnight with 20nM of Actinomycin D, served as positive control. pRb: hypo-phosphorylated Rb; ppRb: hyper-phosphorylated Rb.

4.5 Use of 5-fluorouracil as potent inhibitor of ribosome biogenesis to investigate a possible checkpoint activation in mouse ES cells

Throughout the experiments it was observed that siRNA technology does not work as efficiently in ES cells as in other cell types. Based on the number of GFP-positive cells after transfection with an appropriate expression vector, we estimate that about 70% of the cells can be reached by transfection (Fig.7E). Moreover, since ES cells proliferate very rapidly, siRNA effects would be more transient than in other cells because siRNAs will be quickly diluted out and normally proliferating cells will rapidly overgrow transfected, arrested cells. To overcome these limitations, we studied the effects of a strong nucleolar stress on ES cells to independently assess a possible link between ribosome biogenesis and proliferation in ES cells. To this end, we used the chemotherapeutic agent 5-Fluorouracil (5FU), which is a cytotoxic drug used for the treatment of a variety of solid tumors. Its anti-tumor effect is, at least in part, due to the induction of a p53-dependent cell cycle arrest and apoptosis. At low concentrations (10μM-100μM) 5FU was shown to activate p53 by inhibition of rRNA processing and induction of ribosomal stress, while higher concentrations (100μM-500μM) lead to DNA damage and phosphorylation of p53 at serine 15, possibly due to ATM activation (Gilkes et al., 2006).

4.5.1 Block of rRNA processing and inhibition of CGR8 cell proliferation upon 5FU-treatment

Treatment of CGR8 cells with 10μM and 20μM of 5FU for 22 hours resulted in a major inhibition of rRNA processing analyzed by in vivo labeling of newly synthesized rRNA with radioactive ^{32}P-orthophosphate. Both concentrations of 5FU blocked the maturation of 18S as well as 28S rRNA completely (Fig.20). Moreover, already the maturation of the 36S and 32S rRNA intermediates was strongly reduced. Instead, a slight increase of the 45/47S precursor was detected.

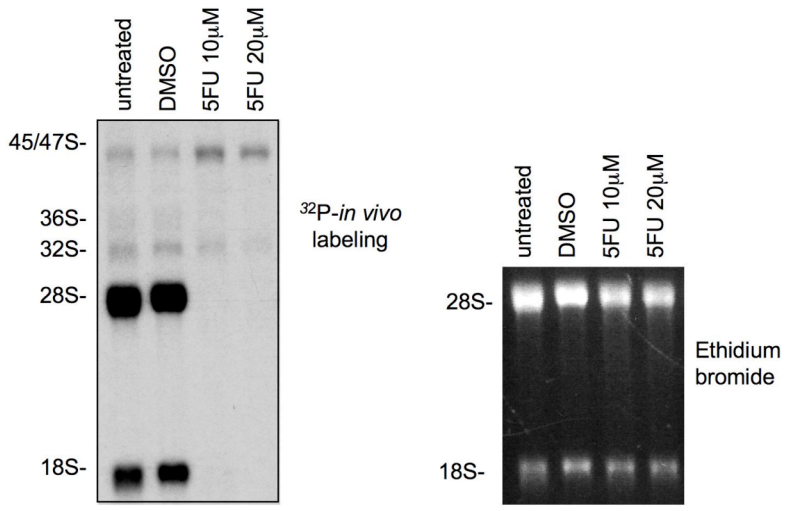

Figure 20: 5FU treatment blocks rRNA processing. CGR8 cells were treated overnight with 10μM and 20μM 5FU, with DMSO (4μl/ml medium) or left untreated. After starvation for 30 minutes in phosphate-free medium cells were pulse-labeled for 1 hour with ^{32}P-orthophosphate, followed by a chase of 3-4 hours. Equal amounts of isolated RNA were resolved on a 1% formaldehyde gel and visualized by autoradiography. Labeled rRNAs are indicated. As loading control, whole RNA was stained with ethidiumbromide.

Cell proliferation of CGR8 and NIH3T3 cells was strongly reduced after 5FU treatment, as shown by GIEMSA staining of cells after fixation with methanol (Fig.21). Staining of control and DMSO-treated cells was much more intensive due to more cells per 6-well plate. Inhibition of cell proliferation was comparable between CGR8 and NIH3T3 cells.

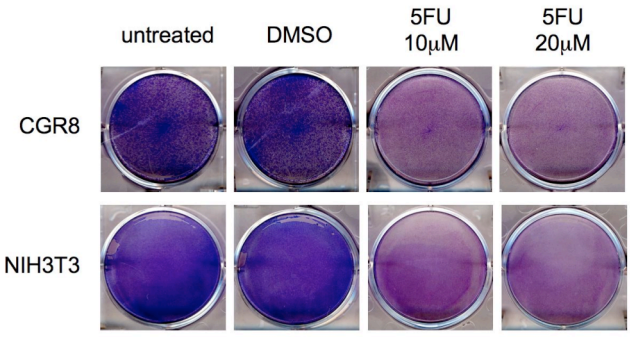

Figure 21: 5FU inhibits cell proliferation. CGR8 and NIH3T3 cells were seeded at equal densities in 6 well plates and treated for 48 hours with 10μM and 20μM 5FU, DMSO (4μl/ml medium) or left untreated. To estimate the amount of cells per well, cells were fixed with methanol and stained with GIEMSA.

4.5.2 Strong induction of p53 and Rb but not p21 upon treatment of CGR8 cells with 5FU

Treatment of CGR8 cells with 5FU resulted in a strong induction of p53 protein levels. Levels of p21 proteins were only marginally induced, with the bands detectable only after an exposure time of 30 minutes or longer (Fig.22 lanes 1-4). Moreover, 5FU-treated CGR8 cells showed an extensive induction of total Rb protein levels with the main increase in the hyper-phosphorylated, inactive form of Rb (ppRb). Conversely, only a weak induction of hypo-phosphorylated, active Rb (pRb) was observed (Fig.22, lanes 1-4). The overall ratio between ppRb:pRb was unchanged. The fact that the ratio was not changed towards active pRb is in line with the impaired induction of p21 that usually inhibits the activities of cyclin/Cdk complexes, which are involved in Rb phosphorylation. Overall, much higher amounts of total Rb seem to be present in CGR8 cells compared to NIH3T3 cells in opposite to the p21 levels, which are undetectable in CGR8 control cells.

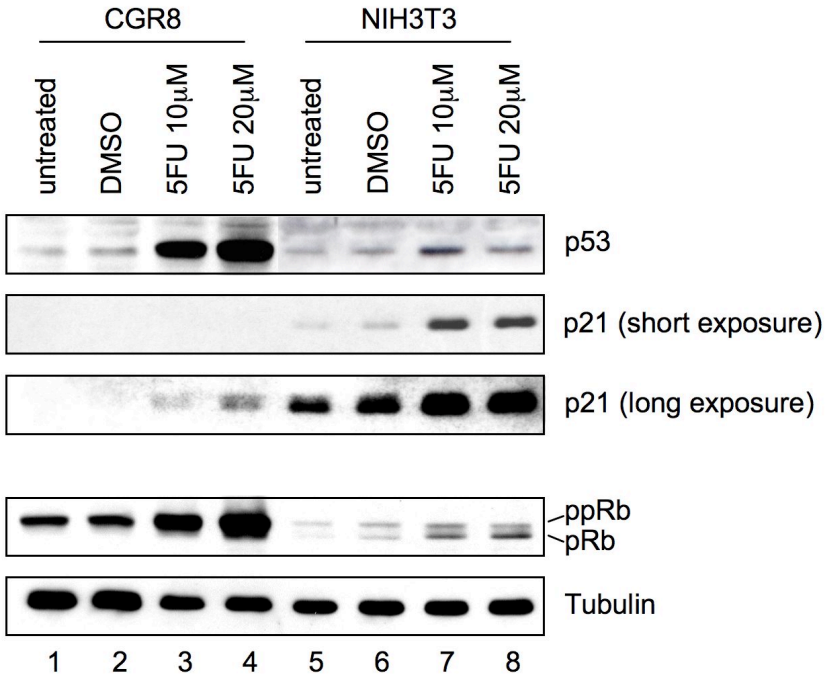

Figure 22: Regulation of Rb, p21 and p53 after 5FU treatment of CGR8 and NIH3T3 cells. CGR8 and NIH3T3 cells were treated with 10μM and 20μM 5FU or DMSO (4μl/ml medium) for 22 hours or left untreated. Total cell lysates were monitored by Western blot analysis for protein levels of p53, p21 and Rb. α-tubulin served as loading control. pRb: hypo-phosphorylated Rb; ppRb: hyper-phosphorylated Rb.

In contrast to ES cells, p21 was highly induced in NIH3T3 cells upon 5FU treatment. In line with this finding, NIH3T3 cells showed an increase in active pRb but not inactive ppRb, compared to an equal, weak expression of pRb and ppRb in untreated and DMSO treated cells. Interestingly, only a very weak induction of p53 was detected (Fig.22, lanes 5-8). Hence, it seems that additional factors might be involved in the induction of p21 in NIH3T3 cells.

4.5.3 Nuclear localization of induced p53

As p53 induction in CGR8 cells after 5FU treatment did not lead to the expected robust induction of p21 or to strong hypo-phosphorylation of Rb, the localization of p53 was investigated. Published data indicated cytoplasmic localization and therefore transcriptionally inactive p53 after cellular stresses like DNA damage (Aladjem et al., 1998; Hong and Stambrook, 2004). Indirect immunofluorescence analysis confirmed an upregulation of p53 protein levels in CGR8 cells and showed also a weak induction in NIH3T3 cells after treatment with 10μM and 20μM of 5FU. The overall expression of p53 in 5FU-treated and non-treated cells was much stronger in CGR8 cells than in NIH3T3 cells (Fig.23A,B). In both cell lines localization of p53 was mainly nuclear. Therefore, the cellular localization cannot explain the lack of p21 upregulation, suggesting a different deficit in inductive mechanisms.

4.5.4 Accumulation of CGR8 cells in S-phase after incubation with 5FU

Next, the cell cycle profiles of CGR8 and NIH3T3 cells after 5FU treatment were monitored. Cells were incubated for 22h and 46h with or without 5FU, followed by FACS analysis of PI stained cells. NIH3T3 cells accumulated in G1- and S-phase with an increase of cells in G1-phase after 22h and 46h of 5FU treatment (Fig.24A). The amount of cells in G2/M-phase was reduced. In contrast, CGR8 cells showed an accumulation of cells in S-phase after 46h of 5FU treatment. After 22h an accumulation at the G1/S-phase boarder was detected (Fig.24B). As the discrimination between G1- and S-phase was difficult in CGR8 cells after PI-staining, due to the high percentage of ES cells in S-phase, the experiment was repeated with BrdU-labeling. BrdU is incorporated into newly synthesized DNA and therefore marks cells within the S-phase.

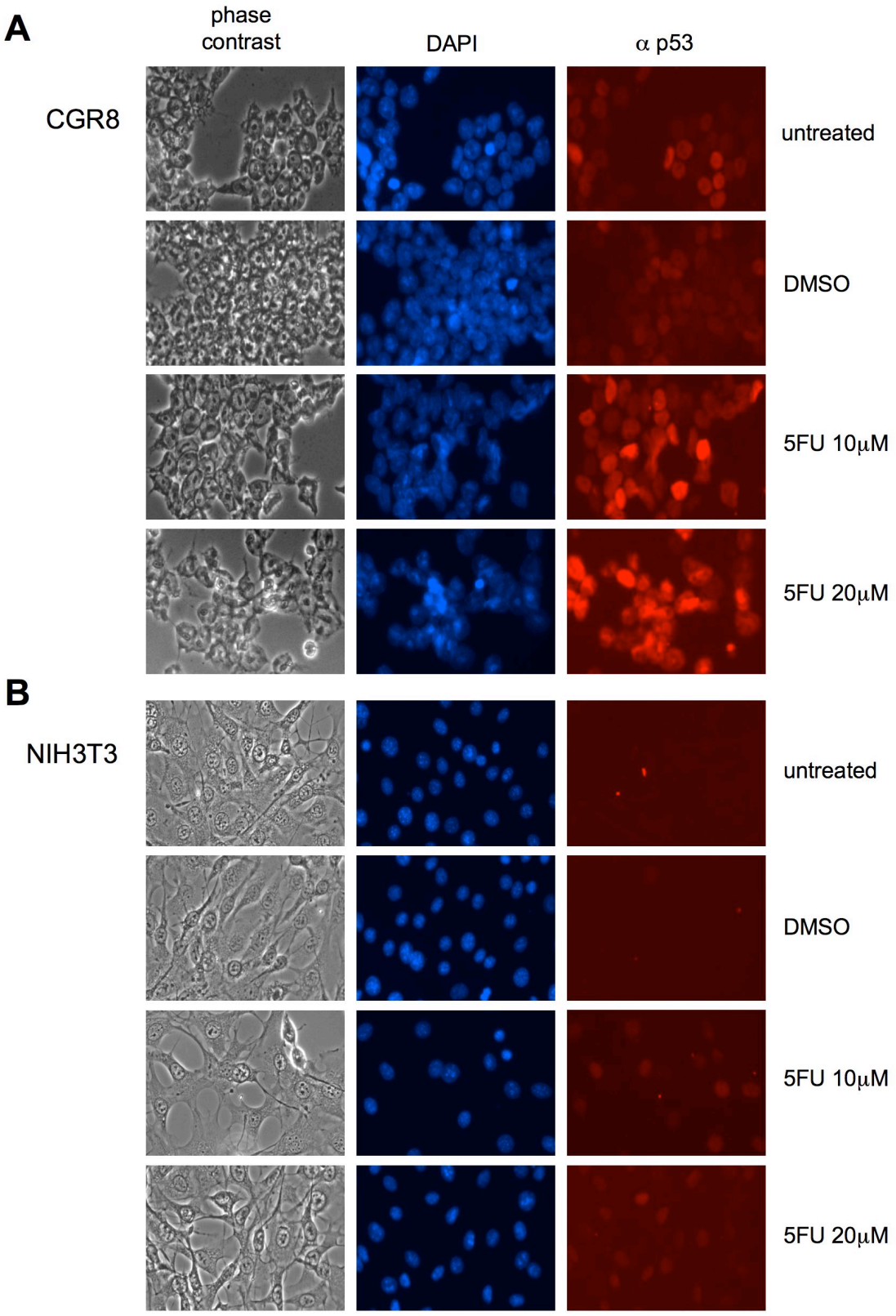

Figure 23: Nuclear localization of p53 in CGR8 and NIH3T3 cells after 5FU treatment. CGR8 **(A)** and NIH3T3 cells **(B)** were treated with 10μM and 20μM 5FU or DMSO (4μl/ml medium) for 22 hours or left untreated. Next, cells were fixed with methanol (CGR8 cells) or methanol/aceton (NIH3T3 cells) and analyzed by indirect immunofluorescence for p53. Nuclei were counterstained with DAPI.

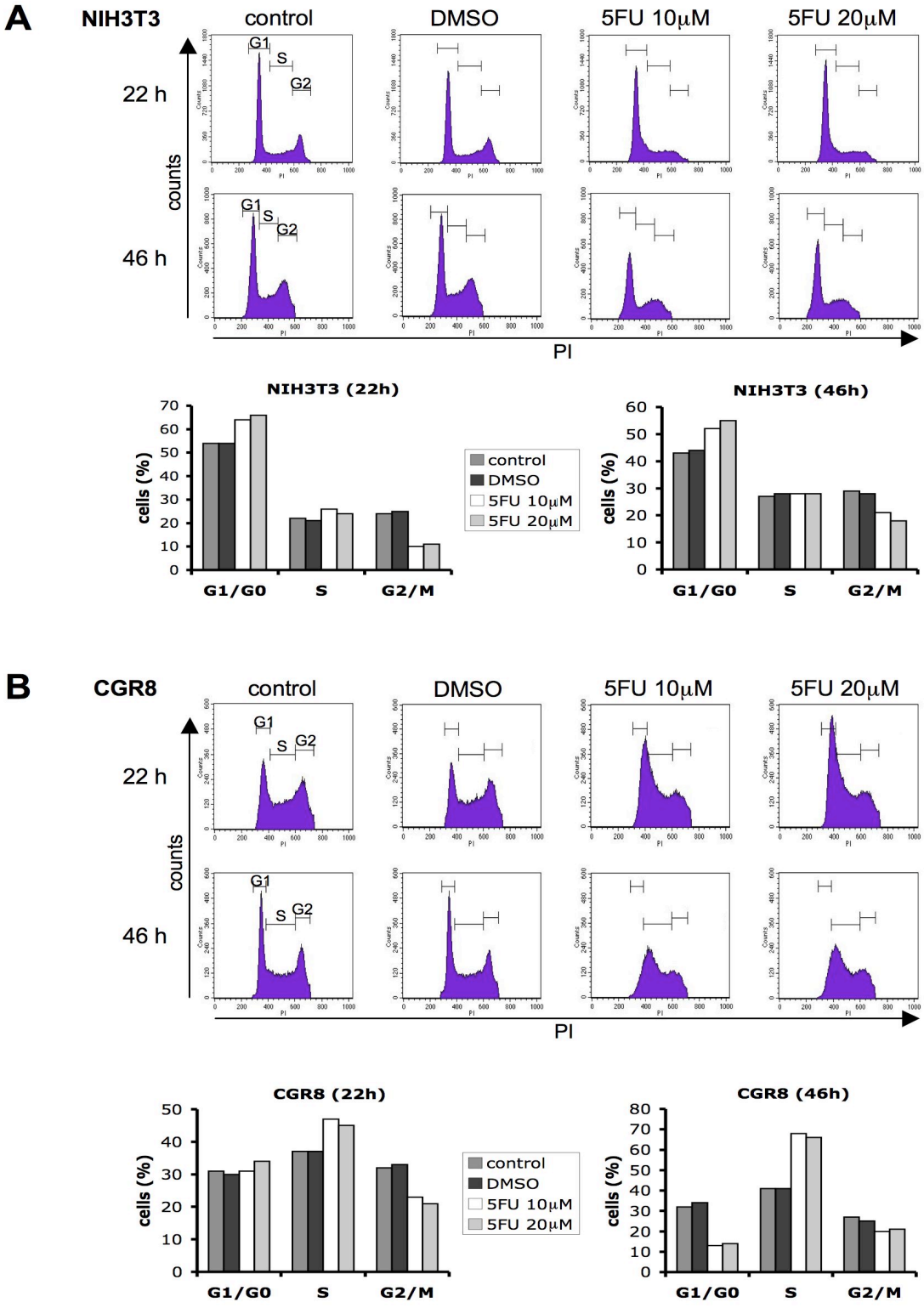

Figure 24: Cell cycle profiles of 5FU-treated CGR8 and NIH3T3 cells analyzed by PI staining. NIH3T3 and CGR8 cells were incubated with 10µM and 20µM of 5FU or DMSO (4µl/ml medium) for 22 hours and 46 hours, respectively, or left untreated. After fixation with EtOH, the DNA content of the cells was evaluated with PI staining and FACS analysis. (**A)** Histograms of cell cycle profiles of NIH3T3 cells and quantitative evaluations, indicating the percentage of cells in G1/G0-, S- and G2/M-phase. Cells with DNA content between 2N and 4N are shown **(B)** As described in A but for CGR8 cells. Calculations were performed using the program Cell Quest.

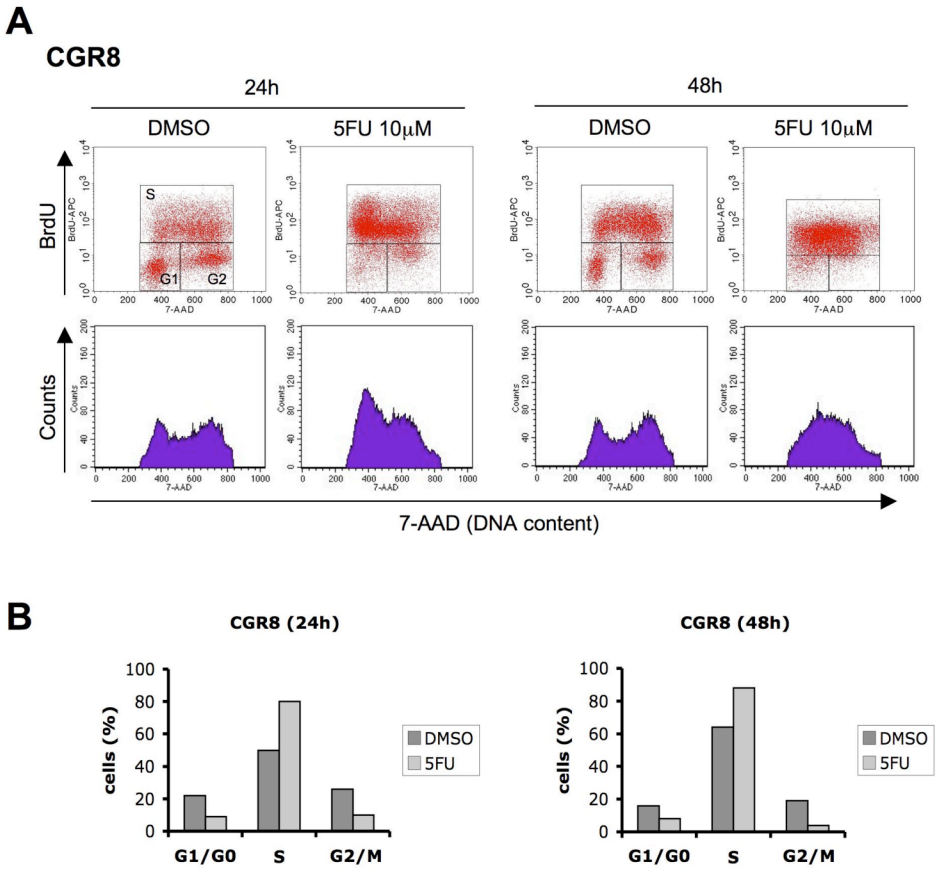

Figure 25: Cell cycle profiles of 5FU-treated CGR8 cells analyzed by BrdU labeling. CGR8 cells were incubated with 10μM 5FU and DMSO (4μl/ml medium) as control for 24 hours and 48 hours, respectively. Cells were labeled for 30 minutes with 10μM BrdU, fixed, stained with an anti-BrdU antibody and 7-AAD and analyzed by FACS analysis. (**A)** Dot blots and respective histograms of BrdU and 7-AAD labelled cells with a DNA content between 2N and 4N **(B)** Quantitative evaluation representing the percentage of cells in G1/G0-, S- and G2/M-phase. Calculations were performed with Cell Quest.

BrdU-positive cells can be subsequently detected by antibody staining and measured by FACS analysis. BrdU-labeling showed an accumulation of CGR8 cells in early S-phase after 24h of 5FU treatment (Fig.25). Cells in G1- and G2/M-phase were reduced according to this assay. After 48h, the majority of cells were in S-phase, but the intensity of the BrdU incorporation was reduced compared to control cells. Nevertheless, the cellular DNA content increased since the measurement after 24h of 5FU treatment. Hence, it seems that replication still took place, as the large majority of cells showed BrdU-incorporation, but it appears to have been hindered. In summary, these results support the hypothesis of an impaired p53-p21-Rb pathway in CGR8 cells, as was already indicated by the depletion studies with Pes1 and Bop1. Upon 5FU treatment, this is additionally reflected by a missing - or at least poorly established and only transient - G1-arrest.

5 DISCUSSION

For efficient proliferation, cells have to coordinate the increase in cell mass with cell division. Deregulation of the two processes is involved in a variety of pathological conditions like cancer, developmental defects and metabolic disorders. The molecular mechanisms controlling the coordination of both processes are still at the onset of investigation. Nevertheless, mutual regulations between cell cycle progression (i.e., cell division) and ribosome biogenesis (one major factor of cell growth) have been described. Embryonic stem (ES) cells display very rapid proliferation, which is slowed down during differentiation. Their high proliferation potential is coupled to an unusual cell cycle, which lacks a regulated G1/S-phase transition. These specific features are strongly suggested to be involved in the maintenance of the self-renewal properties of ES cells. In culture, ES cells show an unlimited proliferation potential without being immortalized. Moreover, similar to tumor cells, they do not undergo senescence, do not show contact inhibition and can grow without serum. Hence, understanding proliferation of ES cells will also further shed light on mechanisms involved in self-renewal and improve our knowledge about transformed cells.
During this work, the expression, complex formation and function of the proteins Pes1, Bop1 and WDR12, which were shown to play a role in ribosome biogenesis and proliferation of mature cells, were examined in ES cells. Thereby, it was aimed to investigate the relation of ribosome biogenesis with proliferation, self-renewal and differentiation of ES cells.

5.1 Nucleolar localization and complex formation as essential factors for functionality of Pes1, Bop1 and WDR12

At the initial stages of this work, the expression and physical interaction of murine Pes1, Bop1 and WDR12 were investigated in the ES cell line CGR8 and the mouse fibroblast cell line NIH3T3. Localization of the proteins was predominantly nucleolar in both cell types. In line with this finding, a function of the proteins for rRNA processing during ribosome biogenesis was confirmed (see chapter 5.2). Murine Pes1, Bop1 and WDR12 were shown by native gel electrophoresis to form a stable complex, including all three

proteins. Taking a look at the protein structure of Pes1, Bop1 and WDR12 reveals that all three proteins contain protein-protein interaction domains.

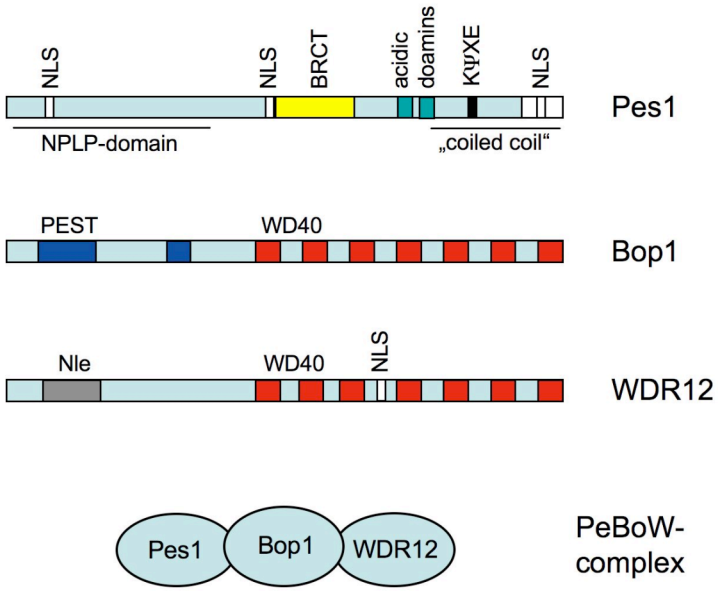

Figure 26: Schematic overview of the protein structures of Pes1, Bop1 and WDR12 and of the PeBoW complex. Pes1 contains a highly conserved N-terminal pescadillo-like domain (NPLP-domain), a BRCT (BRCA1 C-terminal) domain, often involved in protein-protein interactions, and three classical nuclear localization signals (NLS). The C-terminus forms a “coiled coil” structure and contains two acidic stretches of amino acids, a consensus site for sumoylation (KΨXE) and six bipartite NLS. Bop1 contains two PEST sequences, which are often associated with short-lived, regulatory proteins, and seven WD40 domains, usually involved in the formation of multiprotein complexes. WDR12 contains a Notchless-like (Nle) domain at the N-terminus, a NLS and seven WD40 units, which are supposed to form a β-propeller structure. Bop1 is proposed to constitute the core component of the PeBoW-complex, interacting directly with Pes1 and WDR12, which itself interact only indirectly with each other via Bop1.

Pes1 contains a BRCT domain, which is known to facilitate phosphorylation-dependent protein-protein interactions. Bop1 and WDR12 contain several WD40 repeats respectively, which were also reported to be involved in protein-protein interactions and in the formation of multiprotein complexes. Mutations in the WD40 domains of human WDR12 and the BRCT domain of human Pes1 caused aberrant cytoplasmic and nucleoplasmic localization and instability of the proteins, thereby arguing for a defect in complex formation upon loss of those domains (Grimm et al., 2006; Haque et al., 2000; Holzel et al., 2007; Holzel et al., 2005; Strezoska et al., 2000; Strezoska et al., 2002). Hence, the structural properties of the proteins are in support of the detected complex

formation. Further, our results are in consistency with the described complex formation of the human homologues of Pes1, Bop1 and WDR12 (Holzel et al., 2005; Rohrmoser et al., 2007). Whether the complex, detected by native gel electrophoresis, contains additional proteins cannot be excluded, but the fact that stringent conditions for the identification of stable core complexes were used for cell lysis would argue against additional components, which would be expected to bind less stringently. In yeast, a potential homologue of the PeBoW-complex was shown to constitute the core of a bigger complex, involving a variety of other factors, the majority of which is related to ribosome biogenesis, replication and cell cycle regulation (Du and Stillman, 2002; Miles et al., 2005). In mammals such a complex could not be detected so far. However, our data do not exclude this possibility as other proteins may bind *in vivo*, but less stringently or under specific circumstances.

Recent results in our lab revealed that complex formation of human Pes1, Bop1 and WDR12 is an important parameter in the stability and functionality of the proteins. It seems that Bop1 is the core component of the complex, interacting directly with Pes1 and WDR12, while Pes1 and WDR12 interact indirectly with each other via Bop1. Free proteins seem to be highly unstable (Rohrmoser et al., 2007). The results obtained during this work further strengthen this notion since they show a similar behavior of the murine proteins, as no free Pes1 or Bop1 proteins were observed by native gel electrophoresis. Only murine WDR12 showed a substantial amount of free protein, indicating an additional function of WDR12, independent of incorporation into the PeBoW-complex. This was not observed at such intensities in human cell lines. Further, interdependency of the protein levels of murine Pes1 and Bop1 was observed. Depletion of Pes1 by siRNA technology also reduced protein levels of Bop1 and vice versa, indicating instability of free proteins. The effect of Pes1 depletion on the reduction of Bop1 was stronger, suggesting that non-incorporated Bop1 is the most instable one of the three proteins in free form. In accordance with this observation, Bop1 contains two PEST motifs, a domain, which is often found in short-lived proteins with a regulatory function (see Fig.26). Integration of Pes1 into the PeBoW-complex may mask these domains, thereby increasing the stability of the protein. Further, in human cells, instability of the free proteins was shown to be independent of transcriptional regulation, which argues for a regulation by protein destabilization and induced turnover (Rohrmoser et al., 2007).

In contrast to the interdependency of murine Pes1 and Bop1, there was hardly an effect on the levels of murine WDR12 after depletion of Pes1 or Bop1. This observation is in

line with the high amounts of free protein detected by native gel electrophoresis and further strengthens the hypothesis of an additional function of murine WDR12. A biological function of WDR12 independent of ribosome biogenesis and proliferation has not yet been elucidated. Ubiquitous expression of its mRNA during embryogenesis may indicate an additional function during development. Moreover, large amounts of mRNA were found in the thymus and testis of adult mice. An interaction with Notch1-IC, revealed by GST-pulldown experiments, further indicates a role in early T-cell differentiation (Nal et al., 2002). Indirect immunofluorescence analysis during this work gave evidence for a weak cytoplasmic localization of WDR12 in CGR8 cells compared to NIH3T3 cells. This may suggest an additional role for WDR12 in early embryonic development.

Complex formation of Pes1, Bop1 and WDR12 seems to be not only a prerequisite for their stability, but also for nucleolar localization and incorporation into preribosomal complexes and hence for their function. Experiments with several mutants of Pes1 or WDR12 had revealed that all dominant negative mutants integrated into the complex and located within the nucleoli. They are supposed to achieve a dominant negative phenotype by building dead end complexes. Overexpression studies have further revealed that human Bop1 needs the help of Pes1 for translocation into the nucleolus, while WDR12 is suggested to assemble within the nucleolus with Pes1 and Bop1 to the PeBoW complex (Grimm et al., 2006; Holzel et al., 2005; Lapik et al., 2004; Rohrmoser et al., 2007).

In summary, the results obtained in this work present for the first time experimental evidence for the formation of a stable complex of Pes1, Bop1 and WDR12 in mouse cells and embryonic stem cells. Unlike the situation in human cells, a large amount of free WDR12 was present. Generally, the data strongly indicate a similar complex assembly in mouse and in human cells, with Bop1 constituting the core component. As Bop1 protein seems to be highly instable in its free form, the regulation of Bop1 may provide a good target for the fine-tuning of the activity of the PeBoW-complex. In addition to the regulation of mRNA levels of *Pes1, Bop1 and WDR12* by c-Myc, this may account for a second regulatory mechanism linking complex stability and activity to the rate of ribosome biogenesis. A possible additional function for WDR12 needs further investigation. Except for a weak cytoplasmic staining of WDR12 in CGR8 cells, no differences were observed regarding stability, localization and complex formation of Pes1, Bop1 and WDR12 between ES cells (CGR8) and the fibroblast mouse cell line NIH3T3.

5.2 Function of Pes1, Bop1 and WDR12 in ES cells and the relation to self-renewal and differentiation

5.2.1 Role of Pes1 for nucleologenesis and ribosome biogenesis during early embryonic development

Ribosome biogenesis plays an important part already during the early onset of embryonic development. Maternally inherited ribosomes are exhausted during the first three cleavages of the zygote and the first rDNA transcription is proposed to take place between the 2-4-cell stage of mouse development. An increase in ribosome biogenesis was observed at the 6-8-cell stage of the embryo (Geuskens and Alexandre, 1984; Hillman and Tasca, 1969; Hyttel et al., 2000; Kopecny et al., 1995). This is again accelerated during gastrulation, associated with a huge increase in proliferation. Mean generation times as short as 4.4h are estimated in the epiblast at this stage (Snow, 1977; Hogan et al., 1994). In parallel, the nucleolus develops from nucleolar precursor bodies, which start to assemble from the 2-cell stage onwards. The typical nucleolar architecture with a central fibrillar component, containing proteins involved in rDNA transcription, a dense fibrillar component, containing newly synthesized rRNA, and a granular component, consisting of preribosomal particles, starts to be visible by electron microscopy between the 8-cell and the blastula stage.

Studies with Pes1 knockout mice revealed an arrest of the preimplantation embryos at the morula stage, showed impaired formation of nucleoli, and an inhibited accumulation of ribosomes, indicating a function for Pes1 in nucleologenesis and ribosome biogenesis (Lerch-Gaggl et al., 2002). The complex formation of Pes1, Bop1 and WDR12, which was validated during this work in ES cells, suggests a comparable function for Bop1 and WDR12 during early embryonic development and hence an essential role for proliferation and survival of the embryo. Recently, also other nucleolar proteins were shown to be essential factors for proliferation and embryonic development. For instance, embryos depleted for the nucleolar proteins SURF6 or Bysl, both involved in the maturation of the small 40S ribosomal subunits, arrest at the 8-cell morula stage or just before blastocyst formation (Adachi et al., 2007; Romanova et al., 2006). Furthermore, *Nucleostemin* deficient embryos died around embryonic day 4. Nucleostemin is a putative GTPase expressed in the nucleoli with a predicted function in ribosome biogenesis (Beekman et al., 2006).

5.2.2 Function of Pes1, Bop1 and WDR12 for rRNA maturation and proliferation of ES cells

During this work, the functions of Pes1, Bop1 and WDR12 were examined in an ES cell line *in vitro*. High expression levels of the proteins Pes1, Bop1 and WDR12 were detected in the mouse embryonic stem cell line CGR8, which were strongly reduced during differentiation of the cells. In accordance with the nucleolar localization of the proteins, a function for Pes1 and Bop1 during ribosome biogenesis was confirmed in ES cells. WDR12 could not be investigated due to non-functional siRNAs. The observed incorporation of WDR12 (at least partially) into PeBoW-complexes indicates a similar function for WDR12. Pes1 and Bop1 were shown to be involved in the maturation of the large 60S ribosomal subunit of ES cells. Their depletion led to an impaired maturation of the 28S rRNA, while the 18S rRNA, which is part of the small 40S subunit, was not affected. Mechanistically, Pes1 and Bop1 seem to be involved in processing events of the internal transcribed spacers 1 and 2 as an increase in 36S rRNA and a decrease in maturation of 28S rRNA was observed. These results are comparable to effects detected in the mouse cell line NIH3T3, which was investigated in parallel, and also to previous data obtained in other mature mammalian cell lines (Grimm et al., 2006; Holzel et al., 2005; Lapik et al., 2004; Strezoska et al., 2002). Thereby, our data support the view of an evolutionary conserved function of Pes1, Bop1 and WDR12 in ribosome biogenesis. In addition, a function of Bop1 and Pes1 for 5.8S rRNA maturation and processing of the 3'ETS was described in mature cell lines (Lapik et al., 2004; Strezoska et al., 2002). These steps were not investigated in this work, but are likely to be processed in a similar way in ES cells.

In addition to the effect on rRNA processing, proliferation of ES cells was hindered upon depletion of Pes1 and Bop1. The consistent outcomes between depletion levels and either rRNA processing or proliferation rates strongly imply a close link of both processes in ES cells, as documented in other cell types. Whether there exists a direct crosstalk between ribosome biogenesis and cell cycle control or whether impaired proliferation may just be an effect of a depleted ribosome pool is discussed in chapter 5.3.

5.2.3 Regulation of Pes1, Bop1 and WDR12 during differentiation

The rapid proliferation of ES cells is associated with an unusual cell cycle distribution, with the majority of cells detected in S-phase cells and only a short G1-phase. Concordant with this, Cdks show constitutive activity throughout the cycle, except for the mitotic kinase Cdk1/cyclinB1. Moreover, although the pocket proteins Rb and its close homolog p107 are expressed in ES cells, they are constitutively phosphorylated and therefore inactivated during the cell cycle, probably due to the cell cycle-independent activities of the Cdk2- and Cdk6/cyclin complexes. This leads in turn to a constant activity of the transcription factor E2F and allows direct S-phase entry without the control mechanism usually known as G1/S-phase checkpoint (Savatier et al., 1994; Stead et al., 2002). During *in vitro* differentiation of ES cells, their proliferation slows down and the length of the G1-phase increases substantially (White et al., 2005). At the molecular level, this is associated with the establishment of cell cycle regulated Cdk2 activity and the activation of a functional Rb-E2F pathway. Transcription of cyclin E and cyclin A is downregulated and their levels become periodically regulated during the cycle. Moreover the Cdk-inhibitors p21 and p27 are upregulated, which may also be important for the loss of Cdk2 activity during differentiation.

These changes within the cell cycle control-mechanisms at the beginning of differentiation, together with slower proliferation, argue for a lower rate of ribosome biogenesis to adjust the supply of ribosomes to the actual demand. In accordance with this hypothesis, protein levels of Pes1, Bop1 and WDR12 strongly decreased during differentiation from day 6 onwards. Interestingly, the phosphorylation pattern of Rb also showed a switch at the same day to the predominant presence of its active, hypo-phosphorylated form. Thus, the time, when the cell starts to activate a functional Rb-E2F pathway and thereby also an active G1/S-phase checkpoint, seems to be correlated with a reduced rate of ribosome biogenesis. According to the mRNA levels of the gastrulation marker T-bra, which showed specific upregulation at day 3-4 of differentiation, day 6 corresponds to an early differentiation stage post gastrulation. Moreover, at this time, the investigated pluripotency-markers Oct4, Nanog, Sox2 and KLF4 were almost undetectable, while upregulation of Flk1 indicates differentiation of early mesodermal cells. Whether the changes within the cell cycle are a prerequisite for reduced ribosome biogenesis or vice versa remains to be elucidated. In mature cells, ribosome biogenesis is cell cycle controlled and sensitive to nutrient and growth factor signaling. The formation and maintenance of functional nucleoli during interphase is

dependent on Cdk activities (Sirri et al., 2002) and rRNA synthesis largely relies on the availability of nutrients and growth factors. Deprivation of the latter or extra- and intracellular stresses can lead to downregulation of rRNA synthesis by inhibition of Polymerase I (Pol I) via inactivation of the regulatory factor TIF-IA, which abrogates the formation of the transcription-initiation complex (Mayer et al., 2005; Mayer et al., 2004). Furthermore, G1-phase specific Cdk/cyclin complexes are involved in the phosphorylation and activation of the upstream binding factor (UBF), an activator of RNA Pol I (Voit et al., 1999). On the other hand, functional ribosome biogenesis is essential to keep levels of the tumor suppressor p53 down, thereby ensuring proliferation. Disruptions in the structure or function of the nucleolus can inhibit the cell cycle - for example by inducing p53 (Pestov et al., 2001; Rubbi and Milner, 2003). Thus, mutual regulations of both processes might be another reason behind the changes occurring during early differentiation of ES cells.

Surprisingly, during the first two days of differentiation, an increase in the overall amount of Rb was observed, which was reduced again at day 3 of differentiation. Nevertheless, the ratio between active and inactive Rb (hypo-phosphorylated Rb to hyper-phosphorylated Rb) was not changed. The function of this increase remains so far elusive. Active Rb plays also a role for the differentiation of distinct lineages, for instance myogenesis, cardiogenesis or adipogenesis, where it is involved as a coregulator of transcription factors like MyoD, myogenin or C/EBP (Chen et al., 1996; Gu et al., 1993). Thus, the cells might induce total Rb levels to be prepared for further differentiation, to switch rapidly to the active form. The downregulation of total Rb levels at day 3 of differentiation argues against this assumption though. Another hypothesis might be that the cells slightly reduce their proliferation due to the small increase in the active form of Rb. In addition to its negative regulation of G1/S-phase transition, active Rb can also negatively regulate polymerase I transcription and thereby also regulates rRNA transcription. A slight reduction in proliferation might be important for an initial step in differentiation. It was hypothesized that the constitutive transit through G1-phase could constrain the temporal opportunity for chromatin remodeling or the establishment of heritable transcription programs (Burdon et al., 2002). Generally, the gastrulation phase of embryonic development is characterized by an increase in cell proliferation. During *in vitro* differentiation a decrease in Rb levels was observed at day 3/4, together with induction of the gastrulation marker T-bra, indicating accelerated proliferation of differentiating ES cells at this time. Interestingly, an auto-regulation of the *Rb* gene expression is described. The promoter of the *Rb* gene is transactivated by the

transcription factor E2F-1. This leads to an increase in Rb protein, which in its active form binds and inhibits the E2F-1 transcription factor and thereby its own expression (Shan et al., 1994). Thus, the weak increase in active Rb at day 1 and 2 of differentiation might be involved in the decrease at day 3/4.

Triple knockouts of the three related pocket proteins Rb, p107 and p130 in ES cells do not compromise ES cell proliferation, but impair their differentiation capacity in teratocarcinomas (Dannenberg et al., 2000; Sage et al., 2000). In contrast, triple knockout mouse embryonic fibroblasts (TKO MEFs) were insensitive to senescence inducing signals, had an increased proliferation rate and failed to arrest in G1-phase at confluency (Sage et al., 2000). This behavior is reminiscent of ES cells. Mice deficient for Rb are non-viable and show defects in neurogenesis and hematopoesis. Although the pocket proteins seems to have no function for proliferation of ES cells, Rb and p107 are still expressed, but present mainly in their inactive form. This was hypothesized to render ES cells susceptible for a fast switch to differentiation (Burdon et al., 2002). Alternatively, one may hypothesize that a rapid activation of Rb might be involved in cell cycle arrest after distinct cellular stresses. This was not confirmed during this work (see below). Nevertheless, nucleolar stress induced total levels of Rb in a similar manner as during early differentiation.

5.2.4 The PeBoW-complex and self-renewal

The maintenance of pluripotency during self-renewal of ES cells is proposed to be dependent on the prevention of differentiation and the promotion of proliferation (Niwa, 2007). Evidence for this assumption is given by certain factors and pathways, which have an overlapping function in both processes. One important pathway involved in proliferation, survival and self-renewal of ES cells is PI3K signaling. Inhibition of PI3K and Akt, a downstream effector of PI3K, induces differentiation in the presence of LIF, whereas artificial activation of Akt is sufficient to maintain self-renewal in the absence of LIF (Paling et al., 2004; Watanabe et al., 2006). Blocking of PTEN, an inhibitor of PI3K-signaling leads to enhanced proliferation and viability (Sun et al., 1999). PI3K is activated by LIF and additionally by two endogenous modulators, which are specifically expressed in ES cells. These are Eras, a constitutively active form of the Ras-family, and Tcl, which augments Akt by forming a complex with it (Takahashi et al., 2003a; Takahashi et al., 2005). Generally, PI3K signaling is implicated in many cellular

processes including metabolism, cell cycle progression, survival, migration and adhesion. In ES cells, it was reported to play a role in cell cycle progression by regulating cyclin D, and in the phosphorylation of ribosomal S6 proteins, which implies a role in ribosome biogenesis (Jirmanova et al., 2002; Paling et al., 2004). Hence, PI3K signaling may link the short cell cycle of ES cells with self-renewal.

As Pes1, Bop1 and WDR12 seem to be essential factors for the high proliferation of ES cells, the question arises whether the PeBoW-complex might also be involved in the maintenance of pluripotency. One could envision that the PeBoW-complex may be indirectly linked to the maintenance of pluripotency by regulating proliferation via ribosome biogenesis. The expression of Pes1, Bop1 and WDR12 is regulated by the proto-oncogene c-Myc (Holzel et al., 2005). The transcription factor c-Myc is known as a major coordinator of many cellular processes including ribosome biogenesis and cell cycle progression. Recently, c-Myc was shown to be a major factor involved in the maintenance of pluripotency, acting downstream of LIF and Stat3 and probably downstream of the Wnt signaling pathway (Cartwright et al., 2005). Those are the major pathways involved in self-renewal of ES cells *in vitro* and c-Myc was proposed to support self-renewal by inhibition of differentiation. The function of c-Myc as transcription factor involves chromatin remodeling and modification processes. Overexpression of c-Myc, together with Oct4, Sox2 and KLF4, was crucial for de-differentiation of somatic cells into ES-like cells, including remodeling of the chromatin to an ES cell-like state (Wernig et al., 2007). This indicates that the role of c-Myc for self-renewal may include the maintenance of an ES cell chromatin status. By activating the expression of Pes1, Bop1 and WDR12 in ES cells, c-Myc might indirectly coordinate proliferation with the repression of differentiation, thereby linking both processes. In accordance with the function of c-Myc for self-renewal, high levels of c-Myc are present in ES cells, but are rapidly downregulated at the beginning differentiation within 36h following LIF withdrawal (Cartwright et al., 2005). mRNA levels of *c-myc* decrease rapidly and the protein becomes phosphorylated on threonine 58, triggering its GSK3β-dependent degradation. Inactivation of *c-myc* transcriptional regulators, and activation of pathways required for its degradation are proposed to define a point of no return, where cells become committed to differentiate.

Although Pes1 and Bop1 were shown during the course of this work to be essential for proliferation of ES cells, first results argue against induction of differentiation after their depletion and thus against a role for the maintenance of pluripotency. The transcription factors and pluripotency genes *Nanog, KLF4 and Sox2* were not significantly

downregulated after depletion of Bop1 compared to control cells. Moreover, alkaline phosphatase staining and morphology of the colonies did not change significantly, indicating that the majority of the cells remained in the undifferentiated state with no increase in differentiating colonies. This may suggest that inhibition of ribosome biogenesis and proliferation alone do not lead to differentiation. Alternatively, the effect achieved on rRNA maturation by depletion of Pes1 or Bop1 might not be strong enough to overcome self-renewal. Interestingly, after depletion of the protein Bysl in ES cells, which is involved in maturation of the 40S ribosomal subunit, there was also no change in the expression of pluripotency markers observed (Adachi et al., 2007). Moreover, it was mentioned that inhibition of mTOR inhibited proliferation of ES cells, but did not induce differentiation (Watanabe et al., 2006). mTOR is a critical downstream effector for the PI3K/Akt signaling pathway with a major function in the regulation of ribosome biogenesis. Further experiments are necessary, however, to clarify if the regulation of ribosome biogenesis plays a role in self-renewal.

5.3 Crosstalk between ribosome biogenesis and cell cycle machinery in mouse embryonic stem cells

As indicated before, ribosome biogenesis is an important factor for cell growth needed to supply the components for the translational machinery. Doubling of this machinery is essential for continuous proliferation to ensure equilibrium between growth and division. Increasing evidence points towards mutual regulations of both processes. In mature cells, impaired ribosome biogenesis was, for instance, shown to activate a p53-dependent checkpoint via upregulation of the Cdk-inhibitor p21, which in turn inhibits Cdk/cyclin complex activities, which leads to activation (hypo-phosphorylation) of Rb and thereby to an arrest of cells in G1-phase (Grimm et al., 2006; Holzel et al., 2005; Pestov et al., 2001). Based on the different cell cycle kinetics of ES cells, which do not show a G1/S-phase checkpoint during normal proliferation, we were interested to ask whether ribosomal stress may activate such a checkpoint in ES cells, thereby linking ribosome biogenesis actively with cell cycle progression. After a block of ribosome biogenesis, one can generally envisage two scenarios. Either the cells actively adapt to the situation by stopping or slowing down their division rate. This can be regulated, for instance, due to checkpoint mechanisms, which function as sensor for ribosomal stress, as it was indicated for the p53-dependent activation of the G1/S-phase checkpoint.

Alternatively, if these mechanisms are not functional, division of the cells will continue initially unaltered until the progressive depletion of ribosomes upon each cell division no longer allows further proliferation.

To address the question whether ribosomal stress might induce a p53-dependent checkpoint in ES cells, knockdowns of Pes1 and Bop1 were used to inhibit rRNA maturation without a genotoxic effect. During the experiments, it turned out that the effects observed after Pes1 and Bop1 depletion were not as strong as expected, showing a reduction of nascent 28S rRNA levels up to about 50%, but no complete block of maturation. This might be explained by the transient transfection of siRNAs and therefore a transient knockdown. Transfection with an eGFP-reporter plasmid indicated a transfection efficiency of about 70%. This means that at least 30% of the cells might not be reached by transfection and will continue to proliferate normally. Thereby, they might rapidly overgrow transfected, growth-retarded cells. The chemotherapeutical agent 5-Fluorouracil (5FU) was included in the experiments to induce a more potent inhibition of ribosome biogenesis. 5FU was reported to mainly inhibit ribosome biogenesis if applied at low concentrations (Gilkes et al., 2006). Nevertheless, 5FU is a pleiotropic factor whose function is not fully understood and high concentrations of 5FU also exert an inhibitory effect on DNA metabolism.

5.3.1 Effects of ribosomal stress (5FU) in the mature mouse cell line NIH3T3

To investigate checkpoint activation upon 5FU in a mature cell line, NIH3T3 fibroblasts were used. Treatment with 5FU resulted in an accumulation of cells in the G1- and S-phase, with an increase of cells in G1-phase. The entry of cells into the G2/M-phase seemed to be blocked, as the amount of cells with a DNA content of 2N was reduced. Protein levels of the Cdk-inhibitor p21 were strongly induced as well as the hypo-phosphorylated, active form of Rb. This gives strong evidence that p21 inhibits the activity of Cdk2/cyclinE complexes, which in turn leads to reduced Rb phosphorylation and thus to an increase in active, hypo-phosphorylated Rb. As active Rb binds the family of E2F transcription factors, which play a crucial role in progression of cells from G1-phase into S-phase, the observed increase in active Rb is most likely the responsible factor for the accumulation of cells in G1-phase. In addition, p21 induction might also account for the accumulation of cells in S-phase and the decrease of cells in G2/M-phase, since p21 can inhibit S-phase progression by binding to PCNA, a subunit

of the DNA polymerase δ (Flores-Rozas et al., 1994; Waga et al., 1994). Alternatively, other mechanisms could be involved in the decrease of cells in G2/M-phase. Strikingly, the levels of p53 showed only a very weak induction, mainly observed by immunofluorescence. This may give evidence for a defect in the *p53* gene in those cells. However, only a weak induction of p53 protein was reported also after disruption of ribosome biogenesis with a dominant negative mutant of Bop1 in another NIH3T3 cell line. Nevertheless, in this study a p53-dependent induction of p21 as well as G1-arrest was confirmed according to p53 inhibitor studies, which attenuated the observed effects (Pestov, et al., 2001). So the weak induction of p53 may be responsible at least for part of the p21 induction. Alternatively, p53-independent mechanisms for the induction of p21 are reported in literature (Aliouat-Denis et al., 2005; Huang et al., 2006; Kim et al., 2000; Macleod et al., 1995; Serfas et al., 1997; Zeng and el-Deiry, 1996). Mice, deficient for p53, are viable, but are predisposed to a variety of tumors by 6 months of age (Donehower et al., 1992), whereas mice lacking p21 are defective in G1-checkpoint control, but they undergo normal development (Deng et al., 1995).
Overall, the observed results reflect the notion that ribosomal stress can activate a checkpoint, which involves p53, p21 and subsequent activation of Rb, which finally leads to an arrest of cells in the G1-phase.

5.3.2 Effects of ribosomal stress in ES cells

5.3.2.1 Effects on p53, p21 and Rb upon 5FU and depletion of Pes1 and Bop1

A massive increase of p53 protein was observed in ES cells upon knockdown of Pes1 or Bop1 and after 5FU treatment. Although p53 was localized in the nucleus, no induction of its target gene p21 was observed. In contrast, the overall amount of Rb was highly increased, but the ratio between hyper-phosphorylated and hypo-phosphorylated Rb did not change towards the active form. This implies that the activities of Rb-kinases are not inhibited, due to the fact that no p21 inhibitor is expressed. Hence, the p53-p21-Rb pathway seems to be inoperative in ES cells after inhibition of ribosome biogenesis. These data are in line with publications, showing that Rb is constantly inactive (hyper-phosphorylated) during normal proliferation of ES cells and that neither contact inhibition nor serum deprivation appear to affect proliferation (Savatier et al., 1994; Schratt et al., 2001). Moreover, inability of p53 to induce p21 was reported after DNA damage. Several DNA damaging agents as well as nucleotide depletion induced p53

levels but did not lead to an induction of p21. This was explained by an inefficient translocation of p53 into the nucleus, which showed predominantly cytoplasmic localization. ES cells were shown to rather undergo apoptosis and accumulate in S- and G2/M-phase instead of arresting at G1-phase upon DNA damage (Aladjem et al., 1998; Hong et al., 2006; Hong et al., 2007; Hong and Stambrook, 2004). In that context, it was supposed that a missing G1-arrest might favor apoptosis, thereby ensuring genome stability of the ES cell population. During this work, no major increase in apoptosis was observed upon ribosomal stress. Moreover, p53 was located mainly in the nucleus, indicating other reasons for the deficit in p21 induction. One explanation might be that p53 is not transcriptionally active despite its nuclear localization. However, recent data indicate upregulation of numerous p53 target genes after cisplatin treatment of ES cells (Kruse et al., 2007). Another alternative for the lack of p21 induction might be that p21 is transactivated by p53 in ES cells, but the protein is rapidly degraded. The very weak levels of p21, which could be detected in 5FU-treated cells compared to control cells, may favor this hypothesis. Moreover Malashicheva et al. reported increased p21 protein levels upon treatment of ES cells with gamma-irradiation, adriamycin and nocodazol after the addition of the proteasome inhibitor lactacystin (Malashicheva et al., 2002). A third explanation might be inaccessibility of the *p21* gene promoter. For instance, c-Myc was reported to be involved in the methylation of the *p21* gene promoter. Together with the DNA binding factor Miz-1, it targets the methyltransferase Dnmt3a selectively to the promoter of *p21* (Brenner et al., 2005). As c-Myc is highly expressed in ES cells this could be another possibility. Overall, the observed deficit in p21 induction does not exclude the possibility that p53 might fulfill other functions upon ribosomal stress.

In mature cells, induction of p53 upon nucleolar stress is a common feature, which is described in several cases to be regulated by free ribosomal proteins. Such a mechanism is also described for 5FU. Inhibition of rRNA biogenesis by low concentrations of 5FU leads to a deficit of mature rRNAs and thereby to an excess and release of free ribosomal proteins, like L5, L11 and L23 (Sun et al., 2007). Those were detected to interact with Mdm2, an E3 ubiquitin ligase, which usually binds and targets p53 for degradation. Binding of the ribosomal proteins to Mdm2 inhibits the ubiquitylation of p53 by Mdm2, leading to stabilization and activation of p53. As we could observe reduced levels of mature rRNA species after Pes1 and Bop1 depletion, as well as after 5FU treatment, a similar mechanism for p53 induction seems likely in ES cells. Alternatively, the so-called “riding the ribosome” model has been proposed as another possibility for p53 stabilization in response to ribosomal stress. This model

postulates an export of p53-Mdm2 complexes into the cytoplasm via association with pre-ribosomal particles. During functional ribosome biogenesis, a high amount of pre-ribosomal particles is transported into the cytoplasm for their final maturation into ribosomes. Therefore, the cell has enough capacity to cotransport p53 into the cytoplasm, where it is degraded, and keeps the p53 level low. During disturbed ribosome biogenesis, maturation and export of pre-ribosomal particles are diminished and therefore also the export of p53, which accumulates in the nucleus (Sherr and Weber, 2000). Evidence for this model is given by the observations that p53 accumulated in the nucleus after inhibition of nuclear export. Moreover, p53 was found to covalently bind to the 5.8S RNA, and p53-Mdm2 complexes were detected together with the ribosomal proteins L5 and L11 (Fontoura et al., 1997; Marechal et al., 1994).
Generally, Mdm2 is expressed in mouse ES cells (Ginis et al., 2004) and seems to be an important negative regulator of p53. Mdm2 null mice die during early embryonic development before day 5.5 and consist only of few cells. This phenotype was rescued by additional deletion of p53 (Jones et al., 1995; Montes de Oca Luna et al., 1995).

The reason for the increase in total Rb protein levels upon nucleolar stress remains so far elusive, especially as most of the protein remained still in the inactive form and no robust G1-arrest was observed (see below). Interestingly, Mdm2 was reported to have a function for Rb ubiquitylation and degradation (Miwa et al., 2006; Uchida et al., 2005) As we suppose that Mdm2 is inactivated upon 5FU treatment and upon depletion of Pes1 or Bop1, due to free ribosomal proteins, this inactivation might also lead to stabilization and induction of Rb protein levels. One might speculate that induction of total Rb levels is a mechanism to also increase the levels of the hypo-phosphorylated, active form, without changes in the activity of Cdks. Cdk2/cyclinE and Cdk6/cyclinD activities seem to be the main factors for Rb phosphorylation in ES cells (Faast et al., 2004). Their activities were not examined during this work, but due to the strong inactive (hyper-phosphorylated) fraction of Rb a decrease of their activities seems unlikely.

5.3.2.2 Opposing effects on cell cycle distribution of ES cells upon 5FU treatment and depletion of Pes1 and Bop1

Effects upon 5FU treatment:
Although similar effects were observed on p53, p21 and Rb in ES cells upon 5FU treatment and depletion of Pes1 and Bop1, opposing effects were detected on the cell

cycle distribution. Upon 5FU treatment the majority of CGR8 cells accumulated in S-phase and no stable G1-arrest was observed. The amount of cells in G2/M-phase was reduced and thus the entry into G2/M-phase seemed to be blocked, similar as observed in NIH3T3 cells. Whether the accumulation of cells in S-phase is dependent on the observed induction of p53 needs further investigation, for example, in a p53 knockout ES cell line. In the literature both, p53-dependent and -independent mechanisms for an S-phase arrest have been reported, usually after DNA damage (Agarwal et al., 1998; Prost et al., 1998; Toyoshima et al., 2005). Interestingly, overexpression of the nucleolar protein ARF, which usually stabilizes p53 by binding to Mdm2, can exert a delay in S-phase progression, especially if the function of p53 is comprised (Yarbrough et al., 2002). Although 5FU was shown to mainly affect RNA-metabolism at low concentrations, an additional effect on DNA can not be excluded, especially after longer exposure times. Moreover, the relative doses reported to induce certain effects vary between different cell types.

Effects upon depletion of Pes1 or Bop1:

In contrast to an accumulation of cells in S-phase upon 5FU, a weak decrease of cells in S-phase and a weak increase in G1-phase was observed upon depletion of Pes1 and Bop1. As the p53-p21 pathway seems to not be involved, the underlying mechanisms of this effect cannot be fully explained, but the effect might be linked to the slight increase in hypo-phosphorylated, active Rb, which was observed together with the increase in total Rb levels. For Nop7p, the potential homolog of Pes1 in yeast, a function during DNA replication was reported. Nop7p depletion led to an arrest of cells in G1- or G2-phase, with no cells in S-phase, even if ribosome biogenesis was not impaired (Du and Stillman, 2002). In addition, Nop7p was identified as part of a complex, which contained also MCM and ORC proteins. One might also hypothesize a function for murine Pes1 during DNA replication. This in turn might be involved in the weak accumulation of cells in G1-phase.

Generally, the effects observed on cell cycle distribution upon depletion of Pes1 and Bop1 seem rather weak to explain the reduced proliferation of the cells. Moreover, no strong effect on apoptosis was detected. This suggests the involvement of additional mechanisms. In addition to a prolonged G1-phase, cells might perform an overall delayed cell cycle progression. For instance, inhibition of Cdk2 kinase activity with a specific biochemical inhibitor was reported previously to increase the generation time of ES cells without exhibiting a change in cell cycle distribution and without an extension of G1-phase (Stead et al., 2002). This indicates that cell division rates are not necessarily

coupled to the cell cycle structure and implies a role for Cdk2 in transition through all phases of the cycle and not only for the transit from G1- to S-phase (Stead et al., 2002). During this work, Cdk activities were not determined as an inhibition seemed unlikely due to the strong increase in hyper-phosphorylated Rb and as no induction of p21 was observed. Nevertheless, it cannot be completely excluded.

Another explanation for reduced proliferation and overall slower cell cycle progression might be a decreased amount of ribosomes. However, in mature cells no impaired translation efficiency was observed after a knockdown of Bop1 (Pestov et al., 2001). In addition, other publications reported retarded proliferation, but cells still increased their size after impaired ribosome biogenesis (Volarevic et al., 2000). This effect is most likely related to a slower G1/S-phase transition, achieved by the reported G1-arrest after ribosomal stress, which provides more time for protein synthesis. In contrast, data in Rb- and p53-deficient SAOS-2 cells show inability of those cells to arrest in G1- and G2-phase after transient ribosomal stress and indicate unchanged cell division. After prolonged inhibition of ribosome biogenesis this leads to inhibition of cell proliferation due to increased cell death, which was elicited by an insufficient ribosome content (Montanaro et al., 2007). In ES cells, Rb was only weakly activated upon nucleolar stress and no robust arrest in any cell cycle phase was observed upon depletion of Pes1 or Bop1. Thus, a decrease in the ribosome pool due to initially unchanged proliferation, which leads to a progressive reduction of the ribosomal content after each cell division, cannot be excluded. Pes1 depleted embryos, which arrest at the morula stage, showed a strong decrease in ribosomes, but in addition their nucleoli had not differentiated normally (Lerch-Gaggl et al., 2002). In our study, a decrease of ribosomes as main reason for the impaired proliferation seems unlikely due to the incomplete block of rRNA maturation upon Pes1 and Bop1 depletion, which decreased the amount of nascent 28S rRNA only to about 50%. Moreover, the lack of major cell death, together with the accumulation of cells in S-phase upon 5FU treatment, rather implies that ES cells employ active mechanisms to coordinate their cell cycle progression with ribosome biogenesis.

5FU versus depletion of Pes1 and Bop1:

The different effects observed on cell cycle distribution upon 5FU and depletion of Pes1 or Bop1 might be related to the different intensities of both effectors on ribosome biogenesis, with 5FU inducing a much more potent and extensive block (including 18S, 28S rRNA and some pre rRNAs) as depletion of Pes1 or Bop1, which reduced more specifically the maturation of nascent 28S rRNA and those only to about 50%. In

addition the pleiotropic function of 5FU, but also additional functions of the PeBoW-complex like its indicated function in replication could be involved. In contrast to the PeBoW-complex, which is involved mainly in processing steps of the ITS 2, 5FU achieves its effects by conversion into 5-fluorouridine-triphosphate, which incorporates into rRNA and thereby inhibits processing of rRNA (Sun et al., 2007). In addition 5FU can interfere with other RNA species and its conversion into 5-fluoro-dUMP and 5-flouro-dUTP suppresses DNA synthesis and repair, thereby leading to DNA damage. Finally, it has to be considered that mature NIH3T3 cells treated with 5FU also exhibited a block in G2/M-phase entry and despite their arrest in G1-phase showed no decrease of cells in S-phase. Thus, the accumulation of ES cells in the S-phase upon 5FU treatment is not necessarily an ES cell specific response. However, similar upon 5FU treatment and depletion of Pes1 or Bop1, no robust G1-arrest was induced in ES cells. This seems to be related to the impeded induction of p21.

5.3.3 Conclusions

In summary, a function of the PeBoW-complex in ribosome biogenesis of ES cells, and a relation to proliferation could be confirmed during this work. Different to mature cells, the coordination of ribosome biogenesis with the cell cycle machinery is not regulated via the p53-p21-Rb pathway. Nevertheless, the obtained results suggest that ES cells employ other mechanisms to coordinate ribosome biogenesis with proliferation. The precise nature of these mechanisms needs further investigation. One important experiment could be the use of p53-deficient cells, to examine whether p53 is involved in such mechanisms, as indicated by its strong induction. Further, the use of other inhibiting agents for ribosome biogenesis like Actinomycin D could be important to rule out additional side effects of the used effectors.

In addition to revealing the coordination of ribosome biogenesis with proliferation of ES cells, the question whether ribosome biogenesis is linked to the maintenance of pluripotency or whether a defect in ribosome biogenesis just leads to retarded proliferation without an effect on pluripotency or differentiation will be of outstanding importance in understanding how proliferation and self-renewal are regulated in ES cells.

6 SUMMARY

The hallmark of embryonic stem (ES) cells is their ability for self-renewal (capability of unlimited cell division without the loss of pluripotency) as well as for differentiation into all cell types of the adult organism. One factor supposed to be involved in self-renewal is the rapid proliferation rate of ES cells, which is coupled to an unusual cell cycle distribution with the majority of cells in S-phase and a very short G1-phase. This is linked to the lack of a functional G1/S-phase checkpoint, which allows the cells to enter the S-phase almost directly after mitosis. Generally, cells have to closely coordinate growth and cell cycle progression during proliferation to prevent premature division. One important factor for cell growth is ribosome biogenesis. In mature cells, disruptions in ribosome biogenesis are directly linked to the cell cycle machinery by a p53-dependent activation of the G1/S-phase checkpoint, leading to an arrest of cells in G1-phase.

During this work, the function of the proteins Pes1, Bop1 and WDR12, which were shown previously to be involved in ribosome biogenesis of mature cell lines, was investigated in mouse ES cells. Moreover, a putative crosstalk between ribosome biogenesis and proliferation of ES cells was assessed. A high expression of Pes1, Bop1 and WDR12 was observed in ES cells, which strongly decreased during *in vitro* differentiation. Localization of the proteins was predominantly nucleolar and the formation of a stable complex (PeBoW-complex), including all three proteins, was experimentally validated in mature mouse cells as well as in mouse ES cells. The function and stability of the proteins seems to be dependent on incorporation into the PeBOW-complex, as protein levels were interdependent on each other and no free, non-incorporated proteins were observed, except for WDR12. According to their nucleolar localization, depletion of Pes1 and Bop1 were shown to inhibit maturation of the 28S rRNA and thereby the large 60S ribosomal subunit. Further, impaired proliferation of ES cells was observed. Thus, the PeBoW-complex seems to be an essential factor for the rapid proliferation of ES cells and might therefore also be involved in self-renewal. However, first results suggest that the complex is not directly involved in the maintenance of pluripotency. No changes in the expression levels of pluripotency-genes like Nanog, KLF4 and Sox2 were observed. Moreover, alkaline phosphatase activity was equally detectable after depletion of Pes1 or Bop1 and no morphological changes within the ES cell colonies were observed.

Impaired ribosome biogenesis is known to activate a p53-dependent checkpoint in mature cell lines, which leads to an arrest of cells in G1-phase. Treatment of mouse NIH3T3 cells with 5FU, a potent inhibitor of rRNA maturation, confirmed an activation of this checkpoint, leading to weak induction of the tumor suppressor p53, induction of the Cdk-inhibitor p21, an increase in active, hypo-phosphorylated Rb, and to accumulation of cells in the G1- and S-phase with an increase of cells in G1-phase. In contrast, ES cells showed strong induction of p53, but no induction of its target gene p21. The overall levels of Rb were strongly induced, but the ratio between inactive, hyper-phosphorylated Rb and active, hypo-phosphorylated Rb was not changed towards the active form. These results were observed upon 5FU treatment and upon depletion of Pes1 or Bop1. Hence, ribosomal stress does not lead to checkpoint activation via the p53-p21-Rb pathway in ES cells. Moreover, no robust accumulation of cells in G1-phase was observed. 5FU treated ES cells showed an accumulation of cells in S-phase instead. Whether this effect is regulated by the induced p53 needs further investigation. Overall, the results suggest that ES cells use different mechanisms as mature cells to coordinate their proliferation rate with ribosome biogenesis.

7 BIBLIOGRAPHY

Adachi, K., Soeta-Saneyoshi, C., Sagara, H., and Iwakura, Y. (2007). Crucial role of Bysl in mammalian preimplantation development as an integral factor for 40S ribosome biogenesis. Mol Cell Biol *27*, 2202-2214.

Agarwal, M. L., Agarwal, A., Taylor, W. R., Chernova, O., Sharma, Y., and Stark, G. R. (1998). A p53-dependent S-phase checkpoint helps to protect cells from DNA damage in response to starvation for pyrimidine nucleotides. Proc Natl Acad Sci U S A *95*, 14775-14780.

Aktas, H., Cai, H., and Cooper, G. M. (1997). Ras links growth factor signaling to the cell cycle machinery via regulation of cyclin D1 and the Cdk inhibitor p27KIP1. Mol Cell Biol *17*, 3850-3857.

Aladjem, M. I., Spike, B. T., Rodewald, L. W., Hope, T. J., Klemm, M., Jaenisch, R., and Wahl, G. M. (1998). ES cells do not activate p53-dependent stress responses and undergo p53-independent apoptosis in response to DNA damage. Curr Biol *8*, 145-155.

Aliouat-Denis, C. M., Dendouga, N., Van den Wyngaert, I., Goehlmann, H., Steller, U., van de Weyer, I., Van Slycken, N., Andries, L., Kass, S., Luyten, W.*, et al.* (2005). p53-independent regulation of p21Waf1/Cip1 expression and senescence by Chk2. Mol Cancer Res *3*, 627-634.

Allende, M. L., Amsterdam, A., Becker, T., Kawakami, K., Gaiano, N., and Hopkins, N. (1996). Insertional mutagenesis in zebrafish identifies two novel genes, pescadillo and dead eye, essential for embryonic development. Genes Dev *10*, 3141-3155.

Andersen, J. S., Lyon, C. E., Fox, A. H., Leung, A. K., Lam, Y. W., Steen, H., Mann, M., and Lamond, A. I. (2002). Directed proteomic analysis of the human nucleolus. Curr Biol *12*, 1-11.

Anneren, C., Cowan, C. A., and Melton, D. A. (2004). The Src family of tyrosine kinases is important for embryonic stem cell self-renewal. J Biol Chem *279*, 31590-31598.

Armstrong, L., Lako, M., Lincoln, J., Cairns, P. M., and Hole, N. (2000). mTert expression correlates with telomerase activity during the differentiation of murine embryonic stem cells. Mech Dev *97*, 109-116.

Bartek, J., and Lukas, J. (2001). Pathways governing G1/S transition and their response to DNA damage. FEBS Lett *490*, 117-122.

Bates, S., Bonetta, L., MacAllan, D., Parry, D., Holder, A., Dickson, C., and Peters, G. (1994). CDK6 (PLSTIRE) and CDK4 (PSK-J3) are a distinct subset of the cyclin-dependent kinases that associate with cyclin D1. Oncogene *9*, 71-79.

Beekman, C., Nichane, M., De Clercq, S., Maetens, M., Floss, T., Wurst, W., Bellefroid, E., and Marine, J. C. (2006). Evolutionarily conserved role of nucleostemin: controlling proliferation of stem/progenitor cells during early vertebrate development. Mol Cell Biol *26*, 9291-9301.

Bertrand, E., Houser-Scott, F., Kendall, A., Singer, R. H., and Engelke, D. R. (1998). Nucleolar localization of early tRNA processing. Genes Dev *12*, 2463-2468.

Blagosklonny, M. V., and Pardee, A. B. (2002). The restriction point of the cell cycle. Cell Cycle *1*, 103-110.

Boiani, M., and Scholer, H. R. (2005). Regulatory networks in embryo-derived pluripotent stem cells. Nat Rev Mol Cell Biol *6*, 872-884.

Bouchard, C., Thieke, K., Maier, A., Saffrich, R., Hanley-Hyde, J., Ansorge, W., Reed, S., Sicinski, P., Bartek, J., and Eilers, M. (1999). Direct induction of cyclin D2 by Myc contributes to cell cycle progression and sequestration of p27. Embo J *18*, 5321-5333.

Boyer, L. A., Plath, K., Zeitlinger, J., Brambrink, T., Medeiros, L. A., Lee, T. I., Levine, S. S., Wernig, M., Tajonar, A., Ray, M. K.*, et al.* (2006). Polycomb complexes repress developmental regulators in murine embryonic stem cells. Nature *441*, 349-353.

Brenner, C., Deplus, R., Didelot, C., Loriot, A., Vire, E., De Smet, C., Gutierrez, A., Danovi, D., Bernard, D., Boon, T.*, et al.* (2005). Myc represses transcription through recruitment of DNA methyltransferase corepressor. Embo J *24*, 336-346.

Buehr, M., and Smith, A. (2003). Genesis of embryonic stem cells. Philos Trans R Soc Lond B Biol Sci *358*, 1397-1402; discussion 1402.

Burdon, T., Smith, A., and Savatier, P. (2002). Signalling, cell cycle and pluripotency in embryonic stem cells. Trends Cell Biol *12*, 432-438.

Burdon, T., Stracey, C., Chambers, I., Nichols, J., and Smith, A. (1999). Suppression of SHP-2 and ERK signalling promotes self-renewal of mouse embryonic stem cells. Dev Biol *210*, 30-43.

Cartwright, P., McLean, C., Sheppard, A., Rivett, D., Jones, K., and Dalton, S. (2005). LIF/STAT3 controls ES cell self-renewal and pluripotency by a Myc-dependent mechanism. Development *132*, 885-896.

Chambers, I., Colby, D., Robertson, M., Nichols, J., Lee, S., Tweedie, S., and Smith, A. (2003). Functional expression cloning of Nanog, a pluripotency sustaining factor in embryonic stem cells. Cell *113*, 643-655.

Chen, P. L., Riley, D. J., Chen, Y., and Lee, W. H. (1996). Retinoblastoma protein positively regulates terminal adipocyte differentiation through direct interaction with C/EBPs. Genes Dev *10*, 2794-2804.

Dai, M. S., and Lu, H. (2004). Inhibition of MDM2-mediated p53 ubiquitination and degradation by ribosomal protein L5. J Biol Chem *279*, 44475-44482.

Dai, M. S., Zeng, S. X., Jin, Y., Sun, X. X., David, L., and Lu, H. (2004). Ribosomal protein L23 activates p53 by inhibiting MDM2 function in response to ribosomal perturbation but not to translation inhibition. Mol Cell Biol *24*, 7654-7668.

Dannenberg, J. H., van Rossum, A., Schuijff, L., and te Riele, H. (2000). Ablation of the retinoblastoma gene family deregulates G(1) control causing immortalization and increased cell turnover under growth-restricting conditions. Genes Dev *14*, 3051-3064.

Deng, C., Zhang, P., Harper, J. W., Elledge, S. J., and Leder, P. (1995). Mice lacking p21CIP1/WAF1 undergo normal development, but are defective in G1 checkpoint control. Cell *82*, 675-684.

Doetschman, T. C., Eistetter, H., Katz, M., Schmidt, W., and Kemler, R. (1985). The in vitro development of blastocyst-derived embryonic stem cell lines: formation of visceral yolk sac, blood islands and myocardium. J Embryol Exp Morphol *87*, 27-45.

Donehower, L. A., Harvey, M., Slagle, B. L., McArthur, M. J., Montgomery, C. A., Jr., Butel, J. S., and Bradley, A. (1992). Mice deficient for p53 are developmentally normal but susceptible to spontaneous tumours. Nature *356*, 215-221.

Du, Y. C., and Stillman, B. (2002). Yph1p, an ORC-interacting protein: potential links between cell proliferation control, DNA replication, and ribosome biogenesis. Cell *109*, 835-848.

Duval, D., Reinhardt, B., Kedinger, C., and Boeuf, H. (2000). Role of suppressors of cytokine signaling (Socs) in leukemia inhibitory factor (LIF) -dependent embryonic stem cell survival. Faseb J *14*, 1577-1584.

Eichler, D. C., and Craig, N. (1994). Processing of eukaryotic ribosomal RNA. Prog Nucleic Acid Res Mol Biol *49*, 197-239.

Ekholm, S. V., and Reed, S. I. (2000). Regulation of G(1) cyclin-dependent kinases in the mammalian cell cycle. Curr Opin Cell Biol *12*, 676-684.

Evans, M. J., and Kaufman, M. H. (1981). Establishment in culture of pluripotential cells from mouse embryos. Nature *292*, 154-156.

Faast, R., White, J., Cartwright, P., Crocker, L., Sarcevic, B., and Dalton, S. (2004). Cdk6-cyclin D3 activity in murine ES cells is resistant to inhibition by p16(INK4a). Oncogene *23*, 491-502.

Fatica, A., and Tollervey, D. (2002). Making ribosomes. Curr Opin Cell Biol *14*, 313-318.

Flores-Rozas, H., Kelman, Z., Dean, F. B., Pan, Z. Q., Harper, J. W., Elledge, S. J., O'Donnell, M., and Hurwitz, J. (1994). Cdk-interacting protein 1 directly binds with proliferating cell nuclear antigen and inhibits DNA replication catalyzed by the DNA polymerase delta holoenzyme. Proc Natl Acad Sci U S A *91*, 8655-8659.

Fontoura, B. M., Atienza, C. A., Sorokina, E. A., Morimoto, T., and Carroll, R. B. (1997). Cytoplasmic p53 polypeptide is associated with ribosomes. Mol Cell Biol *17*, 3146-3154.

Fromont-Racine, M., Senger, B., Saveanu, C., and Fasiolo, F. (2003). Ribosome assembly in eukaryotes. Gene *313*, 17-42.

Fujii-Yamamoto, H., Kim, J. M., Arai, K., and Masai, H. (2005). Cell cycle and developmental regulations of replication factors in mouse embryonic stem cells. J Biol Chem *280*, 12976-12987.

Geuskens, M., and Alexandre, H. (1984). Ultrastructural and autoradiographic studies of nucleolar development and rDNA transcription in preimplantation mouse embryos. Cell Differ *14*, 125-134.

Gilkes, D. M., Chen, L., and Chen, J. (2006). MDMX regulation of p53 response to ribosomal stress. Embo J *25*, 5614-5625.

Ginis, I., Luo, Y., Miura, T., Thies, S., Brandenberger, R., Gerecht-Nir, S., Amit, M., Hoke, A., Carpenter, M. K., Itskovitz-Eldor, J., and Rao, M. S. (2004). Differences between human and mouse embryonic stem cells. Dev Biol *269*, 360-380.

Grimm, T., Holzel, M., Rohrmoser, M., Harasim, T., Malamoussi, A., Gruber-Eber, A., Kremmer, E., and Eick, D. (2006). Dominant-negative Pes1 mutants inhibit ribosomal RNA processing and cell proliferation via incorporation into the PeBoW-complex. Nucleic Acids Res *34*, 3030-3043.

Gu, W., Schneider, J. W., Condorelli, G., Kaushal, S., Mahdavi, V., and Nadal-Ginard, B. (1993). Interaction of myogenic factors and the retinoblastoma protein mediates muscle cell commitment and differentiation. Cell *72*, 309-324.

Hadjiolova, K. V., Nicoloso, M., Mazan, S., Hadjiolov, A. A., and Bachellerie, J. P. (1993). Alternative pre-rRNA processing pathways in human cells and their alteration by cycloheximide inhibition of protein synthesis. Eur J Biochem *212*, 211-215.

Hao, J., Li, T. G., Qi, X., Zhao, D. F., and Zhao, G. Q. (2006). WNT/beta-catenin pathway up-regulates Stat3 and converges on LIF to prevent differentiation of mouse embryonic stem cells. Dev Biol *290*, 81-91.

Haque, J., Boger, S., Li, J., and Duncan, S. A. (2000). The murine Pes1 gene encodes a nuclear protein containing a BRCT domain. Genomics *70*, 201-210.

Harbour, J. W., and Dean, D. C. (2000). The Rb/E2F pathway: expanding roles and emerging paradigms. Genes Dev *14*, 2393-2409.

Harper, J. W., Elledge, S. J., Keyomarsi, K., Dynlacht, B., Tsai, L. H., Zhang, P., Dobrowolski, S., Bai, C., Connell-Crowley, L., Swindell, E., and et al. (1995). Inhibition of cyclin-dependent kinases by p21. Mol Biol Cell *6*, 387-400.

Haupt, Y., Maya, R., Kazaz, A., and Oren, M. (1997). Mdm2 promotes the rapid degradation of p53. Nature *387*, 296-299.

Helin, K., Harlow, E., and Fattaey, A. (1993). Inhibition of E2F-1 transactivation by direct binding of the retinoblastoma protein. Mol Cell Biol *13*, 6501-6508.

Hillman, N., and Tasca, R. J. (1969). Ultrastructural and autoradiographic studies of mouse cleavage stages. Am J Anat *126*, 151-173.

Hogan, BLM, Beddington RSB, Constantini F and Lacy E. (1994). Manipulating the mouse embryo. 2nd edn. Cold Spring Harbor Laboratory Press

Holzel, M., Grimm, T., Rohrmoser, M., Malamoussi, A., Harasim, T., Gruber-Eber, A., Kremmer, E., and Eick, D. (2007). The BRCT domain of mammalian Pes1 is crucial for nucleolar localization and rRNA processing. Nucleic Acids Res *35*, 789-800.

Holzel, M., Rohrmoser, M., Schlee, M., Grimm, T., Harasim, T., Malamoussi, A., Gruber-Eber, A., Kremmer, E., Hiddemann, W., Bornkamm, G. W., and Eick, D. (2005). Mammalian WDR12 is a novel member of the Pes1-Bop1 complex and is required for ribosome biogenesis and cell proliferation. J Cell Biol *170*, 367-378.

Hong, Y., Cervantes, R. B., and Stambrook, P. J. (2006). DNA damage response and mutagenesis in mouse embryonic stem cells. Methods Mol Biol *329*, 313-326.

Hong, Y., Cervantes, R. B., Tichy, E., Tischfield, J. A., and Stambrook, P. J. (2007). Protecting genomic integrity in somatic cells and embryonic stem cells. Mutat Res *614*, 48-55.

Hong, Y., and Stambrook, P. J. (2004). Restoration of an absent G1 arrest and protection from apoptosis in embryonic stem cells after ionizing radiation. Proc Natl Acad Sci U S A *101*, 14443-14448.

Huang, H. S., Liu, Z. M., Ding, L., Chang, W. C., Hsu, P. Y., Wang, S. H., Chi, C. C., and Chuang, C. H. (2006). Opposite effect of ERK1/2 and JNK on p53-independent p21WAF1/CIP1 activation involved in the arsenic trioxide-induced human epidermoid carcinoma A431 cellular cytotoxicity. J Biomed Sci *13*, 113-125.

Hyttel, P., Laurincik, J., Rosenkranz, C., Rath, D., Niemann, H., Ochs, R. L., and Schellander, K. (2000). Nucleolar proteins and ultrastructure in preimplantation porcine embryos developed in vivo. Biol Reprod *63*, 1848-1856.

Ivanova, N., Dobrin, R., Lu, R., Kotenko, I., Levorse, J., DeCoste, C., Schafer, X., Lun, Y., and Lemischka, I. R. (2006). Dissecting self-renewal in stem cells with RNA interference. Nature *442*, 533-538.

Jin, A., Itahana, K., O'Keefe, K., and Zhang, Y. (2004). Inhibition of HDM2 and activation of p53 by ribosomal protein L23. Mol Cell Biol *24*, 7669-7680.

Jirmanova, L., Afanassieff, M., Gobert-Gosse, S., Markossian, S., and Savatier, P. (2002). Differential contributions of ERK and PI3-kinase to the regulation of cyclin D1 expression and to the control of the G1/S transition in mouse embryonic stem cells. Oncogene *21*, 5515-5528.

Jones, S. N., Roe, A. E., Donehower, L. A., and Bradley, A. (1995). Rescue of embryonic lethality in Mdm2-deficient mice by absence of p53. Nature *378*, 206-208.

Kato, J., Matsushime, H., Hiebert, S. W., Ewen, M. E., and Sherr, C. J. (1993). Direct binding of cyclin D to the retinoblastoma gene product (pRb) and pRb phosphorylation by the cyclin D-dependent kinase CDK4. Genes Dev *7*, 331-342.

Keller, G. (2005). Embryonic stem cell differentiation: emergence of a new era in biology and medicine. Genes Dev *19*, 1129-1155.

Killian, A., Le Meur, N., Sesboue, R., Bourguignon, J., Bougeard, G., Gautherot, J., Bastard, C., Frebourg, T., and Flaman, J. M. (2004). Inactivation of the RRB1-Pescadillo pathway involved in ribosome biogenesis induces chromosomal instability. Oncogene *23*, 8597-8602.

Killian, A., Sarafan-Vasseur, N., Sesboue, R., Le Pessot, F., Blanchard, F., Lamy, A., Laurent, M., Flaman, J. M., and Frebourg, T. (2006). Contribution of the BOP1 gene, located on 8q24, to colorectal tumorigenesis. Genes Chromosomes Cancer *45*, 874-881.

Kim, W. H., Kang, K. H., Kim, M. Y., and Choi, K. H. (2000). Induction of p53-independent p21 during ceramide-induced G1 arrest in human hepatocarcinoma cells. Biochem Cell Biol *78*, 127-135.

Kinoshita, Y., Jarell, A. D., Flaman, J. M., Foltz, G., Schuster, J., Sopher, B. L., Irvin, D. K., Kanning, K., Kornblum, H. I., Nelson, P. S.*, et al.* (2001). Pescadillo, a novel cell cycle regulatory protein abnormally expressed in malignant cells. J Biol Chem *276*, 6656-6665.

Kopecny, V., Landa, V., and Pavlok, A. (1995). Localization of nucleic acids in the nucleoli of oocytes and early embryos of mouse and hamster: an autoradiographic study. Mol Reprod Dev *41*, 449-458.

Kruse, J. J., Svensson, J. P., Huigsloot, M., Giphart-Gassler, M., Schoonen, W. G., Polman, J. E., Jean Horbach, G., van de Water, B., and Vrieling, H. (2007). A portrait of cisplatin-induced transcriptional changes in mouse embryonic stem cells reveals a dominant p53-like response. Mutat Res *617*, 58-70.

Kubbutat, M. H., Jones, S. N., and Vousden, K. H. (1997). Regulation of p53 stability by Mdm2. Nature *387*, 299-303.

Lapik, Y. R., Fernandes, C. J., Lau, L. F., and Pestov, D. G. (2004). Physical and functional interaction between Pes1 and Bop1 in mammalian ribosome biogenesis. Mol Cell *15*, 17-29.

Lavoie, J. N., L'Allemain, G., Brunet, A., Muller, R., and Pouyssegur, J. (1996). Cyclin D1 expression is regulated positively by the p42/p44MAPK and negatively by the p38/HOGMAPK pathway. J Biol Chem *271*, 20608-20616.

Leahy, A., Xiong, J. W., Kuhnert, F., and Stuhlmann, H. (1999). Use of developmental marker genes to define temporal and spatial patterns of differentiation during embryoid body formation. J Exp Zool *284*, 67-81.

Lerch-Gaggl, A., Haque, J., Li, J., Ning, G., Traktman, P., and Duncan, S. A. (2002). Pescadillo is essential for nucleolar assembly, ribosome biogenesis, and mammalian cell proliferation. J Biol Chem *277*, 45347-45355.

Leung, A. K., Trinkle-Mulcahy, L., Lam, Y. W., Andersen, J. S., Mann, M., and Lamond, A. I. (2006). NOPdb: Nucleolar Proteome Database. Nucleic Acids Res *34*, D218-220.

Lohrum, M. A., Ludwig, R. L., Kubbutat, M. H., Hanlon, M., and Vousden, K. H. (2003). Regulation of HDM2 activity by the ribosomal protein L11. Cancer Cell *3*, 577-587.

Macleod, K. F., Sherry, N., Hannon, G., Beach, D., Tokino, T., Kinzler, K., Vogelstein, B., and Jacks, T. (1995). p53-dependent and independent expression of p21 during cell growth, differentiation, and DNA damage. Genes Dev *9*, 935-944.

Maiorana, A., Tu, X., Cheng, G., and Baserga, R. (2004). Role of pescadillo in the transformation and immortalization of mammalian cells. Oncogene *23*, 7116-7124.

Malashicheva, A. B., Kisliakova, T. V., Savatier, P., and Pospelov, V. A. (2002). [Embryonal stem cells do not undergo cell cycle arrest upon exposure to damaging factors]. Tsitologiia *44*, 643-648.

Marechal, V., Elenbaas, B., Piette, J., Nicolas, J. C., and Levine, A. J. (1994). The ribosomal L5 protein is associated with mdm-2 and mdm-2-p53 complexes. Mol Cell Biol *14*, 7414-7420.

Martin, G. R. (1981). Isolation of a pluripotent cell line from early mouse embryos cultured in medium conditioned by teratocarcinoma stem cells. Proc Natl Acad Sci U S A *78*, 7634-7638.

Matoba, R., Niwa, H., Masui, S., Ohtsuka, S., Carter, M. G., Sharov, A. A., and Ko, M. S. (2006). Dissecting oct3/4-regulated gene networks in embryonic stem cells by expression profiling. PLoS ONE *1*, e26.

Matsuda, T., Nakamura, T., Nakao, K., Arai, T., Katsuki, M., Heike, T., and Yokota, T. (1999). STAT3 activation is sufficient to maintain an undifferentiated state of mouse embryonic stem cells. Embo J *18*, 4261-4269.

Mayer, C., Bierhoff, H., and Grummt, I. (2005). The nucleolus as a stress sensor: JNK2 inactivates the transcription factor TIF-IA and down-regulates rRNA synthesis. Genes Dev *19*, 933-941.

Mayer, C., and Grummt, I. (2005). Cellular stress and nucleolar function. Cell Cycle *4*, 1036-1038.

Mayer, C., Zhao, J., Yuan, X., and Grummt, I. (2004). mTOR-dependent activation of the transcription factor TIF-IA links rRNA synthesis to nutrient availability. Genes Dev *18*, 423-434.

Meshorer, E., and Misteli, T. (2006). Chromatin in pluripotent embryonic stem cells and differentiation. Nat Rev Mol Cell Biol *7*, 540-546.

Miles, T. D., Jakovljevic, J., Horsey, E. W., Harnpicharnchai, P., Tang, L., and Woolford, J. L., Jr. (2005). Ytm1, Nop7, and Erb1 form a complex necessary for maturation of yeast 66S preribosomes. Mol Cell Biol *25*, 10419-10432.

Mitchell, J. R., Cheng, J., and Collins, K. (1999). A box H/ACA small nucleolar RNA-like domain at the human telomerase RNA 3' end. Mol Cell Biol *19*, 567-576.

Mitsui, K., Tokuzawa, Y., Itoh, H., Segawa, K., Murakami, M., Takahashi, K., Maruyama, M., Maeda, M., and Yamanaka, S. (2003). The homeoprotein Nanog is required for maintenance of pluripotency in mouse epiblast and ES cells. Cell *113*, 631-642.

Miwa, S., Uchida, C., Kitagawa, K., Hattori, T., Oda, T., Sugimura, H., Yasuda, H., Nakamura, H., Chida, K., and Kitagawa, M. (2006). Mdm2-mediated pRB downregulation is involved in carcinogenesis in a p53-independent manner. Biochem Biophys Res Commun *340*, 54-61.

Montanaro, L., Mazzini, G., Barbieri, S., Vici, M., Nardi-Pantoli, A., Govoni, M., Donati, G., Trere, D., and Derenzini, M. (2007). Different effects of ribosome biogenesis inhibition on cell proliferation in retinoblastoma protein- and p53-deficient and proficient human osteosarcoma cell lines. Cell Prolif *40*, 532-549.

Montes de Oca Luna, R., Wagner, D. S., and Lozano, G. (1995). Rescue of early embryonic lethality in mdm2-deficient mice by deletion of p53. Nature *378*, 203-206.

Nal, B., Mohr, E., Silva, M. I., Tagett, R., Navarro, C., Carroll, P., Depetris, D., Verthuy, C., Jordan, B. R., and Ferrier, P. (2002). Wdr12, a mouse gene encoding a novel WD-Repeat Protein with a notchless-like amino-terminal domain. Genomics *79*, 77-86.

Niwa, H. (2007). How is pluripotency determined and maintained? Development *134*, 635-646.

Niwa, H., Burdon, T., Chambers, I., and Smith, A. (1998). Self-renewal of pluripotent embryonic stem cells is mediated via activation of STAT3. Genes Dev *12*, 2048-2060.

O'Shea, K. S. (2004). Self-renewal vs. differentiation of mouse embryonic stem cells. Biol Reprod *71*, 1755-1765.

Obaya, A. J., and Sedivy, J. M. (2002). Regulation of cyclin-Cdk activity in mammalian cells. Cell Mol Life Sci *59*, 126-142.

Oeffinger, M., Leung, A., Lamond, A., and Tollervey, D. (2002). Yeast Pescadillo is required for multiple activities during 60S ribosomal subunit synthesis. Rna *8*, 626-636.

Oliner, J. D., Pietenpol, J. A., Thiagalingam, S., Gyuris, J., Kinzler, K. W., and Vogelstein, B. (1993). Oncoprotein MDM2 conceals the activation domain of tumour suppressor p53. Nature *362*, 857-860.

Olson, M. O. (2004). Sensing cellular stress: another new function for the nucleolus? Sci STKE *2004*, pe10.

Olson, M. O., Dundr, M., and Szebeni, A. (2000). The nucleolus: an old factory with unexpected capabilities. Trends Cell Biol *10*, 189-196.

Paling, N. R., Wheadon, H., Bone, H. K., and Welham, M. J. (2004). Regulation of embryonic stem cell self-renewal by phosphoinositide 3-kinase-dependent signaling. J Biol Chem *279*, 48063-48070.

Perez-Roger, I., Kim, S. H., Griffiths, B., Sewing, A., and Land, H. (1999). Cyclins D1 and D2 mediate myc-induced proliferation via sequestration of p27(Kip1) and p21(Cip1). Embo J *18*, 5310-5320.

Pesce, M., and Scholer, H. R. (2001). Oct-4: gatekeeper in the beginnings of mammalian development. Stem Cells *19*, 271-278.

Pestov, D. G., Strezoska, Z., and Lau, L. F. (2001). Evidence of p53-dependent cross-talk between ribosome biogenesis and the cell cycle: effects of nucleolar protein Bop1 on G(1)/S transition. Mol Cell Biol *21*, 4246-4255.

Politz, J. C., Yarovoi, S., Kilroy, S. M., Gowda, K., Zwieb, C., and Pederson, T. (2000). Signal recognition particle components in the nucleolus. Proc Natl Acad Sci U S A *97*, 55-60.

Polymenis, M., and Schmidt, E. V. (1997). Coupling of cell division to cell growth by translational control of the G1 cyclin CLN3 in yeast. Genes Dev *11*, 2522-2531.

Polymenis, M., and Schmidt, E. V. (1999). Coordination of cell growth with cell division. Curr Opin Genet Dev *9*, 76-80.

Prost, S., Bellamy, C. O., Clarke, A. R., Wyllie, A. H., and Harrison, D. J. (1998). p53-independent DNA repair and cell cycle arrest in embryonic stem cells. FEBS Lett *425*, 499-504.

Qi, X., Li, T. G., Hao, J., Hu, J., Wang, J., Simmons, H., Miura, S., Mishina, Y., and Zhao, G. Q. (2004). BMP4 supports self-renewal of embryonic stem cells by inhibiting mitogen-activated protein kinase pathways. Proc Natl Acad Sci U S A *101*, 6027-6032.

Rohrmoser, M., Holzel, M., Grimm, T., Malamoussi, A., Harasim, T., Orban, M., Pfisterer, I., Gruber-Eber, A., Kremmer, E., and Eick, D. (2007). Interdependence of Pes1, Bop1, and

WDR12 controls nucleolar localization and assembly of the PeBoW complex required for maturation of the 60S ribosomal subunit. Mol Cell Biol *27*, 3682-3694.

Romanova, L. G., Anger, M., Zatsepina, O. V., and Schultz, R. M. (2006). Implication of nucleolar protein SURF6 in ribosome biogenesis and preimplantation mouse development. Biol Reprod *75*, 690-696.

Rouquette, J., Choesmel, V., and Gleizes, P. E. (2005). Nuclear export and cytoplasmic processing of precursors to the 40S ribosomal subunits in mammalian cells. Embo J *24*, 2862-2872.

Rubbi, C. P., and Milner, J. (2003). Disruption of the nucleolus mediates stabilization of p53 in response to DNA damage and other stresses. Embo J *22*, 6068-6077.

Ruggero, D., and Pandolfi, P. P. (2003). Does the ribosome translate cancer? Nat Rev Cancer *3*, 179-192.

Sage, J., Mulligan, G. J., Attardi, L. D., Miller, A., Chen, S., Williams, B., Theodorou, E., and Jacks, T. (2000). Targeted disruption of the three Rb-related genes leads to loss of G(1) control and immortalization. Genes Dev *14*, 3037-3050.

Santoni-Rugiu, E., Falck, J., Mailand, N., Bartek, J., and Lukas, J. (2000). Involvement of Myc activity in a G(1)/S-promoting mechanism parallel to the pRb/E2F pathway. Mol Cell Biol *20*, 3497-3509.

Sato, N., Meijer, L., Skaltsounis, L., Greengard, P., and Brivanlou, A. H. (2004). Maintenance of pluripotency in human and mouse embryonic stem cells through activation of Wnt signaling by a pharmacological GSK-3-specific inhibitor. Nat Med *10*, 55-63.

Savatier, P., Huang, S., Szekely, L., Wiman, K. G., and Samarut, J. (1994). Contrasting patterns of retinoblastoma protein expression in mouse embryonic stem cells and embryonic fibroblasts. Oncogene *9*, 809-818.

Savatier, P., Lapillonne, H., van Grunsven, L. A., Rudkin, B. B., and Samarut, J. (1996). Withdrawal of differentiation inhibitory activity/leukemia inhibitory factor up-regulates D-type cyclins and cyclin-dependent kinase inhibitors in mouse embryonic stem cells. Oncogene *12*, 309-322.

Scherl, A., Coute, Y., Deon, C., Calle, A., Kindbeiter, K., Sanchez, J. C., Greco, A., Hochstrasser, D., and Diaz, J. J. (2002). Functional proteomic analysis of human nucleolus. Mol Biol Cell *13*, 4100-4109.

Schmitz, J., Weissenbach, M., Haan, S., Heinrich, P. C., and Schaper, F. (2000). SOCS3 exerts its inhibitory function on interleukin-6 signal transduction through the SHP2 recruitment site of gp130. J Biol Chem *275*, 12848-12856.

Schneiter, R., Kadowaki, T., and Tartakoff, A. M. (1995). mRNA transport in yeast: time to reinvestigate the functions of the nucleolus. Mol Biol Cell *6*, 357-370.

Schratt, G., Weinhold, B., Lundberg, A. S., Schuck, S., Berger, J., Schwarz, H., Weinberg, R. A., Ruther, U., and Nordheim, A. (2001). Serum response factor is required for immediate-early gene activation yet is dispensable for proliferation of embryonic stem cells. Mol Cell Biol *21*, 2933-2943.

Serfas, M. S., Goufman, E., Feuerman, M. H., Gartel, A. L., and Tyner, A. L. (1997). p53-independent induction of p21WAF1/CIP1 expression in pericentral hepatocytes following carbon tetrachloride intoxication. Cell Growth Differ *8*, 951-961.

Shan, B., Chang, C. Y., Jones, D., and Lee, W. H. (1994). The transcription factor E2F-1 mediates the autoregulation of RB gene expression. Mol Cell Biol *14*, 299-309.

Sherr, C. J., and Roberts, J. M. (1999). CDK inhibitors: positive and negative regulators of G1-phase progression. Genes Dev *13*, 1501-1512.

Sherr, C. J., and Weber, J. D. (2000). The ARF/p53 pathway. Curr Opin Genet Dev *10*, 94-99.

Sirri, V., Hernandez-Verdun, D., and Roussel, P. (2002). Cyclin-dependent kinases govern formation and maintenance of the nucleolus. J Cell Biol *156*, 969-981.

Smith, A. G., Heath, J. K., Donaldson, D. D., Wong, G. G., Moreau, J., Stahl, M., and Rogers, D. (1988). Inhibition of pluripotential embryonic stem cell differentiation by purified polypeptides. Nature *336*, 688-690.

Solter, D. (2006). From teratocarcinomas to embryonic stem cells and beyond: a history of embryonic stem cell research. Nat Rev Genet *7*, 319-327.

Stead, E., White, J., Faast, R., Conn, S., Goldstone, S., Rathjen, J., Dhingra, U., Rathjen, P., Walker, D., and Dalton, S. (2002). Pluripotent cell division cycles are driven by ectopic Cdk2, cyclin A/E and E2F activities. Oncogene *21*, 8320-8333.

Strezoska, Z., Pestov, D. G., and Lau, L. F. (2000). Bop1 is a mouse WD40 repeat nucleolar protein involved in 28S and 5. 8S RRNA processing and 60S ribosome biogenesis. Mol Cell Biol *20*, 5516-5528.

Strezoska, Z., Pestov, D. G., and Lau, L. F. (2002). Functional inactivation of the mouse nucleolar protein Bop1 inhibits multiple steps in pre-rRNA processing and blocks cell cycle progression. J Biol Chem *277*, 29617-29625.

Suda, Y., Suzuki, M., Ikawa, Y., and Aizawa, S. (1987). Mouse embryonic stem cells exhibit indefinite proliferative potential. J Cell Physiol *133*, 197-201.

Sumi, T., Tsuneyoshi, N., Nakatsuji, N., and Suemori, H. (2007). Apoptosis and differentiation of human embryonic stem cells induced by sustained activation of c-Myc. Oncogene.

Sun, H., Lesche, R., Li, D. M., Liliental, J., Zhang, H., Gao, J., Gavrilova, N., Mueller, B., Liu, X., and Wu, H. (1999). PTEN modulates cell cycle progression and cell survival by regulating phosphatidylinositol 3,4,5,-trisphosphate and Akt/protein kinase B signaling pathway. Proc Natl Acad Sci U S A *96*, 6199-6204.

Sun, X. X., Dai, M. S., and Lu, H. (2007). 5-fluorouracil activation of p53 involves an MDM2-ribosomal protein interaction. J Biol Chem *282*, 8052-8059.

Takahashi, K., Mitsui, K., and Yamanaka, S. (2003a). Role of ERas in promoting tumour-like properties in mouse embryonic stem cells. Nature *423*, 541-545.

Takahashi, K., Murakami, M., and Yamanaka, S. (2005). Role of the phosphoinositide 3-kinase pathway in mouse embryonic stem (ES) cells. Biochem Soc Trans *33*, 1522-1525.

Takahashi, K., and Yamanaka, S. (2006). Induction of pluripotent stem cells from mouse embryonic and adult fibroblast cultures by defined factors. Cell *126*, 663-676.

Takahashi, N., Yanagida, M., Fujiyama, S., Hayano, T., and Isobe, T. (2003b). Proteomic snapshot analyses of preribosomal ribonucleoprotein complexes formed at various stages of ribosome biogenesis in yeast and mammalian cells. Mass Spectrom Rev *22*, 287-317.

Thomas, G. (2000). An encore for ribosome biogenesis in the control of cell proliferation. Nat Cell Biol *2*, E71-72.

Thomson, J. A., Itskovitz-Eldor, J., Shapiro, S. S., Waknitz, M. A., Swiergiel, J. J., Marshall, V. S., and Jones, J. M. (1998). Embryonic stem cell lines derived from human blastocysts. Science *282*, 1145-1147.

Toyoshima, M., Shimura, T., Adiga, S. K., Taga, M., Shiraishi, K., Inoue, M., Yuan, Z. M., and Niwa, O. (2005). Transcription-independent suppression of DNA synthesis by p53 in sperm-irradiated mouse zygotes. Oncogene *24*, 3229-3235.

Tsai, R. Y., and McKay, R. D. (2002). A nucleolar mechanism controlling cell proliferation in stem cells and cancer cells. Genes Dev *16*, 2991-3003.

Tschochner, H., and Hurt, E. (2003). Pre-ribosomes on the road from the nucleolus to the cytoplasm. Trends Cell Biol *13*, 255-263.

Uchida, C., Miwa, S., Kitagawa, K., Hattori, T., Isobe, T., Otani, S., Oda, T., Sugimura, H., Kamijo, T., Ookawa, K*., et al.* (2005). Enhanced Mdm2 activity inhibits pRB function via ubiquitin-dependent degradation. Embo J *24*, 160-169.

Venema, J., and Tollervey, D. (1999). Ribosome synthesis in Saccharomyces cerevisiae. Annu Rev Genet *33*, 261-311.

Vogelstein, B., Lane, D., and Levine, A. J. (2000). Surfing the p53 network. Nature *408*, 307-310.

Voit, R., Hoffmann, M., and Grummt, I. (1999). Phosphorylation by G1-specific cdk-cyclin complexes activates the nucleolar transcription factor UBF. Embo J *18*, 1891-1899.

Volarevic, S., Stewart, M. J., Ledermann, B., Zilberman, F., Terracciano, L., Montini, E., Grompe, M., Kozma, S. C., and Thomas, G. (2000). Proliferation, but not growth, blocked by conditional deletion of 40S ribosomal protein S6. Science *288*, 2045-2047.

Waga, S., Hannon, G. J., Beach, D., and Stillman, B. (1994). The p21 inhibitor of cyclin-dependent kinases controls DNA replication by interaction with PCNA. Nature *369*, 574-578.

Warner, J. R. (1999). The economics of ribosome biosynthesis in yeast. Trends Biochem Sci *24*, 437-440.

Watanabe, S., Umehara, H., Murayama, K., Okabe, M., Kimura, T., and Nakano, T. (2006). Activation of Akt signaling is sufficient to maintain pluripotency in mouse and primate embryonic stem cells. Oncogene *25*, 2697-2707.

Weinberg, R. A. (1995). The retinoblastoma protein and cell cycle control. Cell *81*, 323-330.

Wernig, M., Meissner, A., Foreman, R., Brambrink, T., Ku, M., Hochedlinger, K., Bernstein, B. E., and Jaenisch, R. (2007). In vitro reprogramming of fibroblasts into a pluripotent ES-cell-like state. Nature *448*, 318-324.

White, J., Stead, E., Faast, R., Conn, S., Cartwright, P., and Dalton, S. (2005). Developmental activation of the Rb-E2F pathway and establishment of cell cycle-regulated cyclin-dependent kinase activity during embryonic stem cell differentiation. Mol Biol Cell *16*, 2018-2027.

Williams, R. L., Hilton, D. J., Pease, S., Willson, T. A., Stewart, C. L., Gearing, D. P., Wagner, E. F., Metcalf, D., Nicola, N. A., and Gough, N. M. (1988). Myeloid leukaemia inhibitory factor maintains the developmental potential of embryonic stem cells. Nature *336*, 684-687.

Wobus, A. M., Wallukat, G., and Hescheler, J. (1991). Pluripotent mouse embryonic stem cells are able to differentiate into cardiomyocytes expressing chronotropic responses to adrenergic and cholinergic agents and Ca2+ channel blockers. Differentiation *48*, 173-182.

Yarbrough, W. G., Bessho, M., Zanation, A., Bisi, J. E., and Xiong, Y. (2002). Human tumor suppressor ARF impedes S-phase progression independent of p53. Cancer Res *62*, 1171-1177.

Ying, Q. L., Nichols, J., Chambers, I., and Smith, A. (2003). BMP induction of Id proteins suppresses differentiation and sustains embryonic stem cell self-renewal in collaboration with STAT3. Cell *115*, 281-292.

Zeng, Y. X., and el-Deiry, W. S. (1996). Regulation of p21WAF1/CIP1 expression by p53-independent pathways. Oncogene *12*, 1557-1564.

Zhang, Y., Wolf, G. W., Bhat, K., Jin, A., Allio, T., Burkhart, W. A., and Xiong, Y. (2003). Ribosomal protein L11 negatively regulates oncoprotein MDM2 and mediates a p53-dependent ribosomal-stress checkpoint pathway. Mol Cell Biol *23*, 8902-8912.

Zhao, J., Kennedy, B. K., Lawrence, B. D., Barbie, D. A., Matera, A. G., Fletcher, J. A., and Harlow, E. (2000). NPAT links cyclin E-Cdk2 to the regulation of replication-dependent histone gene transcription. Genes Dev *14*, 2283-2297.

8 ABBREVIATIONS

α	anti / alpha
β-ME	β-mercaptoethanol
µg	microgram
µl	microliter
µM	micromolar
A	adenosine
aa	amino acid
Ab	antibody
AP	alkaline phosphatase
APS	ammonium persulfate
bp	base pair
BrdU	bromodeoxyuridine
BSA	bovine serum albumine
C	cytosine
C-	carboxy-
Cdk	cyclin-dependent kinase
cDNA	complementary DNA
d	day(s)
DAPI	4,6-Diamino-2-phenylindol
DEPC	diethylpyrocarbonate
DMSO	dimethylsulfoxide
DNA	2'-deoxyribonucleic acid
dNTP	3'-deoxyribobucleoside-5'-triphosphate
dpc	days post coitum
EB	embryoid body
EDTA	ethylenediamine tetra-acetic acid
e.g.	for example
EGFP	enhanced green fluorescent protein
ES cells	embryonic stem cells
EtOH	ethanol
ETS	external transcribed spacer
FACS	fluorescence activated cell sorting
FBS	fetal bovine serum
FITC	fluoresceinisothiocyanat
G	guanidine
GFP	green fluorescent protein
h	human, hour(s)
HRP	horseradish peroxidase

ICM	inner cell mass
ITS	internal transcribed spacer
kb	kilo base pairs
kD	kilo Dalton
LIF	leukemia inhibitory factor
m	murine
MAPK	mitogen activated protein kinase
MEK	mitogen activated kinase kinase
MEM	non-essential amino acids
min	minute(s)
mM	millimolar
monocl.	monoclonal
MOPS	3-(N-morpholino) propansulfonic acid
myc	myeloblastom
N-	amino-
nM	nanomolar
PBS	Phosphate –buffered saline
PCR	polymerase chain reaction
PI	propidium iodide
PI3K	phosphatidylinositol-3-kinase
polycl.	polyclonal
pRb	hypo-phosphorylated Rb
ppRb	hyper-phosphorylated Rb
Rb	Retinoblastoma gene product
RNA	ribonucleic acid
RNase	ribonuclease
rpm	rounds per minute
rRNA	ribosomal RNA
RT	room temperature / reverse transcription
SD	standard deviation
SDS-PAGE	sodiumdodecylsulfate-polyacrylamide gel electrophoresis
sec	second(s)
siRNA	small interfering RNA
STAT	signal transducer and activator of transcription
T	thymine
TBS	tris-buffered saline
TE	tris-chloride/EDTA (10:1)
TEMED	N,N,N',N'-tetramethylethylendiamine
TRIS	tris-(hydroymethyl)-ammoniummethan
U	units
UV	ultraviolet

CURRICULUM VITAE

Personal Data

Name:	Iris Pfisterer
Date of birth:	07.04.1974
Place of birth:	Leonberg, Germany

Academic Education

1994-2000	Studies of Biology at the University of Heidelberg and the University of Melbourne (1998), Australia
2000-2001	Diploma thesis at the ZMBH in Heidelberg (Prof. Dr. C. Clayton) Topic: Functional characterization of GIM5, a glycosomal membrane protein from *Trypanosoma brucei*
2001	Diploma in Biology
2003-2007	Doctoral thesis at the GSF Research Center in Munich, at the Institute of Clinical Molecular Biology and Tumor Genetics (Prof. Dr. D. Eick) Topic: The Role of the PeBoW-complex in ribosome biogenesis and proliferation of mouse embryonic stem cells

Publications

Rohrmoser M, Holzel M, Grimm T, Malamoussi A, Harasim T, Orban M, Pfisterer I, Gruber-Eber A, Kremmer E, Eick D. **Interdependence of Pes1, Bop1, and WDR12 controls nucleolar localization and assembly of the PeBoW complex required for maturation of the 60S ribosomal subunit.** Mol Cell Biol. 2007 May;27(10):3682-94.

Langer H, May AE, Daub K, Heinzmann U, Lang P, Schumm M, Vestweber D, Massberg S, Schonberger T, Pfisterer I, Hatzopoulos AK, Gawaz M. **Adherent platelets recruit and induce differentiation of murine embryonic endothelial progenitor cells to mature endothelial cells in vitro.** Circ Res. 2006 Feb 3;98(2):e2-10.

Voncken F, van Hellemond JJ, Pfisterer I, Maier A, Hillmer S, Clayton C. **Depletion of GIM5 causes cellular fragility, a decreased glycosome number, and reduced levels of ether-linked phospholipids in trypanosomes.** J Biol Chem. 2003 Sep 12;278(37):35299-310.

ACKNOWLEDGEMENTS

Here I would like to thank all the people that were involved in the successful completion of this thesis:

First, my supervisors Prof. Dr. Dirk Eick and Dr. Antonis Hatzopoulos for giving me the opportunity to work in their labs and for their support, ideas and critical discussions during the course of this work.

Prof. Dr. Dirk Eick also for the official correction of the thesis.

Prof. Dr. Georg Bornkamm for providing very good scientific facilities at the Institute of Clinical Molecular Biology and Tumor Genetics and for finding some space for me at the "first floor" after the disappearance of the vascular genetics group.

Dr. Elisabeth Kremmer and her group for the generation of monoclonal antibodies.

Dr. Michael Hölzel as initiator of my project and Dr. Gerhard Laux for his support in all computer problems. The members of the Eick lab, Anastassia, Bastian, Michaela and Thomas, for passing on their knowledge about native gels and *in vivo*-labelings. The former members of the vascular genetics group and all other people from KMolbi for providing a very comfortable working atmosphere, help with many methods, critical discussions and many tasty cakes, and the Lunch club for delicious food on Thursdays. Last but not least, my lab-mate Thorsten for many fruitful discussions and for making the time more fun with his humor.